PALAEOMAGNETISM OF THE SKINNER COVE FORMATION OF WESTERN NEWFOUNDLAND AND THE BIRTH OF THE IAPETUS OCEAN

PHILIP JOHN ALBERT McCAUSLAND

Palaeomagnetism of the Skinner Cove Formation of Western Newfoundland and the birth of the Iapetus Ocean.

by

Philip John Albert McCausland

A thesis submitted to the School of Graduate Studies

in partial fulfilment of the requirements for the

degree of Master of Science (Geology)

Department of Earth Sciences

Memorial University of Newfoundland

March 1998

St. John's Newfoundland

0-612-34205-0

ABSTRACT

The 550 Ma Skinner Cove Formation is a structural unit within the Humber Arm Allochthon of western Newfoundland, occurring as an alkali volcanic suite affected only by zeolite facies metamorphism. At 10 sites from its flows and dykes a magnetite-borne, stable characteristic `A' remanence direction (tilt-corrected mean $D$=144°, $I$=31.5°; $\alpha_{95}$=10.8°, k=21.1) is recognized and shown to be a primary thermal remanence by an intraformational conglomerate test. The palaeolatitude calculated for the Skinner Cove Formation from its ten `A' site virtual geomagnetic poles is 18.6°S ±9°.

An original relation between the Skinner Cove Formation and the Iapetan margin of Laurentia is suggested by several lines of evidence: As a structural slice it occupies a lower, less transported position in the Humber Arm Allochthon, implying an original adjacency to underlying slices of Laurentian margin sediments. The Skinner Cove volcanics have a within-plate trace element geochemistry with enriched light rare earth elements (LREE), shared with other alkali volcanics of the northeastern Appalachians Humber Zone. Also, the ~550 Ma Skinner Cove volcanics are of similar age to alkali magmatic activity of Laurentia's Iapetan margin, marked by the ~554 Ma Tibbit Hill metavolcanics of Quebec and the ~555 Ma Lady Slipper Pluton of west Newfoundland. Hence, the 18.6°S palaeolatitude of the Skinner Cove Formation constrains Laurentia to an equatorial position at ~550 Ma.

Comparison with other palaeomagnetically determined high southerly palaeolatitudes for ~570 Ma implies a large rapid northward drift of ~34 cm/yr for Laurentia during the latest Neoproterozoic. The start of Laurentia's rapid northward movement at ~570 Ma may mark

the beginning of Iapetus sea-floor spreading, consistent with Laurentian geological data if thermally-delayed subsidence of the Laurentian margin is assumed. Further well-constrained palaeomagnetic results of ~580 –~550 Ma age from Laurentia and especially its suspected conjugate margins Amazonia and Rio de la Plata are required to test this proposed palaeogeography and to define the birth of the Iapetus Ocean precisely.

ACKNOWLEDGEMENTS:

Somehow, I knew that I would end up writing this at two in the morning on Christmas Eve. I am surrounded by my friends, and some of them are working for me. The University closes for the holidays at noon. More on this later...!

As I am about to leave home to start another thesis project (a glutton for punishment, I guess), my thoughts are most with my parents, Reginald and Jean McCausland, who have supported me throughout with their love and generosity. I owe them much more than any thanks I can write here. My sisters, both near (Cathy) and soon-to-be near (Sue) gave me gentle advice, humour, and boots when necessary.

I gratefully acknowledge the opportunity to pursue this research under the inspiration and direction of Dr. Joseph Hodych, my very patient thesis supervisor. His support, both financial and otherwise, has been vital to this work and to the burgeoning of my own interests. It's been a lot of fun, and I hope someday to be able to repay the debt in kind.

The production of the thesis was largely assisted by Ray Patzold, who continues to impress me by overcoming each week's learning curve (diagrams and figures were produced with at least four programs, of variable stability). Sherri Jordan, Allison Gollop, Karen Patzold, and Letitia Peckford also helped with the layout of tables, and with the measurement of samples along the way. Parks Canada kindly issued permits to collect palaeomagnetic samples; I hope that this work becomes a lasting contribution to the understanding and enjoyment of beautiful Gros Morne National Park.

I am indebted to many people for discussions surrounding the study of palaeomagnetism and the possible geography of the late Neoproterozoic, among them Conall MacNiociall, Greg Dunning, Garry Quinlan, Peter Cawood, Chuck Hurich, Ernie Deutsch, Wulf Gose, Ken Buchan and Richard Ernst. And the discussion continues...

Ken Sooley provided able and amiable field assistance during sample collection in the fall of 1995, and also is a dear friend with a ready humour, and a knack for asking the right questions. Keith Morris, Adam and Amanda Bragg, Damien Spracklin, and Jason King pulled the late-night shift to be here in the end. I'd like to thank Amanda for her care and support; I'm going to miss being here.

Cheers,

-pjam

Keith, on Palaeozoic plate relations: "Africa is a distant cousin to Laurentia, several times removed."

TABLE OF CONTENTS

CHAPTER 4: DISCUSSION

LIST OF TABLES

FIGURE LIST

LIST OF PLATES

Chapter 1: Introduction

1.1 Purpose and scope

Earth in the late Neoproterozoic featured supercontinental breakup and reorganization (Bond et al., 1984) which may have influenced the timing of the emergence and early evolution of macroscopic animals. These events may have been triggered by mechanisms sensitive to palaeogeography such as changes in palaeoclimate (Young, 1995), seawater chemistry and oceanic circulation (Brasier, 1992; Nicholas, 1996), and burial of organic carbon (Knoll and Walter, 1992). The opening of the Iapetus Ocean (Harland and Gayer, 1972), creating an east-west subtropical seaway, might be a key palaeogeographic change which aided the diversification of life (Valentine and Moores, 1970).

Recently several late Neoproterozoic continental reconstructions have been proposed (Hoffman, 1991; Dalziel, 1991; 1992; 1997; Torsvik et al., 1996), offering insights on worldwide palaeogeographic and palaeoclimatic conditions during this seminal period of Earth's history. However, more Neoproterozoic geological and palaeomagnetic data are needed to better constrain the relative positions and movements of cratons involved in the breakup of the supercontinent Rodinia (McMenamin and McMenamin-Schulte, 1990), and in the final dispersal of the proposed late Neoproterozoic supercontinent Pannotia (Powell, 1995; Dalziel, 1997). The need for clarification is especially acute for a craton such as Laurentia, which likely had a high absolute plate velocity during the dispersal (Meert et al., 1993; Gurnis and Torsvik, 1994).

A test for the late Neoproterozoic position of Laurentia in palaeocontinental reconstructions is offered by the ca. 550 Ma flows and dykes of the Skinner Cove Formation in western Newfoundland. Preliminary palaeomagnetic data in abstract form only (Beaubouef et al., 1988; McCausland et al., 1996) are available for these rocks. This work reports on the palaeomagnetism of the volcanics, and discusses their role in constraining the position of the newly formed Iapetus margin of Laurentia, the timing of Iapetus opening, and the palaeogeography of the latest Neoproterozoic.

1.2 Regional setting

In western Newfoundland the Humber Zone of the Appalachian Orogen records the history of the ancient Laurentian continental margin through the opening and closure of the Iapetus Ocean (Williams, 1975), involving late Proterozoic rifting, the Cambrian formation of a stable carbonate platform and its subsequent foundering during the obduction of mid-Ordovician (Taconic) allochthons. The largest of these allochthons is the Humber Arm Allochthon (Stevens, 1970), which consists of five lithologically distinct slice assemblages collected in an imbricate stack (Williams, 1995).

The Skinner Cove Formation comprises the lowermost, least displaced igneous slice assemblage in the Humber Arm Allochthon (Williams, 1975), and overlies melanges and transported slices of Laurentian shelf slope sediments in the Humber Arm Supergroup (Stevens, 1970). The Skinner Cove Formation and correlative units are overlain by higher igneous slice assemblages of island arc volcanics and back-arc ophiolites (Jenner et al., 1991), of which the ophiolite units are topmost and farthest-travelled (Williams, 1975).

Transport of the Skinner Cove Formation appears to have started with its inclusion in the mid-Ordovician assembly of the Humber Arm Allochthon imbricate stack and emplacement onto the Laurentian margin (Williams, 1975). Further movement of some 100-200 km may have occurred in the late Silurian during further cratonward transport of much of western Newfoundland (Stockmal and Waldron, 1993). The structural position of the Skinner Cove Formation in the allochthon as well as its geochemistry and age suggest that it formed close to the Iapetan margin of Laurentia, as will be discussed later.

1.3 General geology of the Skinner Cove Formation

The Skinner Cove Formation (Williams, 1975) was first identified (and mapped) by Troelsen (1947) as the Skinner Cove Volcanics. Rocks of the Skinner Cove Formation are best revealed in coastal bluff and wave cut platform exposures beneath the Table Mountain massif along the frontal edge of the Humber Arm Allochthon. The field area is accessible by a ~4.5 km long trail from highway 431 between Trout River and Woody Point, within the boundary of Gros Morne National Park (Figure 1).

Skinner Cove volcanic rocks are a differentiated assemblage of interlayered volcanic and volcaniclastic units cut by subvolcanic dykes. Most units are laterally discontinuous, remarkably fresh and relatively undeformed, dipping steeply to the

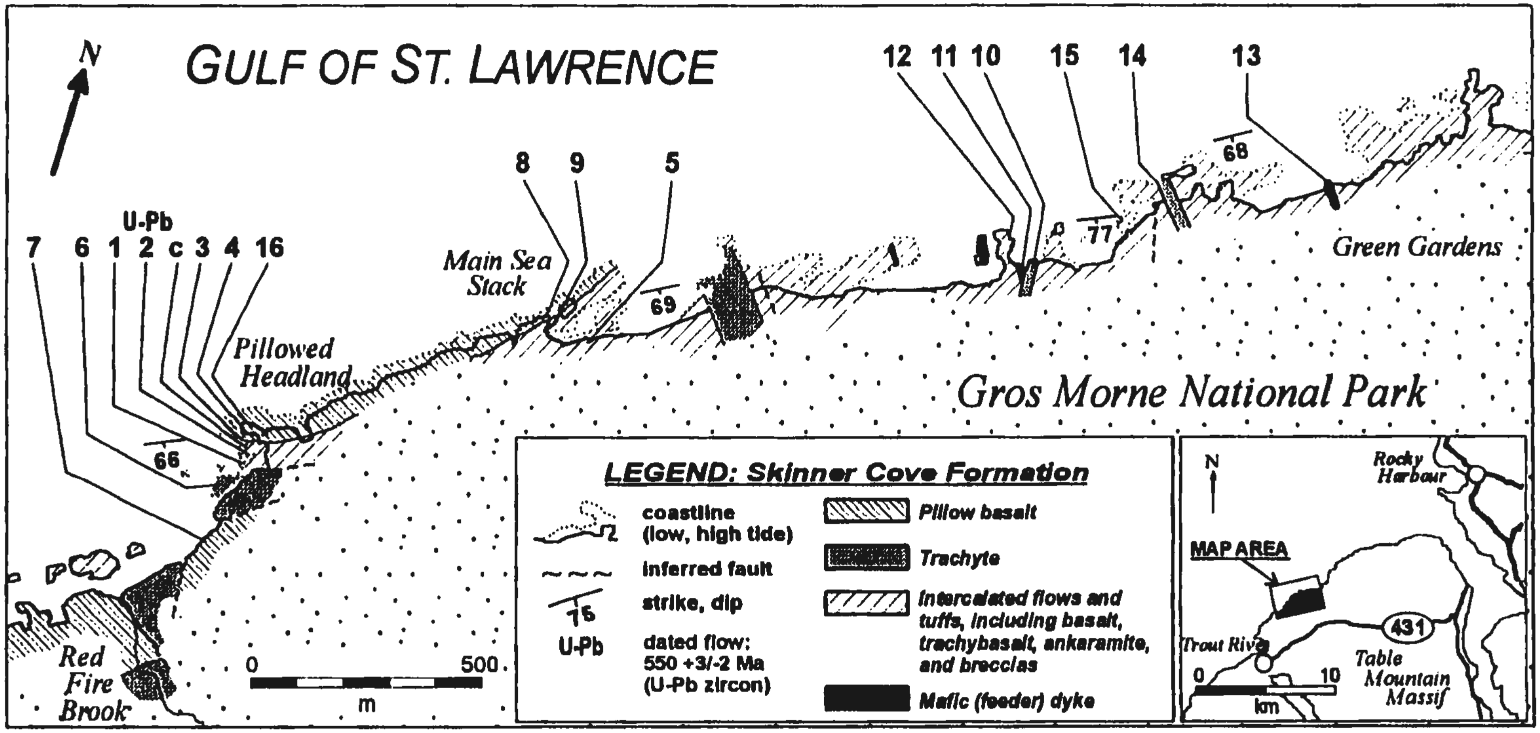

Figure 1. Outcrop sketch map and sampled sites of the Skinner Cove Formation (adapted from Baker, 1979). Regional relation of the Skinner Cove Formation with late Neoproterozoic alkali units of the northeast Appalachians Humber Zone is shown in Figure 7.

southeast and trending northeast-southwest, parallel to the coast.

Units of the type area Trout River slice have been defined in three members: a basal Main Sea Stack member, an extensively brecciated and volcaniclastic rich Wallace Brook member, and the trachyte-only Red Fire Brook member (Baker, 1979). No basal or top contact relations are observed for any of the three members, and their stratigraphic order is established by other local field relations. Little to no penetrative deformation is present in units of the type area Trout River Slice (Baker, 1979; Williams, 1995). Total thickness of the Skinner Cove Formation volcanic pile is estimated at 0.8 km (Baker, 1979).

Four main volcanic compositions are present in the members: Ankaramite, alkali basalt, trachybasalt, and trachyte. The more distinctive lithologies present include: black pillow basalts with limestone filled interstices, purple trachybasalt and dark ankaramite flows, red volcanic breccias, reworked volcaniclastic tuffs with volcanic clasts, brecciated basalt fragments in calcite cement, and massive trachyte.

Major element geochemistry performed on the Skinner Cove volcanics (Strong, 1974; Baker, 1979) shows all rock types present to be strongly alkalic. TiO2 content is typically high in the alkali basalts, averaging 3.24% by weight. Trace element concentrations determined by X-Ray Fluorescence (Baker, 1979) show alkali basalts to have elevated LREE relative to chondrite, with Nb averaging 70 ppm, La 99 ppm, Ce 163 ppm. Zr concentration averages 233 ppm in alkali basalts, and Zr/Y ratios are high, ranging from 5.4 to 12.4, indicating an original alkalic magmatic affinity. Major and trace element abundances are summarized from Baker (1979) in Table 1.

Zeolite facies metamorphism is indicated by the presence of brown fibrous zeolite and analcime-quartz in ankaramite, and analcime-quartz in other rock types. While minor epidote and pumpellyite have been identified in trachyte, this is interpreted to be due to the felsic chemical composition, rather than an indicator of metamorphic condition (Baker, 1979).

Brachiopod fragments and graptolites which implied a late Cambrian-early Ordovician age for the Skinner Cove Formation (Williams, 1975), have since been determined to come from a melange that is not in stratigraphic continuity with other rocks of the formation (Williams, 1995). A U-Pb zircon age of 550.5 +3/-2 Ma (McCausland, 1995) has been obtained from an ankaramite flow (site 2) in the volcanic pile, and is reported in Cawood and others (submitted). The sampled ankaramite flow lies atop greater than 100m thickness of flows and interlayered, reworked tuffs and breccias (Baker, 1979). Hence, the ca. 550 Ma date obtained from the zircons likely represents the age of the Skinner Cove Formation.

U-Pb sampling, 14 of the 16 palaeomagnetic sites, and the conglomerate test were drawn from units of the Main Sea Stack member (Figure 1). Site 7 was obtained from pillow basalt of the Wallace Book member, while site 6 was obtained from trachyte of the Red Fire Brook member. The two trachyte dykes sampled from the Main Sea Stack

Table1: Average major and trace element abundances, Skinner Cove Formation *

	Ankaramite**		Alkali Basalt		Trachybasalt		Trachyte	
	av.	s.d.	av.	s.d.	av.	s.d.	av.	s.d.
SiO_2	40.74	1.16	44.46	2.28	50.16	2.05	60.04	1.74
TiO_2	3.68	0.57	3.24	0.53	1.74	0.52	0.25	0.23
Al_2O_3	13.19	0.88	15.65	0.89	16.73	0.69	18.49	0.55
Fe_2O_3	7.29	1.04	5.49	2.04	4.38	1.68	2.57	1.03
FeO	5.56	1.03	5.8	1.34	4.80	1.65	1.88	0.64
MnO	0.22	0.12	0.29	0.16	0.18	0.06	0.16	0.05
MgO	8.37	2.04	5.14	1.43	3.41	1.54	1.03	0.74
CaO	11.88	1.53	7.13	1.61	4.21	1.81	1.31	0.72
Na_2O	2.22	0.41	4.08	0.84	4.64	1.08	5.56	1.31
K_2O	0.64	0.32	1.58	0.73	3.27	1.95	5.93	1.75
P_2O_5	0.72	0.10	1.10	0.41	0.81	0.17	0.07	0.03
LOI	4.84	0.92	5.50	1.29	4.82	1.14	2.52	0.79
Total	99.34	0.71	99.46	0.98	99.15	0.93	99.80	1.18
Zr	205.9	8.8	233.2	89.7	310.3	60.9	761.3	307.7
Sr	687.7	142.2	740.0	274.3	638.1	164.9	228.9	109.0
Rb	8.4	5.6	18.1	8.5	33.9	22.0	81.4	34.0
Zn	108.4	7.1	119.5	8.4	133.4	11.8	144.9	30.4
Ba	296.2	62.5	823.7	673.2	1503.1	1803.0	431.0	145.3
Nb	46.3	4.3	70.5	13.6	104.9	14.8	203.4	47.2
Ga	18.3	1.1	19.4	2.4	20.1	1.4	19.9	4.9
Pb	6.1	0.3	6.8	0.6	7.4	0.7	10.1	1.7
Ni	139.3	101.0	19.9	21.4	11.1	7.5	16.1	4.2
La	74.1	4.2	99.2	18.3	121.1	15.1	177.5	25.9
Cr	152.5	127.6	26.5	28.6	6.0			
V	262.1	15.3	188.7	53.3	83.6	41.0	4.3	2.6
Y	19.8	1.1	22.7	1.6	26.3	2.9	36.6	7.4
Ce	112.9	9.9	157.0	29.0	194.9	26.4	313.3	146.7
n	10		23		10		8	

Averaged from analyses presented in Baker (1979). n = number of samples averaged

* Major element abundances in wt %; trace element abundances in ppm
** Ankaramite average includes three Ti-rich "pyroxene phyric basalt" samples

member (sites 10, 14) may represent feeder dykes for the Red Fire Brook member. The numbering of sample sites in Figure 1 has no stratigraphic significance.

Chapter 2: Palaeomagnetic methods and results

2.1 Palaeomagnetic sampling and methods

Ninety-seven oriented block samples were collected for palaeomagnetic study from the 16 sites shown in Figure 1. Each site is represented by at least six samples. In addition, 36 oriented block samples were collected for an intraformational conglomerate test from volcanic clasts in a reworked tuff. Block samples were oriented with the aid of a sun compass. Strike and dip at each site were determined from interbedded tuffs. Cylindrical specimens with 2.4 cm diameter and 2.1 cm length were cut from the oriented samples in the laboratory.

Remanent magnetizations in the oriented specimens were measured using a Schonstedt SSM-1 spinner magnetometer. A specimen from each block sample was subjected to stepwise alternating-field (AF) demagnetization using a Schonstedt demagnetizer GSD-1. Some specimens (at least one per site) were subjected to stepwise thermal demagnetization using a Schonstedt TSD-1 demagnetizer. The remanence direction and intensity were measured after each step in demagnetization and are listed in Appendix A for each sample.

Orthogonal vector plots of the detailed stepwise demagnetizations allowed straight line segments to be identified by visual inspection (Zijderveld, 1967), and to be quantitatively resolved with principal-component analysis (Kirschvink, 1980).

2.2 Palaeomagnetic results

Examples of typical demagnetization behaviour for samples from the four main rock types of the Skinner Cove volcanics are shown in tilt-corrected orthogonal vector plots (Figure 2).

A trachybasalt sample from site 3 (Figure 2a) exhibits an initial change in direction during AF demagnetization with the removal of a small viscous component, but above ~20 mT (200 Oe) the remanence maintains a southeasterly down direction as intensity decreases towards the vector plot origin. Thermal demagnetization of a second specimen from the same block sample shows similar behaviour (Figure 2b), with remanence above ~300°C showing little change in its southeasterly down direction. A pair of alkali basalt specimens from a site 4 block sample show broadly similar demagnetization characteristics, with a southeast and down magnetization isolated at coercivities higher than 25 mT (Figure 2c) and at unblocking temperatures higher than 300°C (Figure 2d).

Demagnetizations of trachyte samples tended to be more complex, with behaviours broadly divisible into two families on the basis of NRM intensity. Trachyte with higher NRM intensity (~1 A/m) was evident in nine out of the 22 trachyte samples from three sites, including all six samples of site 6. These nine samples exhibit a low-coercivity remanence that decays towards the origin of an orthogonal vector plot, dominated by a soft viscous magnetization which is mostly removed by 30 mT. Thermal demagnetization and careful AF demagnetization reveal a hard, southeast and down directed remanence of

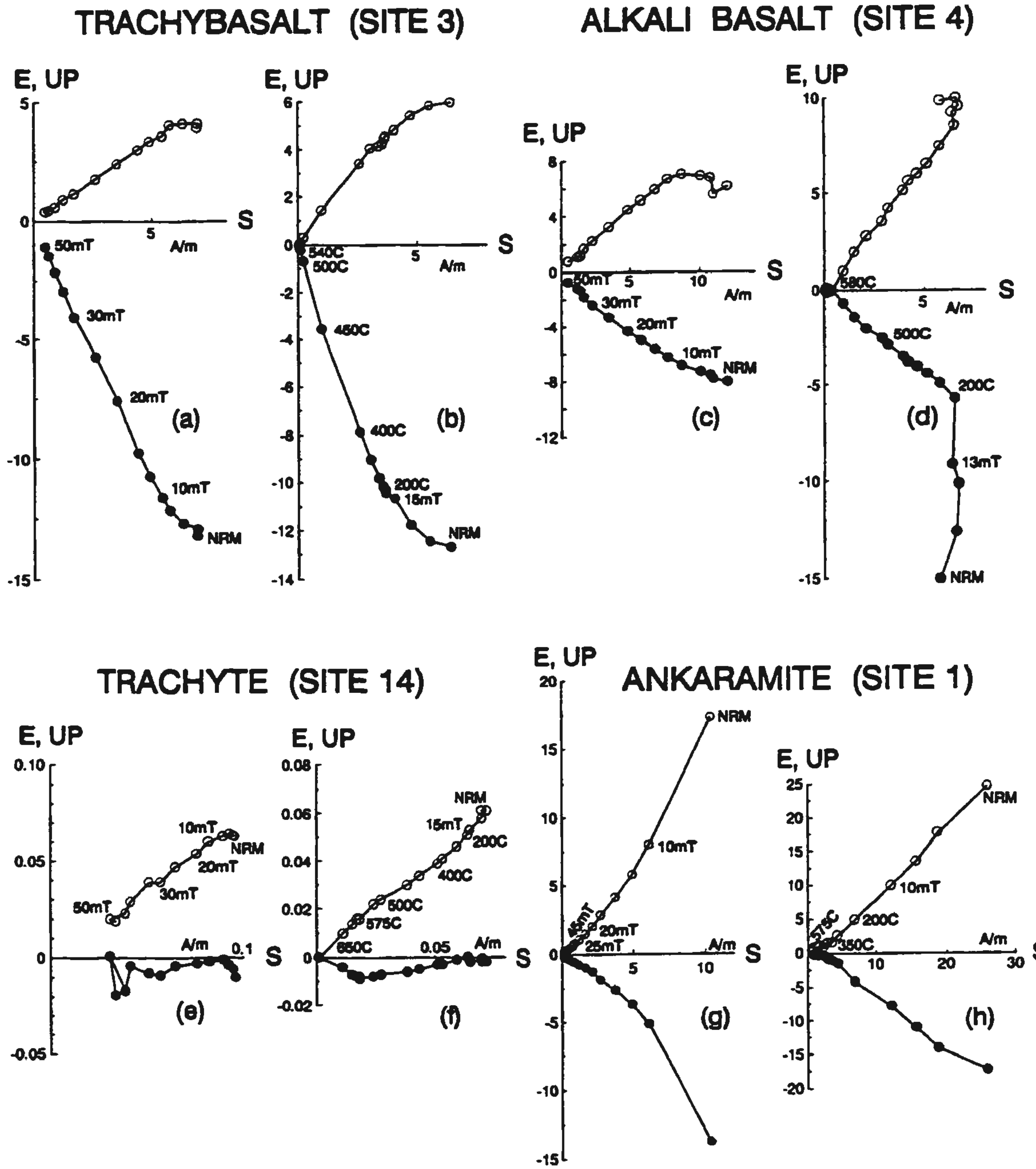

Figure 2. Comparison of alternating field (AF) demagnetizations (a,c,e,g) with thermal demagnetizations (b,d,f,h) for specimens from a site 3 trachybasalt sample (a),(b), a site 4 alkali basalt sample (c),(d), a site 14 trachyte sample (e),(f), and a site 1 ankaramite sample (g),(h). Thermal demagnetizations were preceded by AF demagnetization to 10-15 mT, as indicated. Orthogonal vector plots show decay projected in the UP-S (E-S) plane with closed (open) circles.

typically less than 20% NRM intensity which persists to coercivities of ~50 mT and unblocking temperatures of ~540°C. Thirteen lower NRM intensity trachyte samples (.1 to .01 A/m), including all six from site 10, are difficult to interpret (Figure 2e,f), as the remanence intensity approaches the resolution of the demagnetization and measurement techniques. During AF demagnetization (e.g. Figure 2e), measured remanence directions become unstable at coercivities above ~35 mT, or are undiminished by further AF treatment, suggesting the presence of a haematite-based component. Thermal demagnetization resolves a component between 575°C and 675°C that decays to the origin, corresponding to a component magnetization based in haematite (Figure 2f).

Ankaramite block samples typically exhibit a low coercivity and unblocking temperature remanence, which is removed by ~25 mT or 350°C. In block samples from site 1, an additional remanence of typically less than 20% NRM intensity with a southeast and down direction is resolved at higher coercivity and unblocking temperatures to ~45 mT and 575°C (Figure 2g,h).

The soft viscous remanent magnetization (VRM) initially removed in the specimens of Figure 2 is present in most block samples, and is resolvable in forty-seven. VRM appears to be fully removed by AF demagnetization to 20 mT or thermal demagnetization to 300°C in most specimens. However, a few specimens required 30 mT or 400°C to completely remove VRM. Specimen VRMs typically have a north, steep down in-situ direction, with Formation mean D=351°, I=72.4° (α_{95}=8.2° k=36.2, N=10 sites). This direction is similar to the present Earth field direction (D=335, I=72°) at the sampling sites, and is likely of recent origin.

For 25 specimens, the existence of any component beyond a VRM could not be resolved due to remanence above 25 mT or 350°C being unstable or too weak to be measured. In the other 71 specimens, a stable remanence direction is resolvable by least squares line fitting to vector plots, excluding coercivities below 20 mT and unblocking temperatures below 300°C to avoid contribution from VRM.

A tilt-corrected southeast and down characteristic remanence (here called the `A' component) is resolved in 62 of the specimens with stable remanence, of which 57 contribute to 10 `A' site means (Table 2). It is recognized as a high coercivity and unblocking temperature component that usually decays linearly towards the origin of a vector plot. The `A' component is fully removed between 520°C and 580°C, showing that it is likely carried by magnetite.

Stable component magnetizations carried by magnetite with directions other than `A' have been identified in ten specimens. Four specimens at site 7 retain a high coercivity, high unblocking temperature west-southwest and up `B' component (all directions tilt corrected) which is distinct from VRM and decays toward the origin (Table 2). All five specimens from site 8 along with one sample from site 16 display a high coercivity, high unblocking temperature southeast, up `C' component. These other component directions do not coexist with the `A' component in any specimen or sample.

Table 2: Skinner Cove Formation palaeomagnetic results

	Site	Rock type	Str (°)	Dip (°)	N	A/T	D (°)	I (°)	D′ (°)	I′ (°)	α_{95} (°)	k
A:	6	Trachyte	073	80	6	A&T	17.2	78.2	155.9	19.7	14.0	23.7
	1	Ankaramite	057	70	5	A	98.3	89.3	146.5	19.5	12.0	41.9
	3	Trachybasalt	062	67	6	A&T	341.3	56.3	142.7	56.0	9.2	54.4
	4	Alkali Basalt	062	67	5	A	7.4	71.4	138.5	37.6	5.6	188.9
	9	Alkali Basalt	044	69	6	A	314.8	72.7	133.6	38.3	10.7	40.4
	5	Alkali Basalt	044	69	6	A&T	310.6	51.0	138.3	59.8	13.9	24.1
	12	Ankaramite	053	62	2	A&T	205.4	81.8	150.9	24.0		
	11	Mafic Dyke	057	56	4	A&T	207.6	80.3	156.7	28.8	17.5	28.6
	10	Trachyte Dyke	057	56	3	A&T	151.2	70.1	148.8	14.1	30.2	17.8
	15	Trachybasalt	059	77	5	A&T	345.0	79.4	145.8	23.2	8.5	81.9
	14	Trachyte Dyke	059	72	9	A&T	219.1	87.8	151.1	17.2	11.1	22.4
	13	Mafic Dyke	050	80	5	A&T	16.1	77.2	128.9	16.9	14.5	28.7
MEAN OF 10 'A' SITES		- IN SITU					336.7	78.0			9.7	25.9
		- TILT CORRECTED							144.4	31.5	10.8	21.1
B:	7	Alkali Basalt	020	78	4	A	143.2	-38.2	247.3	-50.5	12.7	53.0
C:	8	Alkali Basalt	044	69	5	A&T	153.5	18.4	161.2	-46.2	20.7	14.6
	16	Mafic Dyke	062	67	1	T	151.8	23.6	151.8	-43.4		

*Sites 10, 12 not used for calculating mean of "A" sites due to insufficient number of samples

Str, Dip = Strike, Dip in degrees of bedding used for tilt correction; N = number of samples which contribute to the site mean; A/T = AF or Thermal demagnetizations; D, I = Declination and Inclination in situ; D′, I′ = Declination and Inclination after tilt correction; α_{95} = circle of 95% confidence about mean direction; k = precision parameter estimate

There appears to be a small magnetization component held by haematite, resolved with thermal demagnetization above 600°C in seven specimens from 6 sites. The resolved haematite magnetization directions define a horizontal swath from southwest to southeast when tilt corrected, and do not seem to have a clear relation to any one of the magnetite-based components.

2.3 Rock magnetism

Curie balance heatings in a 100 mT field for 16 samples representing all four rock types drawn from the ten sites with `A' component remanence and the conglomerate test clasts show that magnetite is the dominant magnetic mineral. Observed Curie points range from ~530°C for the trachyte to ~580°C for most samples of other rock types. A fraction of haematite is also identified in five specimens which remain slightly magnetic at temperatures between 580°C and 640°C. Intensities of magnetization measured during cooling are similar to those found during heating, implying that there is little creation or destruction of magnetic phases during thermal demagnetization.

Hysteresis loops were traced for several samples from ankaramite, alkali basalt, trachybasalt, and trachyte. In all cases the ratio of saturation remanence to saturation magnetization suggests that the magnetite is dominantly pseudo-single domain, rather than single domain.

Backscatter electron microscopy with capability of semi-quantitative analysis was used to examine polished sections from the four rock types. Large (80 μm) magnetite grains in alkali basalt, trachybasalt and ankaramite samples are finely subdivided by intergrowth with a titanium-rich phase, likely ilmenite. Typically, grains in trachyte are smaller ($\tilde{}$10 μm), and contain less Ti than similar grains in the more mafic volcanics, but show patchy Ti-enriched portions which may be due to unresolved exsolution lamellae. Most larger magnetite grains in the alkali pillow basalt (site 4), ankaramite (site 1), and an amygdaloidal basalt conglomerate test clast had ilmenite lamellae in their cores, with titanium-free cracks and margins and a rim of rutile grains (Plate 1).

Plate 1. Backscatter photomicrograph of amygdaloidal clast 18794-2 typical titanomagnetite grains. Rutile occurs as a dark phase along grain boundaries and cracks, while magnetite is brightest, hosting darker grey Fe-Ti rich patches which may represent areas of ilmenite lamellae development.

Chapter 3: Tests for primary remanence

3.1 Fold test

For this study, there is no significant change in the clustering of the 10 characteristic `A' component site mean directions when tilt correction is applied. The fold test is thus inconclusive, as expected since there is little variation in bedding attitude throughout the exposed section.

Previous palaeomagnetic work on the Skinner Cove volcanics is summarized in an abstract by Beaubouef et al. (1988). They report a palaeolatitude of ~12°S and a "large declination anomaly" for remanence of Skinner Cove volcanics from a site at Beverley Head, a nearby slice under the North Arm massif. The presence of Skinner Cove volcanics with similar tilt corrected remanence inclination, but different declination implies that the characteristic remanence predates relative tectonic rotation of the slices in the Humber Arm Allochthon, suggesting that the characteristic remanence predates mid-Ordovician (Taconic) transport (Beaubouef et al., 1988). However, rotation of slices relative to one another could have happened in the late Silurian to mid Devonian during orogenic reactivation (Cawood et al., 1988), or during the movement of much of western Newfoundland as part of a greater Port au Port Allochthon (Stockmal and Waldron, 1993).

3.2 Intraformational conglomerate test

An intraformational conglomerate test (Graham, 1949) was performed using samples collected from clasts of blocky trachybasalt and rounded amygdaloidal basalt in a layered, reworked tuff (Plate 2) that overlies a trachybasalt flow (site 3). The sampling location lies stratigraphically ~2m above the trachybasalt flow and ~10m below the overlying 2m thick U-Pb dated ankaramite flow (site 2). Results for specimens from the 21 trachybasalt and 15 amygdaloidal basalt clasts are presented in Appendix A.

Trachybasalt clast specimens typically display two well resolved component magnetizations (Figure 3a-b). A soft component is removed by ~15 mT (150 Oe) or 300°C. It is resolved in 13 clasts and has a consistent northwest and steep down in situ direction (D=310°, I=81°; α_{95}=22.5°, k=4.3; N=13), which is close to the present Earth's field direction and is likely a recent VRM.

A hard component resolved in 20 clasts has coercivities mainly greater than 30 mT and unblocking temperatures greater than 400°C. This stable, hard component of magnetization has similar demagnetization behaviour to that observed in specimens drawn from the underlying site 3 trachybasalt, and shows a large scatter of directions among the 20 clasts (Figure 4a). A statistical test of randomness (Watson, 1956; Irving, 1964) shows that the 20 scattered hard component directions pass the intraformational conglomerate test (i.e. the specimens' unit vector sum R=5.38 is less than the R_0=7.17 expected for 20 specimens at the 95% confidence level).

Plate 2. Blocky trachybasalt and rounded amygdaloidal (alkali) basalt clasts sampled from an intraformational tuff for the conglomerate test. Scale pen is 14 cm long.

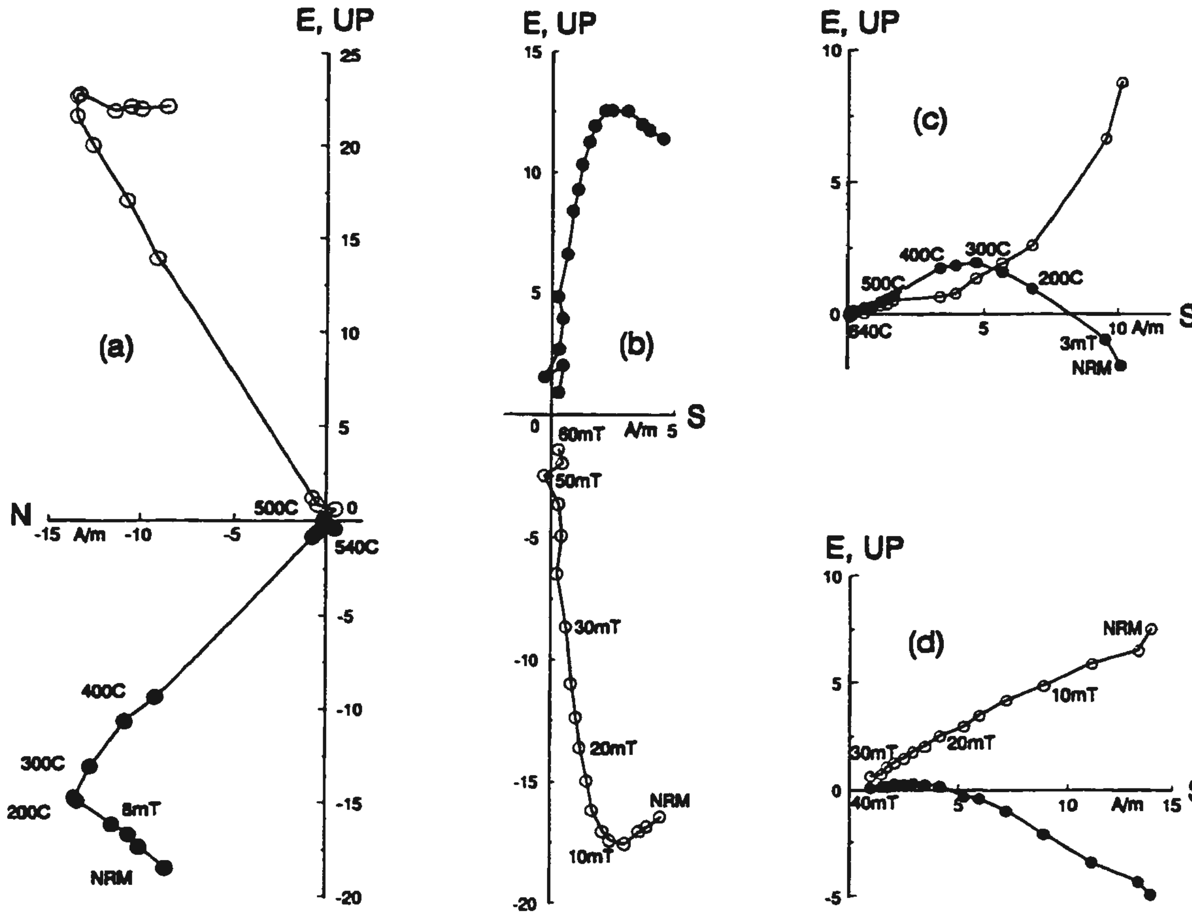

Figure 3. Orthogonal vector plots of thermal (a),(c) and AF (b),(d) demagnetization of representative samples from conglomerate test clasts: Trachybasalt clasts (a),(b); Amygdaloidal alkali basalt clasts (c),(d). Decay paths for each sample are projected in the UP-S (E-S) plane with closed (open) circles.

Amygdaloidal basalt clast specimens typically behave as shown in Figure 3c-d. A soft component is removed by demagnetization to ~25 mT or ~400°C. It is well resolved in all 15 clast specimens, and has a mean in situ direction (D=350°, I=83°; α_{95}=4.8°, k=64.9; N=15) close to the present Earth's field direction and is likely a recent VRM.

A hard component of magnetization is also present in 11 of the 15 amygdaloidal clast specimens, but is more difficult to resolve, since it begins to be removed at ~15 mT or ~300°C while much of the dominant soft component is still present. The amygdaloidal basalt clast hard component directions scatter loosely (Figure 4b), but are not statistically random (unit vector sum R=9.33, greater than R_0=5.28 expected for 11 specimens at the 95% confidence level). The hard remanence appears to be mostly overprinted, with a tilt-corrected mean direction of D=145; I=5.7° (α_{95}=20.0°, k=6.2; N=11).

Equal area stereoplots of hard component directions from trachybasalt and amygdaloidal basalt clasts are presented in Figure 4.

3.3 Primary remanence and evidence for an overprint

The positive conglomerate test (Figure 4a) proves that magnetite-borne remanence in trachybasalt with coercivities above 15 mT and unblocking temperatures above 300°C was acquired before the incorporation of the trachybasalt clasts into the intraformational tuff (Graham, 1949). Hence, the `A' component direction dates from the ca. 550 Ma age of the volcanics.

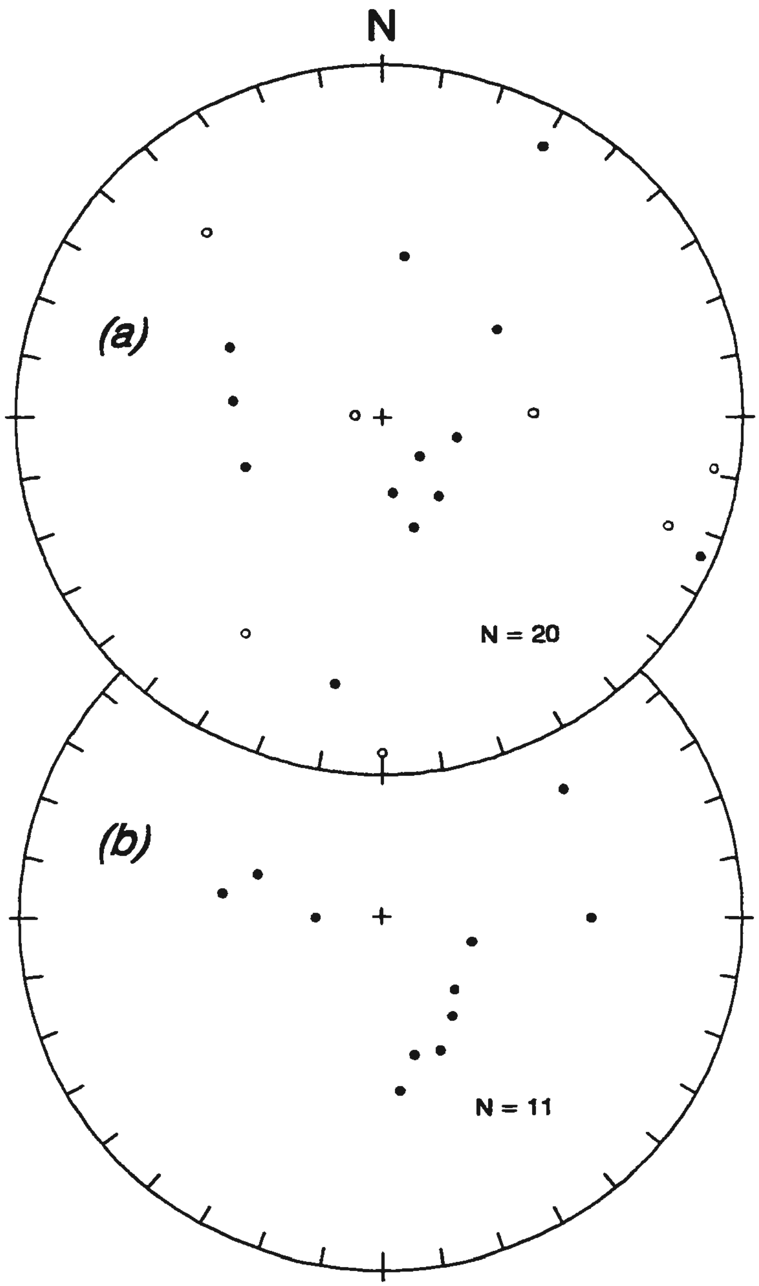

Figure 4. Equal area stereoplots showing the scatter of in-situ hard component directions for conglomerate tests based on (a) 20 trachybasalt clasts, and (b) 11 amygdaloidal basalt clasts. See text for details. Down (up) directions marked by closed (open) circles.

This is consistent with the zeolite facies metamorphism of the Skinner Cove volcanics which implies heating to less than 200°C (Liou et al., 1991; Beiersdorfer and Day, 1995). Even if applied for a million years, heating to 200°C should not have thermoviscously reset magnetite with unblocking temperatures above 300°C, according to single domain theory (Pulliah et al., 1975), whereas the `A' component mostly resides in magnetite with unblocking temperatures above 400°C. Any thermoviscous remagnetization with anomalously high unblocking temperatures (Middleton and Schmidt, 1982) should reside in soft multidomain magnetite (Dunlop et al., 1997) and should have been removed by the AF demagnetization to ~15 mT which preceded all thermal demagnetizations in this study (e.g Figure 3a,c).

The non-randomness of the amygdaloidal basalt clast hard component scatter (Figure 4b) is puzzling, in light of the positive conglomerate test using trachybasalt clasts with similar high coercivity and high unblocking temperature magnetite-borne remanence. The amygdaloidal basalt clasts appear to be overprinted by a high coercivity, high unblocking temperature remanence which cannot be a thermoviscous overprint for the reasons given above.

Amygdaloidal basalt clasts may carry a thermo-chemical overprint of high coercivity and high unblocking temperature, acquired through heating of the conglomerate during emplacement of the overlying flows. This best explains both the source of heating for the thermo-chemical process and the similarity of a partial overprint remanence direction to the `A' remanence direction of the surrounding flows. Although this direction is also similar to the present Earth's field direction, there is no known Tertiary thermal event hot enough to cause the overprint. A Taconic or Siluro-Devonian thermal event is possible, but likely would not have magnetized the rocks in a steep down direction.

The mechanism for the acquisition of a thermo-chemical overprint is uncertain, but may involve the following process. Although basaltic rocks usually crystallize with titanomagnetite of high titanium content, the titanomagnetite in subaerial and intrusive basaltic rocks usually oxidizes during initial cooling to a fine intergrowth of ilmenite and magnetite with Curie point near 580°C (Ade-Hall et al., 1971). However, in submarine basalts the titanomagnetite often remains unexsolved with a Curie point near 150°C (Ade-Hall et al., 1976). Subsequent burial beneath a lava pile can cause zeolite facies metamorphism which often alters the titanomagnetite to a ~580°C Curie point magnetite containing fine rutile granules (Ade-Hall et al., 1971).

This seems to have occurred to the conglomerate test amygdaloidal basalt clasts, except that less oxygen was available to the cores of the titanomagnetite grains, which exsolved ilmenite instead, rutile being mostly restricted to the margins of the grains (e.g Plate 1). That is, the amygdaloidal basalt clasts seem to have been incorporated into the conglomerate with unexsolved titanomagnetite of too low a Curie point for stable remanence. During burial by contemporaneous overlying flows, zeolite facies metamorphism occurred, causing titanomagnetite to exsolve ilmenite (in grain cores) and rutile (at grain margins and in cracks), raising the Curie point to 580°C and stably magnetizing the clasts in the same direction as the overlying flows. This may also have happened in the pillow basalt flow (site 4) which is the only `A' site sampled from an obviously submarine setting.

The likely contemporaneous origin of the overprint in amygdaloidal basalt clasts, and the absence of any overprint in the trachybasalt clasts indicates that the hard `A' component remanence recognized in flows and dykes of the Skinner Cove Formation is likely primary, acquired at ~550 Ma by thermoviscous and possibly in site 4, thermo-chemical mechanisms during the time of flow and conglomerate emplacement at ~550 Ma.

The hard `B' component remanence is found only in site 7 pillow basalt, the only site from the Wallace Brook member (Baker, 1979). It is similar to the `A' component in demagnetization characteristics, and may represent a reversal, although it is not strictly antiparallel to `A'. The hard `C' component remanence may be a Kiaman-type overprint acquired during post-folding orogenic activity, since it is found in samples drawn from the lowermost exposed units (sites 8, 15) in the structural slice and has an in situ south-southeast, shallow down direction.

Figure 5 shows a stereoplot of the 10 `A' sites and their mean. The tilt corrected southeast and down mean direction derived in Table 2 for the Skinner Cove Formation is D=144°, I=31.5°, with α_{95}=10.8° and precision parameter k=21.1. This result yields a palaeolatitude of 17.1°S +7.4°/-6.3°. Calculation of a mean pole and A_{95} from `A' site

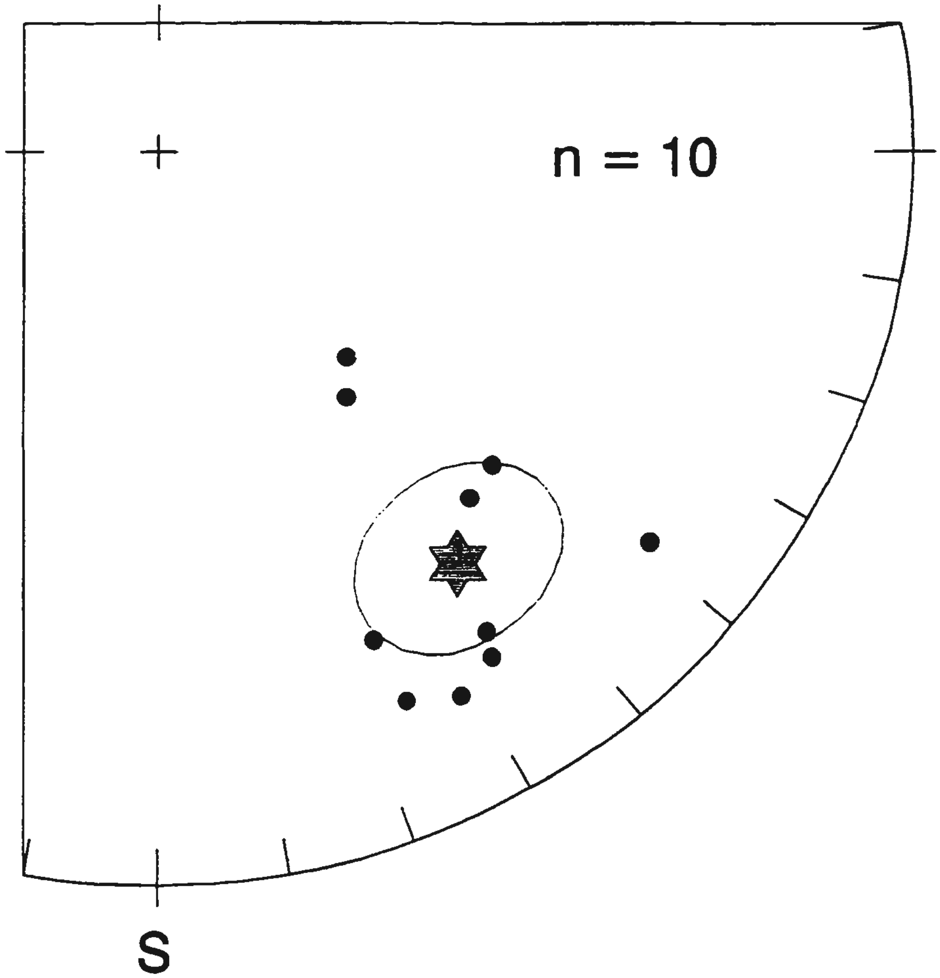

Figure 5. Equal area stereoplot of the ten tilt-corrected `A' component site mean directions (Table 2). The formation mean direction derived from them is D=144°, I=31.5°; α_{95}=10.8°, k=21.1. Down directions marked by closed circles.

virtual geomagnetic poles (VGPs) gives a palaeolatitude of 18.6°S ±9°. The latter will be used below for comparison with palaeolatitudes calculated from other published palaeopoles.

Chapter 4: Discussion

4.1 Relation to Laurentia

Although the Skinner Cove volcanics have been transported, their palaeolatitude should constrain Laurentia at ~550 Ma, since an original relation with Laurentia is implied by local structural associations as well as regional age and trace element geochemistry correlations with other Humber Zone units.

Within the Humber Arm Allochthon imbricate stack, units of the Skinner Cove Formation overlie Laurentian shelf slope sediments of the Humber Arm Supergroup, implying that the two were originally adjacent before their mid-Ordovician obduction. Within the Skinner Cove Formation, the lateral discontinuity of units, evidence for subaqueous eruption of some units and clastic indicators of locally steep palaeoslopes favour an oceanic volcanic setting, while the lack of continentally-derived sediments rules out a strictly continental rift setting. On the basis of these observations, Baker (1979) suggested that the Skinner Cove volcanics formed as an oceanic seamount near the margin of Laurentia.

Tectonic discrimination plots (e.g Meschede, 1986) using immobile elements Zr, Y, Ti, Nb indicate a within-plate setting for the Skinner Cove Formation alkali volcanism (Figure 6), either associated with continental rifting, or with a mantle plume. Titaniferous alkali basalts with similarly high Zr/Y, Nb/Y, and generally enriched LREE are found as

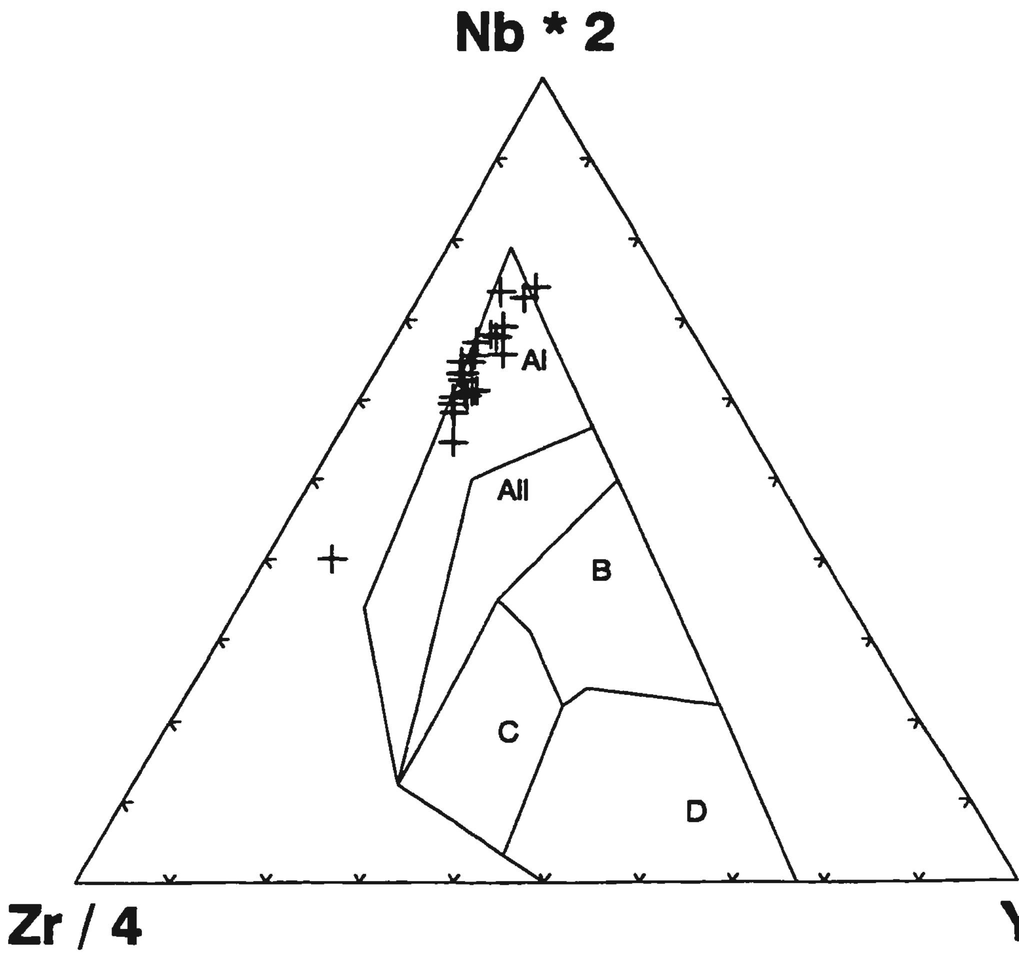

Figure 6. Tectonic discrimination plot (Meschede, 1986) using trace elements Zr, Y, and Nb concentrations. The 23 alkali basalt samples analysed by Baker (1979) from the Skinner Cove volcanics plot in the within-plate alkali field, reflecting their strongly alkali character. AI, AII fields - Within plate alkali; AII, C fields - Within plate tholeiite; B, D fields - Mid Ocean Ridge Basalts; C, D fields - Volcanic arc basalt.

allochthonous units in the Chaudiere River Nappe and Drummondville Olistostrome (Olive et al., 1997), as well as the Ste-Anne River Nappe (Camire et al., 1995), and are interpreted to be lateral equivalents of the Tibbit Hill metavolcanics (St-Julien and Hubert, 1975). These units are thought to have a Laurentia-related seamount origin similar to that of the Skinner Cove volcanics (see Fyffe and Swidden, 1991).

The Tibbit Hill metavolcanics have been dated at 554 +4/-2 Ma (U-Pb zircon. Kumarapeli et al., 1989), and have a confirmed continental setting in the Green Mountains of Vermont, where they rest on Grenville basement (St-Julien and Hubert, 1975). Similar aged magmatism is present in the Humber Zone of western Newfoundland, where the Lady Slipper Pluton occurs in association with allochthonous Grenvillian basement gneiss and unconformably overlying passive margin sediments. A tonalitic gneiss of the pluton was dated at 555 +3/-5 Ma (U-Pb zircon; Cawood et al., 1996), with a ~1500 Ma inherited component interpreted to come from the local Grenville basement of the Laurentian margin. The Lady Slipper Pluton likely represents the margin-intrusive equivalent of the ca. 550 Ma Skinner Cove Formation and other margin-edge Humber Zone alkali volcanics (Cawood et al., submitted).

Figure 7 shows the distribution of selected latest Neoproterozoic failed rift grabens and magmatic features of the northeast Appalachians. Similarity of age, trace element geochemistry and tectonic setting favours a common, regional origin for the Tibbit Hill, Quebec Humber Zone alkali volcanics, Lady Slipper Pluton and Skinner Cove volcanics.

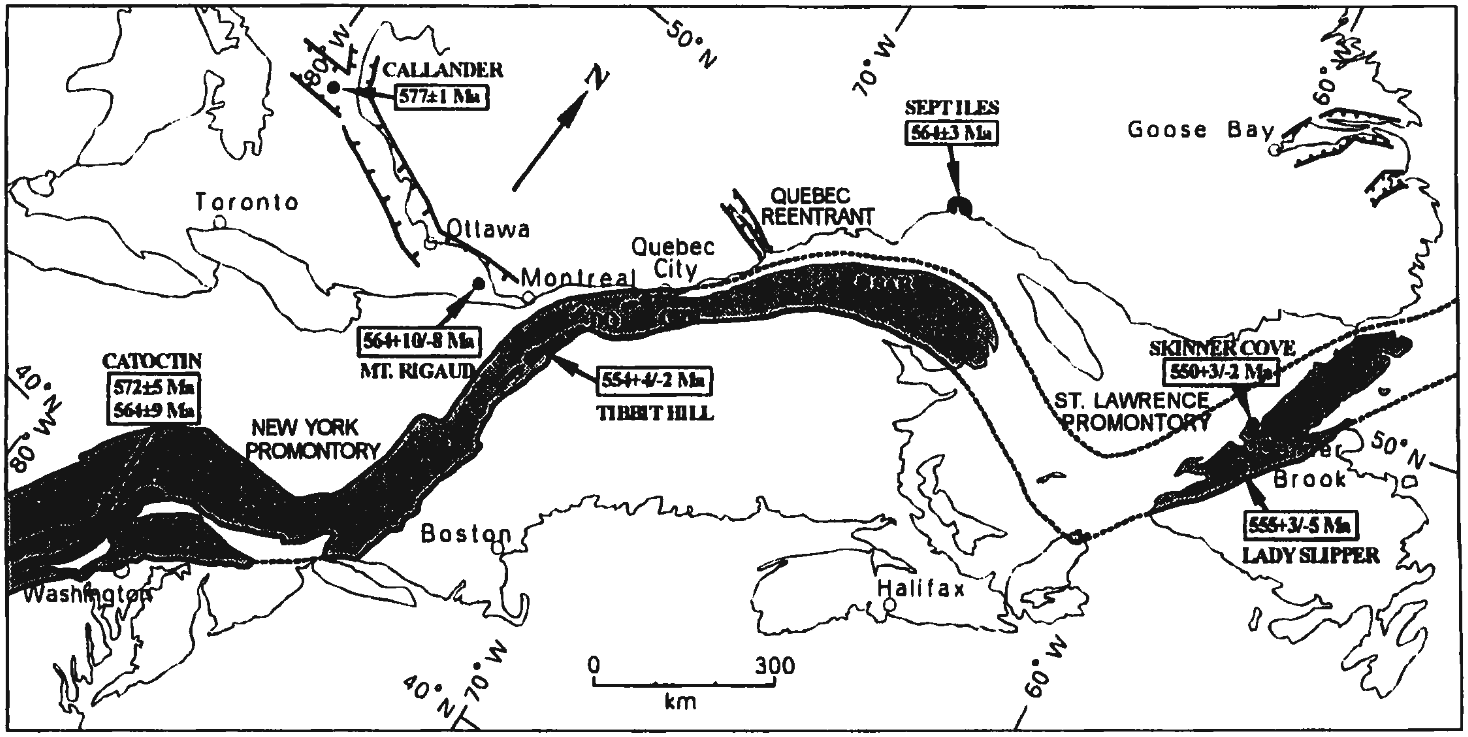

Figure 7. Distribution of selected rift-related and magmatic features along the incipient latest Neoproterozoic Iapetan margin of Laurentia. Deformed, variably transported units of the margin are marked by the Humber Zone (outlined in stipple). Units with ages are dated by the U-Pb zircon method (references in text). Failed rift graben (Kumarapeli, 1993; Murthy et al., 1992) are outlined within spiked line pairs. Abbreviations for Quebec Humber Zone alkali volcanics (Camire et al., 1995) are: CRN - Chaudierre River Nappe; DO - Drummondville Olistostrome; SAR - St. Anne River Nappe.

4.2 Late Neoproterozoic palaeomagnetism of Laurentia

The 18.6°S ±9° palaeolatitude derived from site VGPs for the Skinner Cove Formation constrains the Iapetus margin of Laurentia, implying that Laurentia occupied an equatorial position at ~550 Ma. Figure 8 presents the palaeolatitudinal drift history of the Newfoundland segment of the Laurentian margin, calculated for published Laurentian palaeopoles from 580 Ma to 510 Ma which have well-constrained magnetization ages (Table 3).

Recently tabulated Laurentian poles of ca. 550 Ma age (Meert et al., 1994; MacNiociall and Smethurst, 1994; Torsvik et al., 1996) typically have poor control on the age of magnetization. For example, the Buckingham volcanics of Quebec (Dankers and Lapointe, 1981) have yielded only an imprecise whole-rock K-Ar age of 573 ±32 Ma (Lafleur and Hogarth, 1981). The Long Range Dykes of Labrador have a K-Ar (biotite) date of 553 ±22 Ma (Wanless et al., 1970), which is interpreted as the age of a remagnetization event giving a low-inclination remanence direction (Meert et al., 1994). However, a baked contact test suggests the low-inclination remanence corresponds to the crystallization age of the dykes (Murthy et al., 1992) given by U-Pb zircon and baddelyite dates of 615 ±2 Ma (Kamo et al., 1989) and 614 +6/-4 Ma (Kamo and Gower, 1994). The Double Mer Formation red beds of Labrador (Murthy et al., 1992) have a low-inclination remanence like the Long Range Dykes, but poor age control.

The Buckingham volcanics, Long Range Dykes, and Double Mer Formation poles

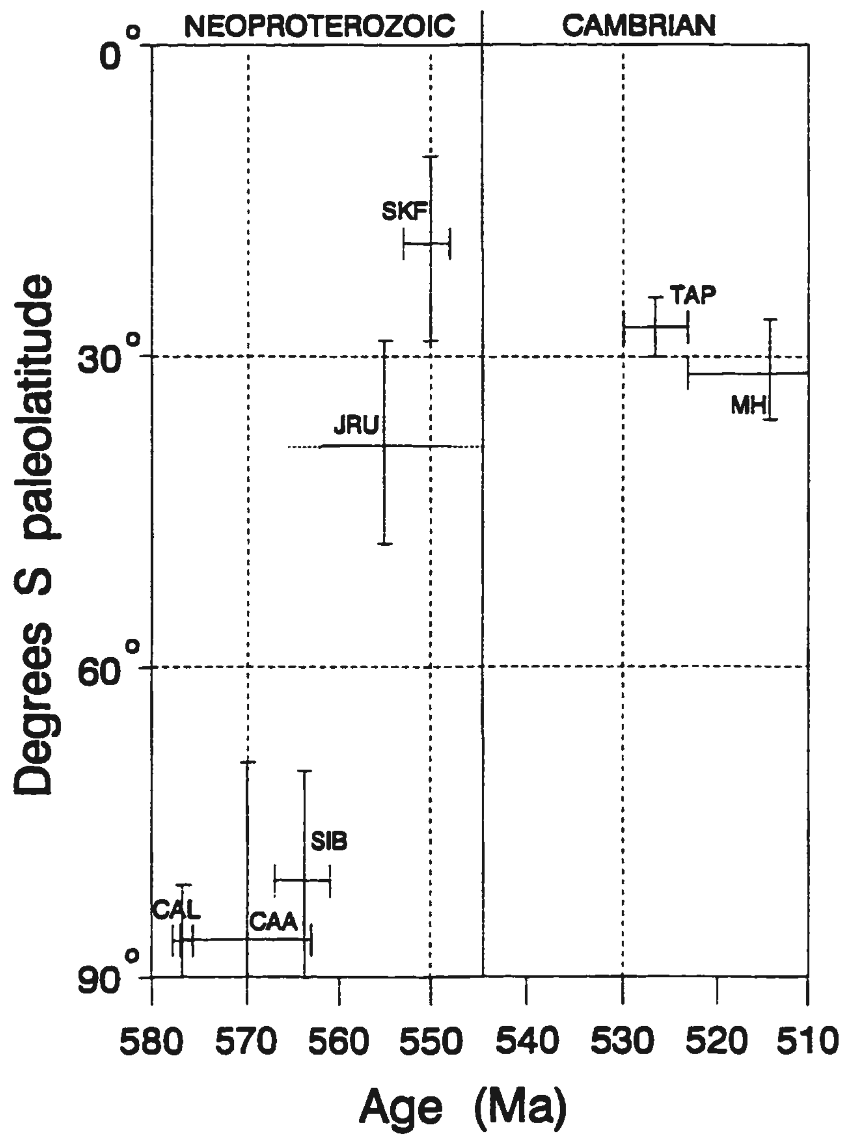

Figure 8. Palaeolatitude plot of the west Newfoundland segment of Laurentia's Iapetan margin calculated from late Neoproterozoic to Cambrian Laurentian palaeopoles (Table 3). Abbreviations are: CAA -Catoctin `A' component; CAL -Callander Complex; JRU -Johnnie Rainstorm Fm, Unrotated; MH -Moores Hollow; SIB -Sept Iles `B' component; SKF -Skinner Cove Formation; TAP -Tapeats Sandstone.

Table 3: Palaeolatitude of the west Newfoundland Iapetan margin between 580 Ma and 510 Ma calculated from published poles for Laurentia.*

Unit	Age (Ma)	Palaeopole**	A_{95}	K	Palaeolatitude
Moore Hollow Gp., TX	505-523 bio	1°S 163°E	5°	94	31° ± 5° S
Tapeats SS, TX	~525 bio	5°N 158°E	3°		27° ± 3° S
Skinner Cove Fm, Nfld	550 +3/-2 U-Pb	(15°N 157°E)ᵃ	9°	31	19° ± 9° S
Johnnie Rainstorm, NV	~555 ?	10°S 162°E	~10°	-	38° ± 10°S
Sept Iles 'B,' Quebec	564 ±3 U-Pb	44°S 135°E	10°	16	80° ± 10°S
Catoctin Basalts 'A,' VA	564 ±9 U-Pb	43°S 118°E	17°	17	86° ± 17°S
Callander Complex, ONT	577 ±1 U-Pb	46°S 121°E	6°	25	87° ± 6° S

*Palaeolatitude calculated for present-day Skinner Cove location 49.5°N, 302°E (see text).
**North palaeopole calculated as the mean of site VGPs (Virtual Geomagnetic Poles), with A_{95} being the circle of 95% confidence about the mean pole direction, and K is the precision parameter.
ᵃSkinner Cove Fm pole is a proxy for Laurentia, but does not account for possible net tectonic rotation relative to the craton.
Ages obtained from biostratigraphic (bio) or radiometric (U-Pb) methods.

are excluded from Figure 8, since their uncertain age of magnetization makes them of only limited support for the discussion below. However, a regional (thermal?) remagnetization event at ~555 Ma most plausibly accounts for the similarity of low-inclination directions between these three studies, and may be related to the regional activity which produced the ca. 555-550 Ma Tibbit Hill, Skinner Cove, and Lady Slipper magmatism.

Sandstones of the dual-polarity Johnnie Formation (Rainstorm member) of Nevada are estimated to be ~10 Ma older than the Precambrian-Cambrian boundary (cf. Meert et al., 1994), giving an age of ~555 Ma using the timescale of Tucker and McKerrow (1995). The (unrotated) pole derived for the Johnnie Formation (van Alstine and Gillett, 1979) implies a low southerly palaeolatitudinal position for Laurentia at roughly 555 Ma (Figure 8), which supports the ~550 Ma Skinner Cove Formation result. An equatorial to low southerly palaeolatitudinal position for Laurentia is also supported by early to mid Cambrian poles (Table 3, and Elston and Bressler, 1977; Farr and Gose, 1991) , implying that Laurentia remained at low palaeolatitudes from ~550 Ma onwards through the Cambrian.

The Callander Complex of Ontario is well-constrained in age (577 $\pm$ 1, U-Pb zircon; Kamo et al., 1995) and carries a primary remanence, demonstrated by a positive baked contact test (Symons and Chiasson, 1991). Comparison of its well-constrained palaeolatitude estimate for the Laurentian margin (87°$\pm$6°S) with the 18.6°$\pm$9°S Skinner Cove Formation result for ~550 Ma implies a northward latitudinal drift rate for Laurentia of ~28 cm/yr (68°/27 Ma), with an uncertainty of ~± 10 cm/yr, if full advantage is taken of the 95% confidence ranges (Figure 8).

An even higher apparent drift rate is implied by palaeopoles for the Catoctin volcanics (Meert et al., 1994) and the Sept Iles anorthosite (Tanczyk et al., 1987). For the Catoctin basalts, U-Pb ages (572 ±5 Ma and 564 ±9 Ma; Aleinikoff et al., 1995) and a remanence that predates Taconic folding (Meert et al, 1994) imply that the Laurentian margin remained at high southerly palaeolatitudes of ~86°S as late as ~570 Ma. The Sept Iles anorthosite `B' component (Tanczyk et al., 1987) is less constrained in magnetization age, there being no proof of primary remanence. However, if the `B' pole is primary, as reinterpreted by Symons and Chiasson (1991), then Laurentia started its rapid northward drift by 564 ±3 Ma (U-Pb zircon, Higgins and van Breemen, in press).

Rapid northward apparent drift appears to have begun within ~7 Ma of 570 Ma, based on the results from the Callander Complex, the Catoctin volcanics and the Sept Iles Anorthosite. A latitudinal drift rate of ~34 ±15 cm/yr for Laurentia seems to be the most reasonable estimate which can be derived from existing late Neoproterozoic Laurentian palaeomagnetic data, calculated for ~68° of drift during the period between ~570 Ma and ~550 Ma. A rapid northward drift of Laurentia from high southerly palaeolatitudes to the equator between 580 Ma and 540 Ma has been proposed (Meert et al., 1993), with interpolated minimum (latitudinal) drift rates as high as 23 cm/yr (Gurnis and Torsvik, 1994). The Skinner Cove Formation result provides support for a high latitudinal drift rate and constrains Laurentia to have reached an equatorial position by ~550 Ma.

Kirschvink and others (1997) recently presented evidence for a major true polar wander (TPW) event of some 90° between ~530 Ma and ~515 Ma to account for much of the inferred rapid apparent motions of Laurentia and an assembled Gondwana, as well as apparent rotations of Siberia and Australia. Results from the Skinner Cove volcanics do not support a mid-Cambrian major TPW event since this would require Laurentia to reside near the south pole until ~530 Ma instead of approaching the equator by ~550 Ma as implied primarily by this study and the Johnnie Rainstorm result. A TPW contribution to apparently rapid latitudinal movements of Laurentia (and Baltica; Gurnis and Torsvik, 1994) is possible (Evans, 1998), but difficult to evaluate since there is a general lack of late Neoproterozoic palaeomagnetic data from other cratons.

4.3 Implications for timing of Iapetus opening

Alkali magmatism of ca. 555-550 Ma age along the Laurentian margin, followed by transgressive sedimentation at the time of the Precambrian-Cambrian boundary (Bond et al., 1984; Williams and Hiscott, 1987; Thomas, 1991) are together interpreted to mark the final stage of rifting between Laurentia and the proto-Andean margin of Gondwana along Rio de la Plata-Amazonia, signalling the birth of the Iapetus Ocean at ~545 Ma (e.g. Dalziel, 1997). The Laurentia-Amazonia-Rio de la Plata association is attractive because it preserves the global budget of late Neoproterozoic rifted margins proposed by Bond and others (1984). An ancestral association of Laurentia with these South American cratons is suggested by a geometrical fit of the reconstructed Labrador-Scotland promontory of Laurentia with the Arica embayment of South America (Dalziel, 1992), and supported by similarities in age of Grenvillian-aged basement (Dalziel et al., 1994; Wasteneys et al., 1995), and possibly by the similarity of the late Neoproterozoic Puncoviscana Formation of northwest Argentina with rift deposits along Laurentia's Iapetan margin (Dalziel et al., 1994).

However, the geological interpretation for a rifting relation between these cratons at the Precambrian-Cambrian boundary is not consistent with ~550 Ma palaeomagnetic data (e.g., Torsvik et al., 1996; this study) which imply a large separation of up to ~75° between Laurentia and Gondwana's proto-Andean margin at that time. Gondwanan ca. 550 Ma palaeopoles from the Mozambique belt (Congo), India and Australia (summarized in Meert and Van der Voo, 1997) would place Laurentia astride the south pole instead of near the equator, if a ca. 550 Ma rifting relation with the proto-Andean margin (Dalziel, 1997) is maintained.

The discussion to follow will explore possibilities for reconciling the late Neoproterozoic palaeomagnetism with the geology, with the aim of proposing a palaeogeographic model for the much-disputed period between ca. 580 Ma and ca. 540 Ma.

4.3.1 Palaeomagnetic constraints

While no palaeomagnetic data for Gondwanan cratons during the critical late Neoproterozoic period are available, several poles of ~550 Ma age are published.

The position of Gondwana at ~550 Ma may be constrained by the Sinyai Dolerite dike of Kenya, which intrudes gneisses of the Mozambique belt in Kenya as a solitary, 150 m wide dyke (Meert and Van der Voo, 1996). It has a remanence that exhibits dual polarities but is interpreted to be a remagnetization, likely acquired at the dike's $^{40}Ar/^{39}Ar$ metamorphic biotite closure age of 547 $\pm$4 Ma. No tilt correction was possible for the result, although local tectonic rotation seems unlikely (Meert and Van der Voo, 1996). The dual polarity of the dyke remanence is considered to indicate that secular variation was likely averaged out over the time of remanence acquisition during the metamorphic cooling of the dyke.

The Sinyai dyke pole is an uncertain constraint on the ~550 Ma position of the Congo craton of Gondwana because the dyke's age of remanence acquisition may not be the biotite closure age, the dyke's palaeomagnetic data may require tilt correction, and the dyke's relation to the Congo craton may have changed since the remanence was acquired. Nevertheless, the similarity of the Sinyai Dyke pole with other ca. 550 Ma Gondwana paleopoles from India (McElhinny et al., 1978) and Australia (summarized in Li and Powell, 1993) support the interpretation of Meert and Van der Voo (1996).

The ca. 550 Ma Gondwanan poles only represent the Rio de la Plata and Amazonia cratons if no significant separations remained between constituent Gondwanan cratons at 550 Ma. Wide separations between Gondwanan cratons appear to be unlikely across basins that are interpreted to be narrow, intracratonic or closed by that time (Unrug, 1996; Trompette, 1997). Assuming an assembled West Gondwana and a Dalziel (1997) reconstruction, the proto-Andean margin of Gondwana and Laurentia would occupy a position at the Sinyai Dyke south pole, instead of the equatorial position implied by the Skinner Cove Formation paleolatitude. The ~550 Ma Gondwanan poles from India and Australia have poorly constrained age (±30 Ma and ±15 Ma, respectively), but still require the proto-Andean margin to reside at high southerly palaeolatitudes, some 60° from Laurentia's Iapetan margin as constrained by the ~550 Ma Skinner Cove result.

Other Gondwanan poles from the Cambrian imply the movement of Amazonia and West Africa cratons across the south pole during the Cambrian (Meert and Van der Voo, 1997), lending support to the polar position of the proto-Andean margin implied by the ca. 550 poles. If the proto-Andean margin and cratons of a nearly assembled Gondwana had travelled rapidly north with Laurentia during the late Neoproterozoic to rift from the its Iapetan margin at low southerly palaeolatitudes at ~550 Ma, they must then have drifted rapidly south to occupy the south polar position implied by ca. 530-510 Ma poles from Gondwana. A continued south polar position for the proto-Andean margin throughout the late Neoproterozoic into the Cambrian, as implied by the poorly constrained ~550 Ma Gondwanan poles, is the most plausible alternative. For the remainder of this discussion the ca. 550 Ma Gondwanan palaeopoles are assumed to be approximately correct in age, representing an assembled or nearly assembled Gondwana supercontinent.

The Laurentian poles have been discussed above, but a few remarks on the basis of their reliability are warranted: The Callander Complex (Symons and Chiasson, 1991) provides a well determined near south polar position for Laurentia at ~577 Ma, along with an adjacent proto-Andean margin of Gondwana, if the Laurentia-Amazonia-Rio de la Plata association and post 570 Ma timing of rifting is correct. The Callander Complex result is broadly supported by similar, but less well constrained high palaeolatitude results from the Catoctin basalts (Meert et al., 1994) and the Sept Iles Anorthosite (Tanczyk et al., 1987).

This study provides results from the ~550 Ma Skinner Cove volcanics, which are not part of the Laurentian craton. If their above argued original relation with the Laurentian margin is correct, then the Skinner Cove volcanics constrain the Iapetan margin of Laurentia to low southerly palaeolatitudes at ~550 Ma. Sandstones of the ~555 Ma Johnnie Formation, Rainstorm member in Nevada also provide a low southerly palaeolatitude position for Laurentia (Figure 8), and are part of the craton, but may have been subject to tectonic rotation (van Alstine and Gillett, 1979). However, like the Skinner Cove volcanics result, a possible tectonic rotation of the Johnnie Rainstorm pole would not alter the latitudinal separation between Laurentia and its palaeopole, only Laurentia's orientation at low latitude would vary. In other words, net tectonic rotation about a vertical axis of the locally tilt-corrected palaeomagnetically sampled units does not alter the unit's distance to its palaeopole. Hence, no net rotation of the Skinner Cove volcanics or Johnnie Rainstorm units would allow Laurentia to be closer to the south pole and the proto-Andean margin of Gondwana at ~550 Ma.

Other ca. 550 Ma cratonic poles for Laurentia (e.g. tabulated in Torsvik et al., 1996) are similar to the Johnnie Rainstorm result, but have ages of magnetization that are less well constrained or tested.

If an ancestral relation between Laurentia and the proto-Andean margin of Gondwana (Bond et al., 1984; Dalziel, 1997) is correct, then the most plausible interpretation of the palaeomagnetic data from Laurentia between 580 Ma and 550 Ma (Figure 8) and ca. 550 Ma Gondwana is that the apparent rapid northward movement of Laurentia away from a south polar proto-Andean margin of Gondwana represents the opening of the Iapetus Ocean between ~570 Ma and ~550 Ma.

4.3.2 Geological constraints

Evidence for rifting along the Appalachian margin of Laurentia prior to the opening of the Iapetus extends back to the mid-Neoproterozoic, involving the emplacement of ca. 750 Ma granitoids, rhyolites and tholeiitic continental flood basalts in units such as the Mt. Rogers and Grandfather Mountain Formations of the southern Appalachians (Aleinikoff et al., 1995). This early rifting activity is of the same age as rifting along Laurentia's proto-Pacific margin (Moores, 1991; Hoffman, 1991; Dalziel, 1991, 1997), but apparently did not proceed to completion, as there is little evidence of ca. 750 Ma plutonic or rifting activity in the northeast Appalachians (Kumarapeli, 1993; Aleinikoff et al., 1995).

Initiation of the continental extension which led to the opening of the Iapetus is first dated by the ~615 Ma Long Range Dykes and ~590 Ma Grenville Dyke swarm (Kumarapeli, 1993). Much of the development of the Ottawa-Bonnechere rift graben and related alkaline intrusions is interpreted to have occurred between ~590 Ma and the ~570 Ma ages of most of the alkaline intrusions (Figure 7), such as the ~577 Ma Callander Complex and the ~564 Ma Sept Iles Anorthosite (Kumarapeli, 1993; Higgins and van Breemen, in press).

Alkali volcanic and plutonic units (e.g., the ~554 Ma Tibbit Hill metavolcanics and ~555 Ma Lady Slipper Pluton) have been interpreted to represent the last stage of rifting prior to initial sea-floor spreading of the Iapetus (Kumarapeli, 1993; Cawood et al., 1996). This is at variance with the palaeomagnetic evidence which suggests that sea-floor spreading began at ~570 Ma. Transgressive sedimentation of latest Neoproterozoic-early Cambrian age is found in passive margin sections along the Appalachians (Williams and Hiscott, 1987; Simpson and Sundberg, 1987; St-Julien and Hubert, 1975; Cawood et al., 1996), and has been interpreted to represent post-rift margin thermal subsidence that marks a transition from rift to drift. This implies that final separation of Laurentia from its conjugate margin occurred near the time of the Precambrian-Cambrian boundary (Williams and Hiscott, 1987; Thomas, 1991), which is also at variance with palaeomagnetic evidence suggesting this final separation occurred at ~570 Ma.

Cambro-Ordovician passive margin strata from Newfoundland and Virginia have also been used in subsidence curve analysis, or `back-stripping,' in which lithification and loading due to overlying sediments is calculated and removed from the section to arrive at an estimate of the thickness of sediment cover, and therefore the subsidence of the margin by comparison with model thermal subsidence curves (McKenzie, 1978). Subsidence curve analysis of Laurentia's Iapetan margin by best visual fit of the calculated curves with modelled subsidence yields an estimated initiation of thermal subsidence at the time of Precambrian-Cambrian boundary (Bond et al., 1984). These analyses are now revised on the basis of biostratigraphic dating of units in the new Cambrian timescale (e.g., Tucker and McKerrow, 1995) to give an age of 550 Ma for the initiation of thermal subsidence, with an age of at most 600 Ma possible, assuming maximum delithification factors in the restored section calculation (Bond, 1997).

Units of the proposed conjugate margin to Laurentia in South America include upper Precambrian to lower Cambrian alkali volcanics of the Puncoviscana Formation in northwest Argentina (Dalla Salda et al., 1992), related granitoids with tholeiitic affinities (Rapela et al., 1990), and a transgressive section (Acenolaza and Durand, 1986). To the north, bordering the southern margin of the Amazonia craton are late Neoproterozoic to early Cambrian sections of the Paraguay and Tucavaca Belts, in which Vendian glaciogenic and turbiditic rocks are overlain by limestones which contain Ediacaran-like fauna indicative of a late Vendian (570-545 Ma) age. The upper part of the Paraguay section consists of poorly sorted, cross-bedded sandstones overlain by red shales, siltstone and arkoses (Pimentel et al., 1996). Subsidence analysis of a section from northwest Argentina (Bond et al., 1984) yields a curve similar to those of the Appalachian margin of Laurentia, implying the onset of thermal subsidence was at the Precambrian-Cambrian boundary.

Information from the proto-Andean margin tends as yet to be less well constrained in age, making comparisons with its proposed conjugate Laurentian margin unclear. Another complication stems from the long-standing convergent aspect of the Andean margin, in which continental subduction arc plutonism, metamorphism, terrane accretion and multiple deformation events act to make analysis of late Neoproterozoic to early Cambrian units more difficult (Dalla Salda et al., 1992).

The simplest interpretation of geological evidence from Laurentia and the proto-Andean margin of Amazonia and Rio de la Plata is that rifting occurred between them at the Precambrian-Cambrian boundary, with subsequent early Cambrian transgressive sedimentation due to thermal subsidence of the rifted margins (e.g Dalziel, 1997). The following section discusses an alternative interpretation of the geologic data that is consistent with the palaeomagnetically inferred ~570 Ma birth of the Iapetus.

4.3.3 Is a ca. 570 Ma birth of Iapetus compatible with the geology?

The timing of Laurentian magmatic and structural events, interpreted to culminate in rifting at ~550-545 Ma (Kumarapeli, 1993; Dalziel, 1997; Cawood et al., submitted), is also consistent with rifting at ~570 Ma. Large volume Catoctin tholeiitic flood basalt and rhyolitic volcanism at ~570 Ma (Burton et al., 1995) may mark the final breakup of Laurentia from its conjugate margin, while ca. 555-550 alkali magmatism of the Laurentian margin can be interpreted as post-rifting activity, occurring as seamounts and intrusions in a manner analogous to Atlantic passive-margin alkali magmatism during the early Cretaceous (Jansa and Pe-Piper, 1985; Oyarzun et al., 1997).

Intersections of major Atlantic oceanic transforms with the North American margin seem to have controlled the location of passive margin alkali seamounts and volcanics (Jansa and Pe-Piper, 1985). A similar controlling mechanism has been suggested for the formation of Humber Zone alkali volcanics in Quebec (Kumarapeli et al., 1988), and could also account for the Skinner Cove volcanics and the margin-intrusive Lady Slipper Pluton. A relation between the promontories and embayments of margins with early transform development is recognized for the modern-day Atlantic, and for the formation of Iapetan transforms with respect to the sinuous Laurentian margin (Stockmal et al., 1987). Opening of the Iapetus at ~570 Ma in Quebec and west Newfoundland may have involved transform development in connection with both the Ottawa-Bonnechere failed rift arm (Kumarapeli, 1993) and with the abrupt bend in the margin at the tip of the St.

Lawrence promontory (Stockmal et al., 1987), thus controlling the later occurrence of alkali magmatism along the Quebec reentrant and St. Lawrence promontory (Figure 7).

Stratigraphic evidence for widespread transgression of the Laurentian margin at ~540 Ma (Thomas, 1991; Cawood et al., 1996) that is interpreted to represent margin subsidence recording a rift-drift transition may have a viable alternative interpretation as well. The first drift sedimentation is recognized at the base of early Cambrian transgressive sections which overlap sediment-filled rift grabens and rift volcanics (Thomas, 1991; Cawood et al., submitted). The nature of the contact between the onlapping transgressive sediments (e.g., Chilhowee Formation, Bradore Formation) and underlying strata is generally uncertain (Thomas, 1991; Simpson and Sundberg, 1987), and in several locations appears to represent a hiatus in deposition (e.g. Cawood et al., submitted), or an erosional surface (e.g. Burton et al, 1995). Transgressive drift sedimentation after a time break is consistent with a post-breakup unconformity and margin subsidence following a rift-drift transition at ~540 Ma, but is also consistent with a longer hiatus in sedimentation following rifting and breakup at ~570 Ma. Early Cambrian transgressive sedimentation may not necessarily reflect the rift-drift transition of the Laurentian margin if anomalous uplift of the margin occurred during the birth of the Iapetus.

Analyses of tectonic subsidence curves from Cambrian to Devonian passive margin sediments indicate that the initiation of Laurentian margin subsidence (the start of Iapetus opening) occurred at ~525 Ma (Bond, 1997). The analyses are based on comparison with kinematic models (McKenzie, 1978; Jarvis and McKenzie, 1980) of thermally-controlled margin subsidence following various degrees of pure shear (uniform) lithospheric extension and thinning during rifting. Uniform stretching models have been successfully compared with observed degrees of extension and sedimentation in modern intracratonic basins and continental margins (e.g Barton and Wood, 1984; Roydon and Keen, 1981). However, margin subsidence modelling that involved significant melt generation during rifting (Bown, 1994; Buck, 1986; Keen, 1986) suggests alternative margin subsidence curves. Indeed, deep borehole data from present-day continental margins indicate that large deviations from post-rift kinematically modelled subsidence can occur, producing a relative uplift of several hundred metres, and delaying first sedimentation by ~10-30 m.y. (e.g Heller et al., 1982).

Anomalous margin subsidence appears to occur in connection with volcanic-type margins (Eldholm et al., 1995), in which the syn-rift and post-rift development of the margin is substantially modified by large-scale magmatic activity. White and McKenzie (1989) attribute the magmatism of volcanic margins to anomalously high upper mantle temperature due to the impact of a mantle plume, leading to much greater melt generation during decompression melting of the asthenospheric mantle underlying the continental rift. Modelling which involves rift-initiated asthenospheric circulation during lithospheric extension (Keen and Boutilier, 1995) also provides a mechanism for producing large volumes of decompression melting and anomalous margin subsidence, without requiring elevated upper mantle temperatures or the involvement of a mantle plume.

In the uniform stretching models of Bown and White (1995), the effect of syn-rift melt production on margin subsidence is related to initially elevated asthenospheric mantle temperatures (modelled for 100°C and 200°C in excess of the upper mantle nominal ~1300°C temperature) brought about by mantle plume involvement in rifting. In the cases of enhanced asthenospheric melt production, the production of a more buoyant depleted mantle and the magmatic addition (underplating) of heated mafic material to lower extended crust results in buoyant support of the rifted margin, slowing, and in some cases reversing the extensional subsidence of the attenuated crust during final stages of rifting (Bown and White, 1995). Post-rifting margin thermal subsidence curves for all elevated asthenospheric mantle temperature cases mimic the form of the nominal 1300°C curves used in subsidence analysis, but are displaced upwards by up to several kilometres, reflecting the slowing or negation of major syn-rift extensional subsidence due to the addition of buoyant crustal material and support from the underlying depleted asthenospheric mantle.

For a subsiding margin this could mean a delay in the onset of transgressive sedimentation compared with that implied by curves for a 'normal' rifted margin. In other words, a freshly rifted volcanic margin may ride several hundred meters to several kilometres higher at the rift-drift transition than would a normal rifted margin, such that subsidence-related transgressive sedimentation atop continental rift grabens and volcanics would be delayed until the volcanic margin had subsided to the eustatic sea level over some tens of millions of years.

Local small-scale circulation of the lithospheric mantle and the asthenosphere below developing rifts may similarly account for localized decompression melting of asthenospheric mantle, and the development of a volcanic margin and anomalous margin subsidence (Keen and Boutilier, 1995). In these models, vigourous rift-initiated circulation appears to require steep lateral thermal gradients in the lithospheric mantle, best developed across a narrow rift (less than 200 km wide), with a narrow transition from unextended to extended continental crust, and with mantle material of comparatively low-viscosity. Continued local mantle circulation under the rifted margin following breakup may continue to provide heat to the margin, resulting in its delayed post-rift subsidence. While continent-ocean lithosphere transitions may not provide sufficient conditions for a continued local mantle convection following final rifting (Keen and Boutilier, 1995), the modelled convection-related delay in post rift subsidence may apply to failed rift arms of the Iapetus. Transgressive sections in Vermont, Quebec, west Newfoundland and northwest Argentina may have been influenced by anomalously delayed subsidence in relation to failed rift arms (Figure 7 and Dalziel, 1994), if conditions for vigourous rift-initiated local mantle circulation prevailed.

The inferred maximum possible age of breakup for Iapetan transgressive sections from Laurentia and Rio de la Plata would be ~570 Ma if syn-rift uplift of the margin displaced first drift sedimentation by 20-30 m.y. Rifted margin buoyancy related to syn-rift melt emplacement would likely involve a ~200-600 m reduction in extensional syn-rift subsidence in order to account for a 20-30 m.y. delay in first transgressive sedimentation, based on melt-modified margin subsidence models (Bown and White, 1995; Keen and Boutilier, 1995), and observations of perturbations in margin subsidence history from present day volcanic margins (e.g. Heller et al., 1982).

A delay in the recording of drift transgressive sedimentation on a volcanic margin would result in a flatter subsidence curve, best fitted to the latter portion of model subsidence curves since the sedimentation would be initiated after much of the uplifted margin's exponentially decaying thermal subsidence had taken place. Tectonic subsidence curves for the Iapetus margin of Laurentia between New York and Greenland are recognized to be surprisingly flat (Bond, 1997), perhaps indicating a delay in the recording of drift sedimentation.

While a rift-drift transition at ~540 Ma is the simplest interpretation of geological data from Laurentia, an alternative interpretation involving initial Iapetan opening at ~570 Ma is also feasible, if the development of a volcanic-type margin (Eldholm et al., 1995) and its likely anomalous subsidence is invoked to account for a ~20-30 m.y. delay in first drift sedimentation. Did rifting to form the Iapetus involve the development of conjugate volcanic-type margins with anomalous margin subsidence? How might this be recognized in the preserved rock record?

Present-day volcanic margins are identified by a number of features related to their extensive magmatism, including 1) onshore rift-setting continental flood basalts; 2) voluminous extrusive basaltic complexes erupted in shallow water or subaerially atop crust of the continent-ocean transition, with intrusive counterparts; 3) sills and low-angle dykes in pre-opening sediments cratonward of the continent-ocean transitional crust; 4) volcanic vents and a regional tephra horizon in coeval strata; 5) thicker than normal oceanic crust adjacent to the continent-ocean transition, and; 6) a lower crustal body of mafic material which underplates the attenuated continental-oceanic transitional crust (Eldholm et al., 1995).

A good deal of the evidence for present-day volcanic margins is found with lithosphere of the continent-ocean transition. What happened to past continent-ocean transitions during collision and orogeny? Is any of it preserved, or accessible? The obduction onto the Laurentian margin of Taconic allochthons and the initiation of subduction along the proto-Andean margin implies that Iapetan continent-ocean transitional lithosphere may have been overridden, to become lost as deep roots in the Appalachian and Andean orogens.

More likely to be preserved are the peripheral products of a volcanic margin, such as continental flood basalts, a regional tephra horizon and possibly sills in pre-opening sediments later preserved in allochthons. Continental flood basalts related to the Iapetus opening are found along the Laurentian margin as the Catoctin volcanics of the Blue Ridge mountains and the Lighthouse Cove Formation of west Newfoundland and southeast Labrador. However, the presence of flood basalts is not itself diagnostic of a volcanic margin.

If a volcanic margin developed in response to the arrival of a mantle plume (White and McKenzie, 1989; Bown and White, 1995), then evidence for the late Neoproterozoic arrival of a mantle plume in the Quebec reentrant portion of the rifting Laurentian margin (Kumarapeli, 1993; Higgins and van Breemen, in press), may be important. Both discussions propose regional (~1000 km) domal uplift of the Laurentian margin in response to the impact of a mantle plume, similar to the plume-related dynamic (thermal) uplift component in the models of Bown (1994) and Bown and White (1995). The direct effects of a plume head impact may extend over no more than an area of 2000 km diameter about it (White and McKenzie, 1989). However, plume-influenced thermal and magmatic uplift along the greater than 3500 km length of Laurentia's incipient Iapetan margin may have occurred if a mantle plume arrived under or near a region of previously thinned continental lithosphere with already heightened upper mantle temperature or fluid content (e.g Thompson and Gibson, 1991; Eldholm et al., 1995). The magmatic and thermal effects on the lithosphere may have extended beyond the region affected by the plume head directly if plume material migrated along a sub-lithospheric channel under the rifting margin (e.g White, 1992; Oyarzun et al., 1997), perhaps influencing the timing and volume of the Catoctin volcanism.

In summary, the start of Iapetus opening at ~570 Ma is implied by palaeomagnetic data, and is permissible within the constraints of geologic data, if the following conditions are invoked: 1) passive margin alkali magmatism to account for ca. 555-550 Ma units of the northeastern Appalachians; and 2) a ~20-30 m.y. delay of the first drift transgressive sedimentation to early Cambrian, due to anomalous margin subsidence. Initial sea-floor spreading of the Iapetus Ocean may have predated ca. 555-550 Ma alkali magmatism by 15-20 million years, and the first Laurentian margin transgressive sedimentation by as much as 30 million years.

Definitive tests to prove or disprove this alternate geological interpretation of ~570 Ma final rifting to form the Iapetus are possible but difficult to find. The identification of continental flood basalts and tephra horizons in coeval strata in cratonic Laurentia and possibly Amazonia and Rio de la Plata would support the possibility of Iapetan volcanic-type margins, and anomalous margin subsidence leading to delayed transgressive sedimentation. On the other hand, the finding of conformable contacts between syn-rift and drift sedimentation would be strong evidence against final rifting at ~570 Ma, as it would imply that there was no break in time in latest Neoproterozoic to early Cambrian sedimentation which records final rifting and the first drift-phase margin subsidence.

4.4 Late Neoproterozoic palaeogeography

Palaeogeographic reconstructions for ~575 Ma and for ~550 Ma which seek to reconcile latest Neoproterozoic palaeomagnetic and geologic data are presented in Figure 9. These reconstructions are consistent with geology for the time (Dalziel, 1997; Trompette, 1997; Unrug, 1996), with reinterpretation for Laurentia and Rio de la Plata as discussed in section 4.3, and are consistent with the palaeomagnetic data available from constituent cratons at the time (Meert and Van der Voo, 1997; Torsvik et al., 1996).

The conjugate margin which rifted from Laurentia at ~570 Ma giving birth to the Iapetus Ocean may have been the Amazonia and Rio de la Plata cratons of West Gondwana, as argued by Dalziel (1992, 1997). Early rifting between Laurentia and Amazonia-Rio de la Plata is shown for the ~575 Ma reconstruction (Figure 9a), marked by syenite and carbonatite rift-related magmatism (e.g. Callander Complex) along the Ottawa-Bonnechere failed rift arm (Kumarapeli, 1993) and volcanism along Laurentia's incipient Iapetan margin (e.g. Catoctin volcanics at ~570 Ma; Burton et al., 1995). An association between Amazonia and Congo-Sao Francisco cratons across the Goias Massif reflects their collision between ~630 Ma and ~600 Ma (Pimentel et al., 1997; Trompette, 1997). By 575 Ma, rocks of the Goias Massif were undergoing extensional uplift (Pimentel et al., 1996), as part of overall extension and dispersal amongst West Gondwana, Laurentia, Baltica and Siberia (e.g. Trompette, 1997; Gurnis and Torsvik, 1994; Torsvik et al., 1996). Other relations between cratons of Gondwana follow Dalziel (1997),

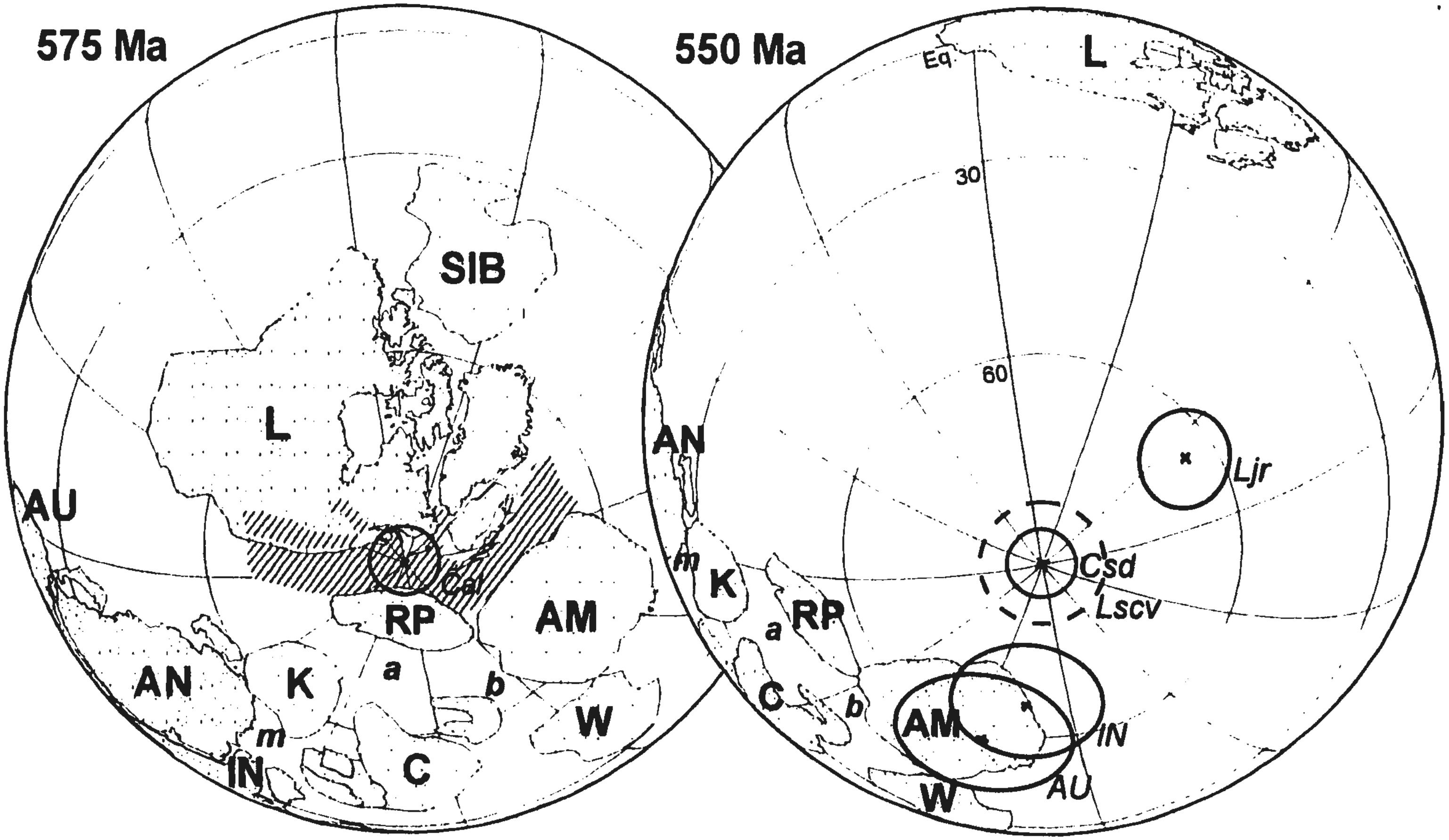

Figure 9. Late Neoproterozoic paleogeography for ~575 Ma and ~550 Ma, based on Dalziel, (1997). Cross-hatched zone in ~575 Ma diagram represents incipient rifting to form the Iapetus, which had opened by the ~550 Ma diagram. Abbreviations: Cal- Callander Complex, Laurentia; Csd-Sinyai Dike, Congo; Ljr- Johnnie Rainstorm, Laurentia, Lscv- Skinner Cove volcanics, Laurentia; a-Adamastor Ocean; b-Brazilide Ocean/Orogen; m-Mozambique Ocean/Orogen; AM-Amazonia; AN-Antarctica; AU-Australia (and pole); C-Congo-Sao Francisco; IN-India (and pole); K-Kalahari; L-Laurentia; RP-Rio de la Plata; SIB-Siberia; W-West Africa. Baltica is omitted for clarity. Poles are plotted with circles of 95% confidence. Diagram created with the assistance of PLATES software from the University of Texas Institute for Geophysics.

although there are many alternative interpretations (e.g Grunow et al., 1996; Unrug, 1996; Meert and Van der Voo, 1997).

By the end of the Neoproterozoic (~550 Ma), the Iapetus Ocean had opened between Laurentia, West Gondwana, and Baltica, as shown in Figure 9b, which resembles the ca. 550 Ma reconstruction of Torsvik et al. (1996). Siberia is shown abutting Laurentia (Pelachaty, 1996), but it may have rifted away by 550 Ma (Torsvik et al., 1996). Laurentian margin ca. 555-550 Ma alkalic magmatism (Tibbit Hill, Lady Slipper Pluton, Skinner Cove Volcanics and others) would in this view have postdated rifting, perhaps erupting from remaining mantle plume material in response to a major rearrangement of plate boundaries and motions (e.g., Jansa and Pe-Piper, 1985), marked by the cessation of Laurentia's rapid northward drift (Figure 8); Laurentia may have stalled at the equator in a geoid low over a mantle sink (Gurnis and Torsvik, 1994). Gondwana is shown to be consolidated, although final closure of the Adamastor Ocean may have been at ~540 Ma (Hoffman, 1997), and final consolidation of Gondwana by ~530 Ma (Meert and Van der Voo, 1997).

Cambrian movement of Gondwana's Amazonia and West Africa cratons across the south pole (Meert et al., 1996; Dalziel, 1997) reflects the beginning of Iapetus closure and the initiation of subduction along the Gondwanan palaeo-Pacific margins of Antarctica and Rio de la Plata cratons (Grunow et al., 1996) and the Avalonian-Cadomian arcs (e.g Dalziel, 1997, Figure 14).

These reconstructions allow for the possible fleeting existence of a Pannotia supercontinent between the unifying ~630 Ma Himalayan-style collision of Amazonia with Congo-Sao Francisco cratons (Pimentel et al., 1996; 1997) and the rifting of Baltica and Laurentia-Siberia from the consolidating Gondwanan cratons between ~600 Ma and ~565 Ma (Torsvik et al., 1996). The existence of Pannotia also depends on the timing of Gondwana assembly, which is variously estimated to have taken place between ~700 and ~600 Ma (Stern, 1994) or by ~530 Ma at latest (Meert and Van der Voo, 1997). However, the existence of Laurentia united with Gondwana in the Pannotia supercontinent is not palaeomagnetically supportable by ca. 550 Ma.

Pannotia may best be viewed as a loose, transitional assembly of cratons at the end of the Neoproterozoic, during a period of apparently intense global reorganization of plate boundaries and sometimes rapid cratonic movement. The dispersal of Pannotia resulted in the consolidation of Gondwana and its separation from Laurentia, Siberia and Baltica by the Iapetus Ocean. These cratons ultimately assembled through closure of the Iapetus to form Pangea.

Chapter 5: Concluding remarks

Alkali volcanic flows and dykes of the ca. 550 Ma Skinner Cove Formation in western Newfoundland retain a characteristic `A' remanence in ten sites which is interpreted to be primary on the basis of a positive intraformational conglomerate test. The palaeolatitude calculated from the ten tilt-corrected `A' site virtual geomagnetic poles is 18.6°S ±9°, and is interpreted to represent the Iapetan margin of Laurentia at ~550 Ma, based on the age of the Skinner Cove Formation and geological evidence for its original relation with Laurentia.

The low southerly palaeolatitude of the Skinner Cove Formation constrains Laurentia to have occupied an equatorial position by ~550 Ma. Comparison with other palaeomagnetic results from Laurentia suggests it drifted rapidly northward from near south polar palaeolatitudes at ~575 Ma (Figure 8). The rapid northward drift of Laurentia may accommodate the opening of a wide Iapetus by ~550 Ma, following initial spreading some 20 million years beforehand (Figure 9a,b). Subsidence of the Laurentian margin recorded in early Cambrian transgressive sections may not necessarily record its rift to drift transition, if anomalous margin subsidence due to large-scale syn-rift magmatic activity is invoked.

Of abiding interest are questions involving the apparent rapid movement of continents during the late Precambrian and Cambrian. Rapid northward movement of

Laurentia and Baltica during the late Neoproterozoic, followed by the movement of West Gondwana across the south pole in the early-mid Cambrian (Meert et al., 1996) suggests differing periods of apparently rapid cratonic movement. While rapid cratonic motion of ~34 ±15 cm/yr is implied by existing late Neoproterozoic palaeomagnetic data for Laurentia, the reconstructions proposed here do not require a role for true polar wander, although late Neoproterozoic TPW cannot be ruled out. Mechanisms to account for the driving forces of rapidly moving continents are much debated, and may act in concert in some cases. In the case of late Neoproterozoic Laurentia, several mechanisms for movement have been proposed, including slab pull during distant subduction of the proto-Pacific plate attached to Laurentia (Grunow et al., 1996; Dalziel, 1997), Iapetan spreading ridge push (Jurdy et al., 1995), or mantle push off of a thermal high under the late Neoproterozoic supercontinent, perhaps involving gravity as a motivator from a geoid high at the thermal anomaly to a geoid low over a mantle sink (Gurnis and Torsvik, 1994).

If the Iapetus Ocean began to open at ~570 Ma, and rapidly attained a ~7500 km width by ~550 Ma, as implied by palaeomagnetic data, then what are the consequences of such rapid seafloor spreading and the production of so much young, buoyant ocean crust? Eustatic sea level rise during the late Neoproterozoic and into the Cambrian may be due to Iapetan ridge-volume displacement and the replacement of old ocean crust at convergent margins with new more buoyant Iapetan crust (Thomas and Whiting, 1995).

Final rifting between Laurentia and an adjacent craton to form the Iapetus opened an ocean which provided a new, subtropical east-west seaway and new flooded margins by the Precambrian-Cambrian boundary. The ca. 549-543 Ma diversification of Ediacaran life (Grotzinger et al., 1995) may have been aided by a new, more vigorous subtropical circulation and eustatic sea level rise (Valentine and Moores, 1970) amongst more dispersed cratons in a radically altered palaeogeography.

The results reported here encourage further precisely dated and tested palaeomagnetic investigation of units from Laurentia, Amazonia, Rio de la Plata and other cratons to resolve their role in the formation of the Iapetus and to evaluate palaeogeographic reconstructions such as that proposed here. For the late Neoproterozoic-early Cambrian period of apparently rapid cratonic movement and changing plate boundaries, a finer resolution of magnetization and geological events to within $\pm 1\%$ of age (± 5 Ma) may be required to clearly establish relations between the cratons involved in the possible existence of Pannotia, its dispersal, and the assembly of Gondwana.

REFERENCES

Acenolaza, F.G., and Durand, F.R. 1986. Upper Precambrian-Lower Cambrian biota from the northwest of Argentina. Geological Magazine, 124: pp 367-375.

Ade-Hall, J.M., Palmer, H.C., and Hubbard, T.P. 1971. The magnetic and petrological response of basalts to regional hydrothermal alteration. Geophysical Journal of the Royal Astronomical Society, 24: pp 137-174.

Ade-Hall, J.M., Fink, L.K., and Johnson, H.P. 1976. Petrography of opaque minerals, Leg 34, *in* Initial reports of the Deep Sea Drilling Project, Volume XXXIV, Washington (US Government Printing Office): pp 349-364.

Aleinikoff, J.N., Zartman, R.E., Walter, M., Rankin, D.W., Lyttle, P.T., and Burton, W.C. 1995. U-Pb ages of metarhyolites of the Catoctin and Mount Rogers Formations, Central and southern Appalachians: Evidence for two pulses of Iapetan rifting. American Jounal of Science, 295: pp 428-454.

Baker, D.F. 1979. Geology and geochemistry of an alkali volcanic suite (Skinner Cove Formation) in the Humber Arm Allochthon, Newfoundland. Unpublished M.Sc. dissertation, Memorial University of Newfoundland. 314p.

Barton, P., and Wood, R. 1984. Tectonic evolution of the North Sea basin: crustal stretching and subsidence. Geophysical Journal of the Royal Astronomical Society, 79: pp 987-1022.

Beaubouef, R.T., Casey, J.F., and Hall, S.A. 1988. A paleomagnetic study of the Skinner Cove Volcanic Assemblage, Western Newfoundland. Poster-Abstract; Eos, 69: no.44.

Beiersdorfer, R.E., and Day, H.W. 1995. Mineral paragenesis of pumpellyite in low-grade mafic rocks, *in* Low-grade metamorphism in mafic rocks (Schiffman, P., and Day, H.W., eds), Boulder, Colorado, GSA Special Paper 296: pp 5-27.

Bond, G.C. 1997. New constraints on Rodinia breakup ages from revised tectonic subsidence curves, *in* GSA Abstracts with Programs, 1997, vol. 29: p A-280.

Bond, G.C., Nickerson, P.A., and Kominz, M.A. 1984. Breakup of a supercontinent between 625 and 555 Ma- New evidence and implications for continental histories. Earth and Planetary Science Letters, 70: pp 325-345.

Bown, J.W., 1994. Melting and subsidence at rifts. Ph.D. Dissertation, University of Cambridge: 238 p.

Bown, J.W., and White, R.S. 1995. Finite duration rifting, melting and subsidence at continental margins, *in* Rifted Ocean-Continent Boundaries (Banda, E., et al., eds.). Kluwer, Netherlands: pp 31-54.

Brasier, M.D. 1992. Global ocean-atmosphere change across the Precambrian-Cambrian transition. Geological Magazine, 129: pp 161-168.

Buck, W.R. 1986. Small-scale convection induced by passive rifting: the cause for uplift of rift shoulders. Earth and Planetary Science Letters, 77: pp 362-372.

Burton, W.C., Froelich, A.J., Pomeroy, J.S., and Lee, K.Y. 1995. Geology of the Waterford Quadrangle, Virginia and Maryland, and the Virginia part of the Point of Rocks Quadrangle. USGS Bulletin, 2095: 30 pp.

Camire, G., La Fleche, M.R., and Jenner, G.A. 1995. Geochemistry of pre-Taconian mafic volcanism in the Humber Zone of the northern Appalachians, Quebec, Canada. Chemical Geology, 119: pp 55-77.

Cawood, P.A., McCausland, P.J.A., and Dunning, G.R. submitted. Opening Iapetus: Constraints from the Laurentian margin in Newfoundland. Geology

Cawood, P.A., van Gool, J.A.M., and Dunning, G.R., 1996, Geological development of eastern Humber and western Dunnage zones: Corner Brook - Glover Island region, Newfoundland: Canadian Journal of Earth Sciences, v. 33, p. 182-198.

Cawood, P.A., Williams, H., O'Brien, S.J., and O'Neill, P.P. 1988. Trip A1. A Geologic cross-section of the Appalachian Orogen. Field trip guidebook, Geological Association of Canada, 160p.

Dalla Salda, L.H., Cingolani, C.A., and Varela, R. 1992. The early Paleozoic orogenic belt of the Andes in southwestern South America: Result of Laurentia-Gondwana collision? Geology, 20: pp 617-620.

Dankers, P., and Lapointe, P. 1981. Paleomagnetism of Lower Cambrian volcanics and a crosscutting Cambro-Ordovician diabase dyke from Buckingham, (Quebec). Canadian Journal of Earth Sciences, 18: pp 1174-1186.

Dalziel, I.W.D. 1991. Pacific margins of Laurentia and east Antarctica-Australia as a conjugate rift pair: Evidence and implications for an Eocambrian supercontinent. Geology, 19: pp 598-601.

Dalziel, I.W.D. 1992. On the organization of American plates during the Neoproterozoic and the breakout of Laurentia. GSA Today 2:11, pp 237-241.

Dalziel, I.W.D. 1994. Precambrian Scotland as a Laurentia-Gondwana link -Origin and significance of cratonic promontories. Geology, 22: pp 589-592.

Dalziel, I.W.D. 1997. Neoproterozoic-Paleozoic geography and tectonics: Review, hypothesis, environmental speculation. GSA Bulletin, 109: pp 16-42.

Dalziel, I.W.D., Dalla Salda, L.H., and Gahagan, L.M. 1994. Paleozoic Laurentia-Gondwana interaction and the origin of the Appalachian-Andean mountain system. GSA Bulletin, 106: pp 243-252.

Dunlop, D.J., Ozdemir, O., and Schmidt, P.W. 1997. Paleomagnetism and paleothermometry of the Sydney Basin II. Origin of anomalously high unblocking temperatures. Journal of Geophysical Research, in press.

Eldholm, O., Skogseid, J, Planke, S., and Gladczenko, T.P. 1995. Volcanic margin concepts, *in* Rifted Ocean-Continent Boundaries (Banda, E., et al., eds.). Kluwer, Netherlands: pp 1-16.

Elston, D.P., and Bressler, S.L. 1977. Palaeomagnetic poles and polarity zonation from Cambrian and Devonian strata of Arizona. Earth and Planetary Science Letters, 36: pp 423-433.

Evans, D.A. 1998. True polar wander, a supercontinental legacy. Earth and Planetary Science Letters, in press.

Farr, M.R., and Gose, W.A. 1991. Palaeomagnetism of the Cambrian Moore Hollow Group, Texas: Evidence for a primary magnetization carried by detrital magnetite. Journal of Geophysical research, 96: pp 9895-9907.

Fyffe, L.R. and Swinden, H.S. 1991. Paleotectonic setting of Cambro-Ordovician rocks in the Canadian Appalachians. Geoscience Canada, 18: No. 4., pp 145-157.

Graham, J.W. 1949. The stability and significance of magnetism in sedimentary rocks. Journal of Geophysical Research, 54: pp 131-167.

Grotzinger, J.P., Bowring, S.A., Saylor, B.Z., Kaufman, A.J. 1995. Biostratigraphic and geochronologic constraints on early animal evolution. Science, 270: pp 598-604.

Grunow, A., Hanson, R., Wilson, T. 1996. Were aspects of the Pan-African deformation linked to Iapetus opening? Geology, 24: pp 1063-1066.

Gurnis, M., and Torsvik, T.H. 1994. Rapid drift of large continents during the late Precambrian and Palaeozoic: Palaeomagnetic constraints and dynamic models. Geology, 22: pp 1023-1026.

Harland, W.B. and Gayer, R.A. 1972. The Arctic Caledonides and earlier oceans. Geological Magazine, 109: pp 289-314.

Heller, P.L., Wentworth, C.M., and Poag, C.W. 1982. Episodic post rift subsidence of the U.S. Atlantic margin. GSA Bulletin, 93: pp 379-390.

Higgins, M.D., and van Breemen, O. in press. The age of the Sept Iles layered intrusion, Canada: Implications for the late Neoproterozoic/Cambrian history of south-eastern Canada. Journal of Geology.

Hoffman, P.F. 1991. Did the breakout of Laurentia turn Gondwana inside-out? Science, 252: pp 1409-1412.

Irving, E. 1964. Paleomagnetism and its application to geological and geophysical problems. New York, John Wiley and Sons, Inc., 399p.

Jansa, L.F., and Pe-Piper, G. 1985. Early Cretaceous volcanism on the northeastern American margin and implications for plate tectonics. Geological Society of America Bulletin, 96: pp 83-91.

Jarvis, G.T., and McKenzie, D.P. 1980. Sedimentary basin formation with finite extension rates. Earth and Planetary Science Letters, 48: pp 42-52.

Jenner, G.A., Dunning, G.R., Malpas, J., Brown, M., and Brace, T. 1991. Bay of Islands and Little Port complexes, revisited: Age, geochemical and isotopic evidence confirm suprasubduction-zone origin. Canadian Journal of Earth Sciences, 28: pp 1635-1652.

Jurdy, D.M., Stefanick, M., and Scotese, C.R. 1995. Paleozoic plate dynamics. Journal of Geophysical Research, 100: pp 17965-17975.

Kamo, S.L., and Gower, C.F. 1994. Note: U-Pb baddeleyite dating clarifies age of characteristic paleomagnetic remanence of Long Range dykes, southeastern Labrador. Atlantic Geology, 30: pp 259-262.

Kamo, S.L., Gower, C. F., and Krogh, T.E. 1989. A birthdate for the Iapetus Ocean? A precise U-Pb zircon and baddeleyite age for the Long Range dykes, S.E. Labrador. Geology, 17: pp 602-605.

Kamo, S.L., Krogh, T.E., and Kumarapeli, P.S. 1995. Age of the Grenville dyke swarm, Ontario-Quebec: implications for the timing of Iapetan rifting. Canadian Journal of Earth Sciences, 32: pp 273-280.

Keen, C.E. 1986. The dynamics of rifting: deformation of the lithosphere by active and passive driving forces. Geophysical Journal of the Royal Astronomical Society, 80: pp 95-120.

Keen, C.E., and Boutilier, R.R. 1995. Lithosphere-asthenosphere interactions below rifts, *in* Rifted Ocean-Continent Boundaries (Banda, E., et al., eds.). Kluwer, Netherlands: pp 17-30.

Kirschvink, J.L. 1980. The least-squares line and plane and the analysis of paleomagnetic data. Geophysical Journal of the Royal Astronomical Society, 62: pp 699-718.

Kirschvink, J.L., Ripperdan, R.L., and Evans, D.A. 1997. Evidence for a large-scale reorganization of early Cambrian continental masses by inertial interchange true polar wander. Science, 277: pp 541-545.

Knoll, A.H, and Walter, M.R,. 1992. Latest Proterozoic stratigraphy and Earth history. Nature, 356: pp 673-678.

Kumarapeli, P.S. 1993. A plume-generated segment of the rifted margin of Laurentia, Southern Canadian Appalachians, seen through a completed Wilson Cycle. Tectonophysics, 219: pp 47-55.

Kumarapeli, P.S., St. Seymour, K., Pintson, H., and Hasselgren, E. 1988. Volcanism on the passive margin of Laurentian early Paleozoic analogue of Cretaceous volcanism on the northeastern American margin. Canadian Journal of Earth Sciences, 25: pp 1824-1833.

Kumarapeli, P.S., Dunning, G.R., Pintson, H., and Shaver, J. 1989. Geochemistry and U-Pb age of comenditic metafelsites of the Tibbit Hill Formation, Quebec Appalachians. Canadian Journal of Earth Sciences, 26: pp 1374-1383.

LaFleur, J., and Hogarth, D.D. 1981. K-Ar age determinations. Geological Survey of Canada, Paper 81-C, pp 27-34.

Li, Z.X. and Powell, C.M. 1993. Late Proterozoic to early Palaeozoic palaeomagnetism and the formation of Gondwana, *in* Gondwana 8: Assembly, evolution and dispersal (Findlay, R.H., et al., eds.) Rotterdam, A.A. Balkema: pp 9-21

Liou, J.G., de Capitani, C., and Frey, M. 1991. Zeolite equilibria in the system CaAlSi2O8-SiO2-H2O. New Zealand Journal of Geology and Geophysics, 34: pp 293-301.

MacNiociall, C., and Smethurst, M.A. 1994. Palaeozoic palaeogeography of Laurentia and its margins: A reassessment of palaeomagnetic data: Geophysical Journal International, 116: pp 715-725.

Malka, E., Stevenson, R.K., and David, J. 1996. The petrology and petrogenesis of the Mt. Rigaud alkaline syeno-granite, Quebec, *in* GAC-MAC annual meeting, Program with abstracts, Winnipeg: p A-61.

McCausland, P.J.A. 1995. Palaeomagnetism and U-Pb zircon age of the Skinner Cove Volcanics of western Newfoundland. Unpublished B.Sc. dissertation, Memorial University of Newfoundland. 87p.

McCausland, P.J.A., Hodych, J.P., and Dunning, G. 1996. Palaeomagnetism and U-Pb age of the Skinner Cove Volcanics of western Newfoundland: Implications for the late Neoproterozoic breakup of Rodinia, *in* Proterozoic evolution in the North Atlantic realm (compiled by Gower, C.F.) COPENA-ECSOOT-IBTA conference, Goose Bay, Labrador, Program with abstracts: p 122.

McElhinny, M.W., Cowley, J.A., and Edwards, D. 1978. Paleomagnetism of some rocks from peninsular India and Kashmir: Tectonophysics, 50: pp 41-54.

McKenzie, D.P. 1978. Some remarks on the development of sedimentary basins. Earth and Planetary Science Letters, 40: pp 25-32.

McMenamin, M.A.S., and McMenamin-Schulte, D.L.S. 1990. The Emergence of Animals: The Cambrian Breakthrough. Columbia University Press, New York, 217p.

Meert, J.G., and Van der Voo, R., 1996, Paleomagnetic and $^{40}Ar/^{39}Ar$ Study of the Sinyai Dolerite, Kenya: Implications for Gondwana Assembly: Journal of Geology, v. 104, p. 131-142.

Meert, J.G., and Van der Voo, R., 1997, The assembly of Gondwana 800-540 Ma: Journal of Geodynamics, v. 23, p. 223-235.

Meert, J.G., Van der Voo, R., Powell, C.McA., Li, Z.X., McElhinny, M.W., Chen, Z., and Symons, D.T.A. 1993. A plate tectonic speed limit? Nature, 363: pp 216-217.

Meert, J.G., Van der Voo, R., and Payne, T.W. 1994. Paleomagnetism of the Catoctin volcanic province: A new Vendian-Cambrian apparent polar wander path for North America. Journal of Geophysical Research, 99: B3, pp 4625-4641.

Meschede, M. 1986. A method of discriminating between different types of mid-ocean ridge basalts and continental tholeiites with the Nb-Zr-Y diagram. Chemical Geology, 56: pp 207-218.

Middleton, M.F., and Schmidt, P.W. 1992. Paleothermometry of the Sydney Basin. Journal of Geophysical Research, 87: pp 5351-5359.

Moores, E.M. 1991. Southwest U.S.-East Antarctic (SWEAT) connection: A hypothesis. Geology, 19: pp 425-428.

Murthy, G., Gower, C., Tubrett, M., and Patzold, R. 1992. Paleomagnetism of Eocambrian Long Range dykes and Double Mer Formation from Labrador, Canada. Canadian Journal of Earth Sciences, 29: pp 1224-1234.

Nicholas, C.J. 1996. The Sr isotopic evolution of the oceans during the `Cambrian Explosion' Geological Society of London Journal, 153: pp 243-254.

Olive, V., Hebert, R., Vermette, D., Loubet, M. 1997. Geochemistry of Iapetus volcanic rocks, Quebec Appalachians: Nd, Sr isotopic compositions. American Journal of Science, 297: pp 418-439.

Oyarzun, R., Doblas, M., Lopez-Ruiz, J., and Maria Cebria, J. 1997. Opening of the central Atlantic and asymmetric mantle upwelling phenomena: Implications for long-lived magmatism in western North Africa and Europe. Geology, 25: pp727-730.

Pelechaty, S.M. 1996. Stratigraphic evidence for the Siberia-Laurentia connection and early Cambrian rifting. Geology, 24: pp 719-722.

Pimentel, M.M., Whitehouse, M.J., das G. Viana, M., Fuck, R.A., and Machado, N. 1997. The Mara Rosa Arc in the Tocantins Province: further evidence for Neoproterozoic crustal accretion in Central Brazil. Precambrian Research, 81: pp 299-310.

Pimentel, M.M., Fuck, R.A., and Jose Souza de Alvarenga, C. 1996. Post-Braziliano (Pan-African) high-K granitic magmatism in central Brazil: the role of Late Precambrian-early Cambrian extension. Precambrian Research, 80: pp 217-238.

Powell, C.M. 1995. Are Neoproterozoic glacial deposits preserved on the margins of Laurentia related to the fragmentation of two supercontinents?: Comment. Geology, 23: pp 1053-1054.

Pulliah, G., Irving, E., Buchan, K.L., and Dunlop, D.J. 1975. Magnetisation changes caused by burial depth and uplift. Earth and Planetary Science Letters, 28: pp 133-143.

Rapela, C., Toselli, A., Heaman, L., and Saavedra, J. 1990. Granite plutonism of the Sierras Pampeanas: An inner cordilleran Paleozoic arc in the southern Andes, *in* Plutonism from Antarctica to Alaska (Kay, S., and Rapela, C., eds.): pp 77-90.

Roydon, L., and Keen, C.E. 1980. Rifting process and thermal evolution of the continental margin of eastern Canada determined from subsidence data. Earth and Planetary Science Letters, 51: pp 343-361.

Simpson, E.L., and Sundberg, F.A. 1987. Early Cambrian age for synrift deposits of the Chilhowee Group of southwestern Virginia. Geology, 15: pp 123-126.

St-Julien, P., and Hubert, C. 1975. Evolution of the Taconian orogen in the Quebec Appalachians: American Journal of Science, 257A: pp 337-367.

Stern, R.J. 1994. Arc assembly and continental collision in the Neoproterozoic East African orogen: Implications for the consolidation of Gondwanaland. Annual Reviews of Earth and Planetary Science, 22: pp 319-351.

Stevens, R.K. 1970. Cambro-Ordovician flysch sedimentation and tectonics in west Newfoundland and their possible bearing on a Proto-Atlantic Ocean, *in* Flysch sedimentology in North America (Lajoie, J., ed), GAC Special paper, 7: pp 165-177.

Stockmal, G.S., and Waldron, J.W.F. 1993. Structural and tectonic evolution of the Humber Zone, western Newfoundland, 1: Implications of cross section through the Appalachian structural front, Port au Port Peninsula, Tectonics 12: pp 1056-1075.

Stockmal, G.S., Colman-Sadd, S.P., Keen, C.E., O'Brien, S.J., and Quinlan, G. 1987. Collision along an irregular margin: a regional plate tectonic interpretation of the Canadian Appalachians. Canadian Journal of Earth Sciences, 24: pp 1098-1107.

Strong, D.F. 1974. An "off-axis" alkali volcanic suite associated with the Bay of Islands ophiolites, Newfoundland. Earth and Planetary Science Letters, 21: pp 301-309.

Symons, D.T.A., and Chiasson, A.D. 1991. Paleomagnetism of the Callander Complex and the Cambrian apparent polar wander path for North America. Canadian Journal of Earth Sciences, 28: pp 355-363.

Tanczyk, E. I., Lapointe, P., Morris, W.A., and Schmidt, P.W. 1987. A paleomagnetic study of the layered mafic intrusion at Sept-Isles, Quebec. Canadian Journal of Earth Sciences, 24: pp 1431-1438.

Thomas, W.A. 1991, The Appalachian-Ouachita rifted margin of southeastern North America: Geological Society of America, Bulletin, v. 103, p. 415-431.

Thomas, W.A., and Whiting, B.M. 1995. The Alabama promontory: Example of the evolution of an Appalachian-Ouachita thrust-belt recess at a promontory of the rifted continental margin, *in* Current perspectives in the Appalachian-Caledonian Orogen (Hibbard et al., eds), GAC Special Paper 41: pp 3-20.

Thompson, R.N., and Gibson, S.A. 1991. Subcontinental mantle plumes, hotspots, and pre-existing thinspots. Journal of the Geological Society of London, 148: pp 973-977.

Troelsen, J. 1947. Stratigraphy and structure of the Bonne Bay-Trout River area. Ph.D. dissertation, Yale University, New Haven, Connecticut, USA.

Torsvik, T.H., Smethurst, M.A., Meert, J.G., Van der Voo, R., McKerrow, W.S., Brasier, M.D., Sturt, B.A., and Walderhaug, H.J., 1996, Continental break-up and collision in the Neoproterozoic and Paleozoic - A tale of Baltica and Laurentia: Earth Science Reviews, v. 40, p. 229-258.

Trompette, R., 1997, Neoproterozoic (~600 Ma) aggregation of Western Gondwana: a tentative scenario: Precambrian Research, v. 82, p. 101-112.

Tucker, R.D., and McKerrow, W.S. 1995. Early Paleozoic chronology: A review in light of new U-Pb zircon ages from Newfoundland and Britain. Canadian Journal of Earth Sciences, 32: pp 368-379.

Unrug, R. 1996. The assembly of Gondwanaland. Episodes, 19: pp 11-20.

Valentine, J.W., and Moores, E.M. 1970. Plate-tectonic regulation of faunal diversity and sea level: a model. Nature 228: p 657.

van Alstine, D.R., and Gillett, S.L. 1979. Palaeomagnetism of the upper Precambrian sedimentary rocks from the Desert Range, Nevada. Journal of Geophysical Research, 84: pp 4490-4500.

Wanless, R.K., Stevens, R.D., Lachance, G.R., and Delabio, R.N. 1970. Age determinations and geological studies. Geological Survey of Canada, Paper 69-2A.

Wasteneys, H.A., Clark, A.H., Farrar, E., Langridge, R.J. 1995. Grenvillian granulite-facies metamorphism in the Arequipa Massif, Peru: a Laurentia-Gondwana link. Earth and Planetary Science Letters, 132: pp 63-73.

Watson, G.S. 1956. A test for randomness of directions. Monthly notices of the Royal Astronomical Society, Geophysics Supplement, 7: pp 160-161.

White, R.S. 1992. Magmatism during and after continental break-up, *in* Magmatism and the causes of continental break-up (Storey, B.C., et al., eds.): Special paper of the Geological Society of London, 68: pp 1-16.

White, R.S., and McKenzie, D. 1989. Magmatism at rift zones: The generation of volcanic continental margins and flood basalts. Journal of Geophysical Research, 94: pp 7685-7729.

Williams, H. 1973. Bay of Islands map-area, Newfoundland. Geological Survey of Canada, Paper 72-34.

Williams, H. 1975. Structural succession, nomenclature, and interpretation of transported rocks in western Newfoundland. Canadian Journal of Earth Sciences, 12: pp1874-1894.

Williams, H. 1978. Tectonic Lithofacies map of the Appalachian Orogen. Map 1, Memorial University of Newfoundland.

Williams, H. 1979. Appalachian Orogen in Canada: Canadian Journal of Earth Sciences, 16: pp 729-807.

Williams, H., 1995, Geology of the Appalachian-Caledonian Orogen in Canada and Greenland, Volume F-1 in Decade of North American Geology: Ottawa, Geological Survey of Canada, p. 944.

Williams, H., and Hiscott, R.N. 1987. Definition of the Iapetus rift-drift transition in western Newfoundland. Geology, 15: pp 1044-1047.

Wilson, J.T. 1966. Did the Atlantic close and then re-open? Nature, 211: pp 676-681.

Young, G.M. 1995. Are Neoproterozoic glacial deposits preserved on the margins of Laurentia related to the fragmentation of two supercontinents? Geology, 23: pp 153-156.

Zijderveld, J.D.A. 1967. A.C. demagnetization of rocks: Analysis of results. in Methods in Paleomagnetism (Collinson et el., eds.), Elsevier, New York, pp 254-286.

APPENDIX A

The declination (DECL) and inclination (INCL.) in degrees and the magnetic moment (MOMENT) in c.g.s. units are listed during stepwise demagnetizations for each specimen carrying a stable component of remanence. Magnetization in c.g.s. units can be obtained by dividing the magnetic moment by simple volume which is ~10 cm^3. These c.g.s. magnetizations can then be converted to A/m by multiplying by 10^3.

The alternating field strengths (FIELD) are given in Oersteds and should be divided by 10 to obtain the mT equivalent. The temperatures used in thermal demagnetization (TEMP) are listed in °C. Thermal demagnetization was usually preceded by alternating field demagnetization to 15 or 20 mT and are indicated between 0 and the 200°C initial step of thermal demagnetization.

A list of sites and their constituent samples follows.

Site 6 Trachyte
19794-22.2
19794-23.2A
19794-24.2
19794-25.1
19794-26.1
19794-27.1

Site 3 Trachybasalt
18794-6.2b
18784-7.3
18794-8.1
18794-9.1
18794-10.1
18794-12.1a

Site 1 Ankaramite
17794-1.2.2
17794-2.2A
17794-3.1B
17794-4.1C
17794-5.3
21794-25.1c

Site 4 Pillowed Headland Basalt
19794-16.1
19794-17.1
19794-18.1
19794-19.1
19794-21.1a
19794-20.1

Site 9 Alkali Basalt
21794-7.1
21794-8.2
21794-9.1
21794-10.1
21794-11.1
21794-12

Site 5 Alkali Basalt
21794-13.1
21794-14.3
21794-15.1a
21794-16.1a
21794-17b
21794-18b

Site 12 Pinnacle
13995-1.1b
13995-6.1b
13995-2.1
13995-3.2
13995-5.2b
13995-5.2a

Ankaramite Site 11 Mafic Dyke
12995-8.2b
12995-9.2b
12995-11.1a
12995-12.1a
12995-7.1a
12995-10.2

Site 10 Trachyte Dyke
12995-1.1b
12995-5.2
12995-6.2
12995-2.1a
12995-3.1a
12995-4.2.2

Site 15 Trachybasalt
16995-2.2a
16995-3.1
16995-4.2a
16995-6.1
16995-20.2
16995-5.1
16995-1.2a

Site 14 Trachyte Dyke
13995-13.2b
13995-15a
16995-17.2
16995-18.1b
16995-19
13996-1.2
13996-2.2b
13996-3.2
13996-4.1a
13995-14.2a

Site 13 Mafic Dyke
13995-8.3
13995-9A
13995-10.1a
13995-11.1
13995-12.2
13995-7.1b

Site 7 Cliff Pillow Basalt
21794-19.1a
21794-20.1a
21794-21.2
21794-22.1a
21794-23.1a
21794-24.1a

Site 8 Main Sea Stack
Pillows
21794-1.1a
21794-3.1b
21794-4.2
21794-5.1a
21794-6.2

Site 2 Ankaramite (U-Pb Dated)
17994-6.1b
17794-9.2
17794-10.2b
17794-7.1a
17794-8.1
21794-26.1a

Site 16 Pillowed Headland
Mafic Dyke
16995-26.1
16995-22
16995-24
16995-25

Conglomerate Test Clasts

Amygdaloidal Alkaki Basalt
17794-11.2
17794-12.2b
17794-13.1A
17794-14.1a
17794-15.2
18794-1.3a
18794-2.1A
18794-3.3
18794-4.2
18794-5
19794-11.2A
19794-12.1A
19794-13.2
19794-14.2A
19794-15

Trachybasalt
19794-1.4
19794-2.1
19794-3.1
19794-4.1
19794-5.2
19794-6
19794-7
19794-8
19794-9
19794-10
1993-1.1A
1993-2B1A
1993-3
1993-4.1
1993-5.1
1993-6.1A
18794-13.1
18794-14.1
18794-15.1
18794-16.2
18794-17.2

SPEC. NAME: 18794-6.2B Site 3

TEMP	DECL.	INCL.	MOMENT
0	347.1	55.9	1.545E-02
5	348.9	53.4	1.484E-02
10	349.4	51.5	1.381E-02
15	349.5	50.6	1.238E-02
200	349.1	49.1	1.197E-02
250	349.1	49.2	1.180E-02
300	348.0	48.9	1.157E-02
350	348.2	48.7	1.118E-02
400	350.3	48.6	1.037E-02
450	349.5	48.0	8.961E-03
500	349.2	45.6	3.971E-03
520	348.7	49.8	7.971E-04
540	345.4	57.9	2.684E-04
560	308.0	75.6	9.684E-05
580	244.4	58.1	9.227E-05
600	211.6	67.2	8.629E-05

SPEC. NAME: 18794-7.3 Site 3

FIELD	DECL.	INCL.	MOMENT
0	360.0	50.9	9.926E-03
25	1.4	51.5	9.281E-03
50	357.4	52.9	8.611E-03
75	357.0	53.3	7.468E-03
100	358.8	53.2	6.142E-03
125	2.2	52.6	4.883E-03
150	3.0	52.6	4.034E-03
175	3.0	53.7	3.305E-03
200	5.2	52.8	2.850E-03
250	6.9	53.3	1.989E-03
300	6.2	53.8	1.496E-03
350	6.1	54.1	1.071E-03
400	12.1	55.1	7.168E-04

SPEC. NAME: 18794-8.1 Site 3

FIELD	DECL.	INCL.	MOMENT
0	330.6	67.0	1.051E-02
25	323.5	61.9	1.011E-02
50	323.4	63.4	9.756E-03
75	316.6	61.8	8.315E-03
100	312.3	58.2	7.225E-03
125	313.2	58.9	6.107E-03
150	312.6	55.2	4.852E-03
175	312.5	54.9	3.953E-03
200	313.6	54.7	3.239E-03
250	316.0	56.7	2.162E-03
300	315.7	58.5	1.475E-03
350	316.6	58.6	1.030E-03

SPEC. NAME: 18794-9.1 Site 3

FIELD	DECL.	INCL.	MOMENT
0	351.3	61.8	1.090E-02
25	349.0	59.3	1.051E-02
50	348.2	60.9	9.697E-03
75	347.7	60.0	8.380E-03
100	346.1	59.3	7.005E-03
125	347.8	57.7	5.513E-03
150	348.7	58.2	4.565E-03
200	351.4	58.8	3.333E-03
250	352.1	59.1	4.800E-03
251	352.1	59.1	2.400E-03
300	351.1	57.9	1.761E-03
350	352.6	60.5	1.344E-03
400	350.5	59.0	9.987E-04

SPEC. NAME: 18794-10.1 Site 3

FIELD	DECL.	INCL.	MOMENT
0	352.4	59.9	9.356E-03
25	351.1	60.9	9.215E-03
50	349.4	60.2	8.749E-03
75	348.9	60.2	8.130E-03
100	346.6	59.7	7.356E-03
150	345.6	59.6	5.852E-03
200	345.4	59.5	4.308E-03
250	346.3	60.3	3.348E-03
300	347.7	60.1	2.561E-03
400	350.0	62.4	1.434E-03
500	359.3	63.2	8.613E-04

SPEC. NAME: 18794-12.1a Site 3

FIELD	DECL.	INCL.	MOMENT
0	333.1	59.5	2.451E-02
25	332.2	59.4	2.423E-02
50	329.7	59.2	2.355E-02
75	328.3	59.1	2.264E-02
100	326.8	59.3	2.144E-02
125	325.6	59.2	2.016E-02
150	323.7	59.1	1.871E-02
175	322.6	59.1	1.667E-02
200	322.3	59.0	1.482E-02
250	321.1	59.1	1.139E-02
300	319.3	59.3	8.281E-03
350	319.5	58.9	5.799E-03
400	321.0	59.2	4.268E-03
500	312.1	61.1	2.078E-03

SPEC. NAME: 12995-7.1A Site 11

FIELD	DECL.	INCL.	MOMENT
0	97.8	82.4	3.158E-02
25	95.4	88.4	2.263E-02
50	87.4	86.2	1.771E-02
75	112.5	87.3	1.291E-02
100	152.6	87.1	9.273E-03
125	165.9	86.6	6.756E-03
150	176.1	85.6	5.126E-03
200	205.8	86.5	3.117E-03
250	192.4	82.4	2.093E-03

SPECIMEN NAME:12995-8.2B Site 11

FIELD	DECL.	INCL.	MOMENT
0	235.8	73.3	8.546E-05
25	230.5	69.6	7.682E-05
50	232.6	68.9	7.495E-05
75	233.4	68.7	7.188E-05
100	232.6	68.2	6.668E-05
150	226.7	71.2	5.810E-05
200	224.8	70.7	4.702E-05
250	219.1	69.1	3.892E-05
300	213.1	75.1	3.200E-05
400	358.1	68.0	1.690E-05
500	234.3	31.4	3.263E-05

SPECIMEN NAME:12995-9.2B Site 11

TEMP	DECL.	INCL.	MOMENT
0	143.8	-4.1	1.845E-04
5	143.8	-4.2	1.865E-04
10	147.0	-3.8	1.767E-04
300	11.7	44.2	6.534E-05
350	176.0	61.1	1.458E-04
400	181.3	62.6	1.303E-04
475	179.0	-26.8	4.813E-05
500	184.6	-32.6	4.576E-05

SPECIMEN NAME:12995-10.2 Site 11

FIELD	DECL.	INCL.	MOMENT
0	254.0	53.8	7.150E-05
25	266.2	50.1	6.634E-05
50	258.2	46.4	6.163E-05
75	255.8	44.7	5.747E-05
100	257.5	41.5	5.259E-05
150	257.0	36.1	4.626E-05
200	268.9	31.4	3.391E-05
250	258.0	21.6	3.060E-05
300	262.9	43.7	2.378E-05

SPEC. NAME: 12995-11.1A Site 11

TEMP	DECL.	INCL.	MOMENT
0	337.3	75.5	4.067E-02
3	332.4	75.6	3.878E-02
5	340.2	76.8	3.400E-02
200	342.4	81.2	1.620E-02
250	346.7	83.3	1.211E-02
300	341.9	85.5	9.182E-03
350	359.0	86.3	7.710E-03
400	28.2	87.9	6.157E-03
450	108.0	88.5	4.899E-03
500	122.9	84.7	2.997E-03
520	142.4	84.7	2.820E-03
540	129.3	85.5	2.269E-03
560	177.8	88.3	1.979E-03
580	218.7	64.1	7.327E-04
600	206.5	37.3	2.932E-04
620	229.3	20.8	1.357E-04
640	219.5	14.5	1.141E-04

SPEC. NAME: 12995-12.1A Site 11

FIELD	DECL.	INCL.	MOMENT
0	232.7	73.5	3.942E-05
25	232.5	73.6	3.412E-05
50	234.4	74.6	3.383E-05
75	232.9	75.4	3.316E-05
100	234.0	75.5	3.155E-05
150	230.4	76.3	2.707E-05
200	223.7	78.6	2.253E-05
250	226.2	77.3	1.884E-05
300	203.8	81.7	1.536E-05
400	15.0	78.0	8.255E-06

SPEC. NAME: 13995-1.1b TH Site12

TEMP	DECL.	INCL.	MOMENT
0	341.9	67.7	3.994E-03
5	329.9	73.2	3.309E-03
10	318.9	73.2	2.423E-03
15	327.4	76.7	1.825E-03
200	248.2	76.1	9.387E-04
300	228.5	78.9	7.202E-04
350	236.7	80.6	5.986E-04
400	263.3	81.6	5.362E-04
450	234.5	71.4	3.947E-04
475	242.4	69.2	2.966E-04
500	245.5	68.5	2.259E-04
525	221.4	67.6	1.155E-04
550	200.8	-0.6	5.430E-05

SPEC. NAME: 13995-2.1 Site 12

FIELD	DECL.	INCL.	MOMENT
0	281.4	39.3	1.439E-02
25	279.0	38.4	1.411E-02
50	276.1	37.7	1.343E-02
75	273.2	35.3	1.279E-02
100	272.5	35.2	1.271E-02
150	270.8	29.4	1.124E-02
200	271.0	25.5	9.831E-03
250	269.3	21.8	9.032E-03
300	272.2	23.1	7.027E-03
350	277.3	20.2	5.443E-03
400	267.3	19.6	4.665E-03
500	282.8	26.6	2.366E-03
600	295.8	13.5	1.401E-03

SPEC. NAME: 13995-3.2 Site 12

FIELD	DECL.	INCL.	MOMENT
0	239.0	68.8	7.127E-03
25	242.3	67.5	6.977E-03
50	240.8	65.3	6.667E-03
75	240.6	60.3	6.179E-03
100	241.7	58.3	5.611E-03
125	239.7	53.7	4.915E-03
150	242.0	50.5	4.612E-03
200	245.7	48.5	3.938E-03
250	255.6	45.1	3.131E-03
300	253.2	38.3	2.748E-03
400	265.1	54.5	1.292E-03
500	325.3	40.3	7.051E-04

SPEC. NAME: 13995-5.2A Site 12

FIELD	DECL.	INCL.	MOMENT
0	297.6	61.1	1.612E-02
25	295.7	57.4	1.530E-02
50	289.6	57.7	1.402E-02
75	284.3	53.2	1.257E-02
100	278.2	50.7	1.114E-02
125	273.2	48.6	1.037E-02
150	274.3	44.8	9.200E-03
200	273.7	39.2	7.568E-03
250	274.2	35.0	6.053E-03
300	274.1	30.5	5.043E-03
350	275.9	30.2	3.924E-03
400	283.2	27.4	3.053E-03
500	270.3	28.5	1.964E-03
600	304.9	40.1	1.082E-03

SPEC. NAME:13995-5.2b TH Site 12

TEMP	DECL.	INCL.	MOMENT
0	299.0	53.7	1.043E-02
5	285.6	45.3	1.119E-02
10	278.8	32.6	1.055E-02
15	274.4	24.5	9.676E-03
20	274.2	17.2	8.735E-03
25	276.2	13.0	7.491E-03
200	270.0	8.5	8.455E-03
300	273.8	7.9	8.192E-03
350	274.9	2.8	8.098E-03
400	278.4	0.6	7.688E-03
450	277.6	-3.0	6.920E-03
475	278.8	-4.7	6.687E-03
500	279.3	-7.4	6.260E-03
525	281.4	-9.3	4.718E-03
550	273.4	-6.6	3.479E-04
575	224.4	19.5	1.624E-04

SPEC. NAME: 13995-6.1B Site 12

FIELD	DECL.	INCL.	MOMENT
0	142.5	76.2	2.164E-02
25	147.2	77.8	2.023E-02
50	144.0	79.7	1.656E-02
75	141.6	80.4	1.256E-02
100	147.2	79.8	9.318E-03
125	142.2	80.4	7.466E-03
150	146.8	80.2	5.648E-03
175	146.6	80.5	4.355E-03
200	141.7	78.8	3.373E-03
225	145.3	78.6	2.684E-03
250	142.3	79.3	2.234E-03
300	133.3	80.8	1.540E-03

SPEC. NAME: 17794-1.2.2 Site 1

FIELD	DECL.	INCL.	MOMENT
0	264.1	84.2	3.659E-02
100	262.0	82.5	1.235E-02
125	257.1	81.4	8.900E-03
150	257.6	80.5	6.274E-03
175	262.0	79.3	4.504E-03
200	261.2	78.9	3.336E-03
225	263.0	77.4	2.472E-03
250	261.5	75.3	1.820E-03
300	264.5	74.1	1.185E-03
325	272.6	73.0	8.777E-04
350	277.0	72.2	6.961E-04
375	255.9	76.0	5.919E-04
400	299.9	78.0	3.912E-04

SPEC. NAME: 17794-2.2A Site 1

FIELD	DECL.	INCL.	MOMENT
0	277.9	75.6	2.077E-02
100	203.8	83.4	1.118E-02
125	202.2	82.6	8.046E-03
150	199.7	80.8	5.443E-03
175	197.4	79.7	3.904E-03
200	200.4	77.7	2.886E-03
225	205.2	79.5	2.107E-03
250	203.8	78.4	1.494E-03
275	211.6	78.6	1.148E-03
300	206.3	74.8	9.459E-04
325	219.8	71.9	6.354E-04
350	207.0	79.0	4.612E-04
375	215.0	81.7	4.185E-04
400	202.3	72.3	2.732E-04
425	272.3	76.1	1.822E-04

SPEC. NAME: 17794-3.1B Site 1

FIELD	DECL.	INCL.	MOMENT
0	11.1	59.7	2.243E-02
100	36.7	73.8	6.946E-03
125	53.6	78.1	4.771E-03
150	76.5	78.8	3.340E-03
200	105.8	77.6	1.686E-03
225	117.4	74.3	1.286E-03
250	117.3	71.6	9.648E-04
275	123.1	72.7	7.227E-04
300	130.2	73.3	5.880E-04
325	110.4	62.6	3.420E-04
350	150.9	71.8	2.452E-04

SPEC. NAME: 17794-4.1C Site 1

FIELD	DECL.	INCL.	MOMENT
0	19.8	63.0	2.447E-02
100	31.9	70.7	1.132E-02
125	33.2	73.9	8.489E-03
150	33.9	75.7	6.202E-03
175	29.8	76.9	4.411E-03
200	35.5	80.1	3.275E-03
225	30.0	81.1	2.458E-03
250	15.2	80.8	1.807E-03
275	19.1	80.0	1.350E-03
300	0.5	81.6	1.139E-03
325	359.4	79.4	7.851E-04
350	357.6	80.5	6.500E-04
375	18.9	81.6	5.851E-04
400	354.4	70.6	2.982E-04
425	325.5	76.0	3.082E-04
450	14.7	72.6	3.811E-04

SPEC. NAME: 17794-5.3 Site 1

FIELD	DECL.	INCL.	MOMENT
0	335.6	74.8	3.952E-02
100	349.5	77.1	1.672E-02
125	349.3	77.6	1.264E-02
150	355.5	77.7	9.414E-03
175	347.6	77.4	7.284E-03
200	341.3	75.9	5.699E-03
225	342.7	80.9	4.566E-03
250	342.7	80.0	3.448E-03
275	341.6	79.0	2.716E-03
300	347.7	82.5	2.141E-03
325	339.1	84.0	1.749E-03
350	328.0	79.0	1.572E-03
375	315.8	77.8	1.116E-03
400	111.8	85.3	1.074E-03
425	320.4	74.5	6.623E-04
450	247.2	85.9	6.934E-04

SPEC. NAME: 21794-25.1c Site 1

FIELD	DECL.	INCL.	MOMENT
0	220.1	62.8	2.913E-02
100	201.0	50.3	5.351E-03
125	197.5	62.0	6.601E-03
150	198.1	63.6	4.659E-03
175	198.4	60.5	3.518E-03
200	220.6	60.7	2.379E-03
225	215.9	63.9	1.772E-03
250	217.8	55.6	1.445E-03
275	235.8	46.1	1.187E-03
300	230.2	48.9	8.430E-04
325	232.4	52.1	6.096E-04
350	254.2	36.1	6.624E-04
350	275.3	22.0	6.268E-04
375	285.1	18.9	7.993E-04

SPEC. NAME: 19794-16.1 Site 4

FIELD	DECL.	INCL.	MOMENT
0	23.0	72.3	1.816E-02
25	21.2	73.2	1.744E-02
50	13.5	71.4	1.535E-02
75	10.2	72.7	1.320E-02
100	10.6	73.0	1.100E-02
125	8.8	72.3	8.958E-03
150	7.3	71.9	7.139E-03
175	7.1	71.3	5.727E-03
200	8.2	70.7	4.382E-03
250	11.6	71.0	2.963E-03
300	6.4	70.2	2.083E-03
350	16.6	70.8	1.427E-03

SPEC. NAME: 19794-17.1 Site 4

FIELD	DECL.	INCL.	MOMENT
0	347.5	58.3	2.519E-02
25	343.0	66.9	2.195E-02
50	345.3	69.8	1.924E-02
75	344.8	71.6	1.630E-02
100	345.2	70.9	1.311E-02
125	345.7	69.8	1.033E-02
150	346.0	68.7	7.979E-03
175	344.4	67.1	6.288E-03
200	344.1	65.7	4.704E-03
250	341.6	65.8	3.130E-03
300	339.8	62.7	2.107E-03

SPEC. NAME: 19794-18.1 Site 4

FIELD	DECL.	INCL.	MOMENT
0	54.7	70.6	2.224E-02
25	54.3	69.9	2.170E-02
50	53.6	72.5	1.930E-02
75	42.8	74.9	1.641E-02
100	37.2	75.6	1.410E-02
125	28.4	76.7	1.170E-02
150	21.1	76.6	9.799E-03
175	19.0	76.3	8.044E-03
200	18.9	76.8	6.637E-03
250	21.2	77.0	4.473E-03
300	17.8	76.4	3.053E-03
350	13.2	77.6	2.151E-03

SPEC. NAME: 19794-19.1 Site 4

FIELD	DECL.	INCL.	MOMENT
0	326.4	82.2	1.576E-02
25	325.9	80.6	1.461E-02
50	356.9	81.5	1.481E-02
75	6.9	80.2	1.424E-02
100	18.3	77.1	1.314E-02
125	22.6	75.6	1.199E-02
150	21.3	75.2	1.065E-02
175	20.3	74.5	9.226E-03
200	20.3	73.6	7.917E-03
250	15.9	72.4	5.816E-03
300	13.9	70.5	4.023E-03
350	15.0	69.3	2.974E-03
400	7.5	73.3	2.268E-03
450	8.4	71.3	2.012E-03
500	22.4	61.1	1.163E-03

SPEC. NAME: 19794-20.1 Site 4

FIELD	DECL.	INCL.	MOMENT
0	275.5	37.4	1.469E-02
25	280.8	38.4	1.350E-02
50	283.0	38.4	1.211E-02
75	284.0	43.3	9.743E-03
100	284.4	44.6	7.631E-03
125	285.1	46.5	5.902E-03
150	285.7	47.7	4.548E-03
175	285.7	48.0	3.649E-03
200	286.3	48.0	2.891E-03
250	282.8	49.9	1.903E-03
300	289.6	55.6	1.252E-03

SPEC. NAME: 19794-21.1a Site 4

FIELD	DECL.	INCL.	MOMENT
0	31.2	65.9	1.562E-02
25	20.9	68.1	1.493E-02
50	20.3	69.5	1.353E-02
75	19.6	69.2	1.182E-02
100	14.8	68.7	1.017E-02
125	15.9	68.0	8.655E-03
150	14.9	68.1	7.525E-03
200	12.8	67.4	5.696E-03
250	15.3	64.7	4.331E-03
300	16.4	64.4	3.338E-03
350	14.5	63.9	2.665E-03
400	18.8	63.4	2.156E-03
450	18.4	63.5	1.629E-03
500	23.4	59.9	1.353E-03

SPEC. NAME: 19794K-22.2 TH Site 6

TEMP	DECL.	INCL.	MOMENT
0	210.9	83.9	5.024E-04
5	193.2	79.3	4.626E-04
8	190.1	77.6	4.410E-04
10	188.6	74.3	4.330E-04
15	182.9	71.4	4.028E-04
20	182.5	68.8	3.802E-04
200	178.1	64.8	3.552E-04
300	178.9	64.0	3.120E-04
350	177.6	63.9	2.891E-04
400	178.5	64.6	2.403E-04
450	177.4	65.0	2.060E-04
475	175.4	64.2	1.888E-04
500	175.5	63.0	1.719E-04
525	179.3	62.3	1.626E-04
550	178.0	61.4	1.491E-04
575	177.8	60.6	1.473E-04
600	172.6	57.6	1.274E-04
625	174.0	58.9	1.143E-04
650	175.0	60.5	8.574E-05
675	187.1	54.1	2.858E-06

SPEC. NAME: 19794-23.2A Site 6

FIELD	DECL.	INCL.	MOMENT
0	12.8	75.6	3.019E-03
100	11.7	77.0	1.886E-03
125	12.5	77.4	1.513E-03
150	10.9	75.5	1.191E-03
175	357.9	77.5	9.363E-04
200	13.8	82.3	7.443E-04
225	3.3	81.4	6.145E-04
250	12.1	80.4	5.033E-04
275	35.8	83.5	4.185E-04
300	46.1	82.6	3.370E-04
325	68.8	82.2	3.035E-04
350	25.3	82.4	2.318E-04
375	280.0	88.7	2.191E-04
400	136.0	79.0	1.863E-04
425	161.8	72.7	1.629E-04
450	204.9	80.3	1.340E-04
475	216.1	68.0	1.011E-04
500	221.8	9.4	5.646E-05
500	222.7	50.9	8.954E-05
525	174.7	69.7	7.470E-05
550	69.3	48.0	9.430E-05
500	195.8	64.1	5.487E-05
525	196.7	60.5	4.877E-05
550	243.6	46.2	3.761E-05

SPEC. NAME: 19794-24.2 Site 6

TEMP	DECL.	INCL.	MOMENT
0	303.0	70.5	3.778E-03
5	303.5	70.5	3.414E-03
10	302.5	70.3	2.458E-03
200	7.6	73.5	8.236E-04
250	34.5	81.1	4.297E-04
300	127.0	79.4	2.776E-04
350	157.2	79.3	2.477E-04
400	75.0	62.0	2.276E-04
450	186.9	72.0	1.364E-04
500	143.6	40.3	6.887E-05
520	192.6	46.7	4.966E-05

SPEC. NAME: 19794-25.1 Site 6

FIELD	DECL.	INCL.	MOMENT
0	358.3	80.2	9.143E-04
25	10.0	79.0	8.075E-04
50	358.9	83.1	7.430E-04
75	24.1	83.1	6.455E-04
100	35.0	86.2	5.863E-04
125	51.8	88.2	4.942E-04
150	114.4	89.1	4.459E-04
200	162.6	85.7	3.545E-04
250	151.9	81.1	2.896E-04
300	149.6	79.0	2.483E-04
350	176.3	74.9	2.312E-04
400	140.5	70.3	2.068E-04
450	141.8	66.8	1.947E-04
500	137.8	80.4	2.050E-04
550	187.0	64.9	2.072E-04
600	132.2	61.5	1.777E-04
625	190.0	62.8	2.092E-04

SPEC. NAME: 21794-26.1 Site 6

FIELD	DECL.	INCL.	MOMENT
0	333.0	63.1	1.034E-03
25	334.7	61.9	9.497E-04
50	329.9	66.0	8.355E-04
75	331.6	67.6	7.653E-04
100	333.0	69.8	6.264E-04
125	329.1	75.2	5.200E-04
150	325.4	75.3	4.597E-04
200	317.3	82.2	3.451E-04
250	271.0	86.3	2.719E-04
300	209.9	86.0	2.294E-04
400	181.8	81.6	1.947E-04
500	207.0	72.1	1.875E-04

SPEC. NAME: 19794-27.3 Site 6

FIELD	DECL.	INCL.	MOMENT
0	353.6	65.6	2.186E-03
100	346.0	83.5	1.506E-03
125	355.1	68.3	1.455E-03
150	351.3	68.7	1.185E-03
175	353.2	68.9	9.813E-04
200	357.8	69.3	7.788E-04
225	354.6	68.9	6.619E-04
250	4.4	72.6	5.226E-04
275	1.4	76.0	4.444E-04
300	352.2	76.4	3.830E-04
325	23.5	70.2	3.272E-04
350	41.7	75.5	2.772E-04
375	0.6	74.4	2.268E-04
400	268.0	82.7	1.957E-04
425	183.0	76.3	1.518E-04
450	19.2	62.0	1.325E-04
475	202.4	25.8	2.578E-04
500	118.5	53.3	9.149E-05
525	326.1	65.3	5.487E-05
550	232.4	36.6	9.101E-05

SPEC. NAME: 21794-7.1 Site 9

FIELD	DECL.	INCL.	MOMENT
0	343.7	75.5	8.637E-03
25	338.9	76.6	7.936E-03
50	341.8	77.9	6.777E-03
75	342.1	78.4	5.584E-03
100	340.1	78.0	4.409E-03
125	341.9	79.0	3.807E-03
150	339.9	80.5	3.295E-03
200	347.7	81.8	2.591E-03
250	349.1	84.0	2.032E-03
300	352.1	86.5	1.590E-03
400	155.9	83.7	9.721E-04
450	150.9	77.3	7.055E-04
500	151.7	70.5	5.950E-04
550	157.6	62.3	4.836E-04
600	159.9	62.8	4.335E-04
700	158.8	58.6	4.089E-04

SPEC. NAME: 21794-8.2 Site 9

FIELD	DECL.	INCL.	MOMENT
0	342.9	67.1	1.133E-02
25	344.6	68.7	1.015E-02
50	339.9	67.3	9.260E-03
75	338.4	66.9	7.671E-03
100	337.6	68.4	6.423E-03
150	339.6	68.5	4.478E-03
200	340.9	71.3	3.345E-03
250	339.6	73.8	2.523E-03
300	338.3	77.2	1.820E-03
400	319.6	86.0	1.038E-03

SPEC. NAME: 21794-9.1 Site 9

FIELD	DECL.	INCL.	MOMENT
0	328.6	68.8	1.668E-02
25	323.6	66.8	1.573E-02
50	326.9	66.4	1.515E-02
75	325.2	65.5	1.385E-02
100	325.0	64.8	1.264E-02
150	325.3	64.4	1.013E-02
200	324.9	64.4	7.913E-03
250	326.0	65.5	6.170E-03
300	329.6	64.4	4.569E-03
350	330.3	66.1	3.598E-03
400	331.8	69.5	2.846E-03
500	335.8	70.2	1.604E-03

SPEC. NAME: 21794-10.1 Site 9

FIELD	DECL.	INCL.	MOMENT
0	281.6	75.4	4.034E-02
25	285.5	74.4	4.063E-02
50	288.0	74.2	4.035E-02
75	289.4	73.3	3.967E-02
100	290.9	72.5	3.871E-02
125	291.9	71.7	3.715E-02
150	292.1	70.9	3.550E-02
200	293.2	69.6	3.113E-02
250	293.4	68.6	2.611E-02
300	297.8	66.9	2.079E-02
350	295.7	67.0	1.585E-02
400	296.7	64.6	1.265E-02
450	309.6	62.1	8.402E-03
500	291.3	70.9	6.093E-03
550	298.6	61.8	5.448E-03
600	335.6	46.1	2.638E-03

SPEC. NAME: 21794-11.1 Site 9

FIELD	DECL.	INCL.	MOMENT
0	292.5	45.1	3.452E-03
50	294.1	57.2	2.306E-03
100	288.5	67.9	1.467E-03
125	293.3	65.8	1.206E-03
150	297.3	66.9	8.973E-04
175	294.4	67.9	7.354E-04
225	296.8	71.8	4.466E-04
250	282.1	73.6	3.774E-04
275	275.7	68.5	2.590E-04
300	277.9	70.7	1.506E-04
325	268.7	57.7	1.239E-04
350	255.1	64.2	1.404E-04
375	223.7	58.5	1.061E-04
400	234.4	73.3	6.754E-05
425	348.8	61.2	8.911E-05

SPEC. NAME: 21794-12 Site 9

TEMP	DECL.	INCL.	MOMENT
0	182.6	71.8	1.154E-02
3	185.2	71.4	9.691E-03
5	177.3	70.3	8.517E-03
10	175.9	70.8	6.241E-03
15	174.6	70.7	4.686E-03
200	152.0	66.6	2.263E-03
300	140.8	62.8	1.963E-03
350	147.1	59.1	1.796E-03
400	140.9	59.5	1.766E-03
450	148.5	50.8	1.059E-03
475	149.3	48.7	8.232E-04
500	162.9	52.6	3.814E-04
525	163.1	45.1	1.986E-04

SPEC. NAME: 21794-13.1 Site 5

FIELD	DECL.	INCL.	MOMENT
0	322.5	47.7	3.077E-02
25	321.4	46.9	3.148E-02
50	321.7	45.3	3.115E-02
75	321.9	44.2	3.070E-02
100	321.0	43.2	2.967E-02
125	321.2	42.6	2.801E-02
150	320.8	41.8	2.612E-02
175	320.4	41.9	2.370E-02
200	320.9	41.8	2.083E-02
225	321.0	41.2	1.825E-02
250	320.7	41.3	1.577E-02
300	321.2	41.4	1.175E-02
350	323.7	40.2	8.699E-03
400	317.0	40.8	5.900E-03
450	326.5	44.3	4.045E-03
500	333.7	35.9	3.647E-03
550	293.2	41.0	2.400E-03

SPEC. NAME: 21794-14.3 Site 5

TEMP	DECL.	INCL.	MOMENT
0	315.6	62.0	7.151E-03
5	317.5	63.7	6.697E-03
10	318.2	62.1	4.746E-03
200	321.6	61.2	4.165E-03
250	321.6	59.0	3.913E-03
300	322.9	58.3	3.671E-03
350	323.1	57.8	3.394E-03
400	324.3	59.1	2.980E-03
450	318.6	59.3	1.961E-03
500	315.5	70.4	4.170E-04
520	233.2	71.0	2.157E-04
540	218.6	75.6	2.256E-04
560	213.5	67.1	1.079E-04
580	187.3	58.3	1.967E-04
600	196.7	43.4	1.477E-04
620	183.9	52.0	1.001E-04
640	168.7	50.6	1.002E-04
660	126.7	8.9	1.911E-05

SPEC. NAME: 21794-15.1a Site 5

FIELD	DECL.	INCL.	MOMENT
0	295.7	33.9	2.254E-02
25	295.7	34.0	2.229E-02
50	294.9	33.4	2.217E-02
75	294.4	32.3	2.182E-02
100	294.1	32.1	2.102E-02
150	292.9	31.3	1.843E-02
200	293.0	30.6	1.465E-02
250	293.1	30.6	1.083E-02
300	292.6	29.4	7.785E-03
350	293.5	29.6	5.413E-03
400	293.2	30.2	3.692E-03
500	288.5	14.1	2.111E-03

SPEC. NAME: 21794-16.1a Site 5

FIELD	DECL.	INCL.	MOMENT
0	289.8	56.5	1.348E-02
25	295.1	55.9	1.261E-02
50	298.7	57.5	1.177E-02
75	300.3	55.7	1.083E-02
100	302.5	55.1	9.742E-03
150	305.0	53.0	7.876E-03
200	304.9	49.6	5.881E-03
250	304.5	49.4	4.489E-03
300	304.8	50.1	3.494E-03
400	309.4	47.3	1.949E-03
450	298.1	53.4	1.408E-03
500	301.3	57.1	1.217E-03

SPEC. NAME: 21794-17b Site 5

FIELD	DECL.	INCL.	MOMENT
0	352.2	76.4	1.054E-02
25	349.6	76.4	9.508E-03
50	342.7	74.9	8.251E-03
75	343.7	73.1	6.447E-03
100	343.1	72.5	4.638E-03
125	349.5	74.0	3.485E-03
150	348.3	74.7	2.642E-03
200	351.1	77.6	1.606E-03
250	18.2	80.8	1.037E-03

SPEC. NAME: 21794-18b Site 5

FIELD	DECL.	INCL.	MOMENT
0	313.8	56.9	1.283E-02
25	314.4	56.4	1.209E-02
50	312.6	55.8	1.157E-02
75	310.8	55.5	1.003E-02
100	309.8	53.2	8.665E-03
150	309.8	52.8	5.907E-03
200	308.8	53.0	3.845E-03
250	307.2	54.3	2.522E-03
300	307.2	57.4	1.591E-03
350	312.9	59.7	1.110E-03

SPEC. NAME: 12995-1.1b Site 10

TEMP	DECL.	INCL.	MOMENT
0	141.1	58.0	1.534E-04
5	140.2	56.8	1.460E-04
10	139.7	55.6	1.359E-04
200	137.9	51.2	1.196E-04
250	138.5	51.2	1.160E-04
300	138.9	52.2	1.075E-04
350	139.6	53.4	9.949E-05
400	140.3	54.2	8.888E-05
450	140.3	57.3	7.560E-05
500	139.5	63.8	4.533E-05
520	138.6	64.4	4.365E-05
540	140.1	66.0	3.824E-05
560	140.6	67.2	3.660E-05
580	140.0	67.1	3.434E-05
600	135.0	68.4	3.163E-05
620	140.0	67.8	2.875E-05
640	148.3	67.5	2.198E-05
660	112.0	-24.4	1.652E-06

SPEC. NAME: 12995-2.1A Site 10

FIELD	DECL.	INCL.	MOMENT
0	145.0	58.0	1.220E-04
25	146.6	56.7	1.193E-04
50	147.9	54.9	1.171E-04
100	150.2	53.4	1.100E-04
150	150.7	52.4	1.025E-04
200	148.3	51.4	9.183E-05
250	152.2	50.6	7.730E-05
300	153.4	50.3	6.655E-05
350	150.0	49.9	5.728E-05
400	147.5	48.7	4.489E-05
450	156.9	46.3	4.219E-05
500	147.2	46.8	4.015E-05
600	142.9	46.2	2.988E-05
700	161.5	37.8	3.600E-05

SPEC. NAME: 12995-3.1A Site 10

FIELD	DECL.	INCL.	MOMENT
0	135.6	69.9	1.087E-04
25	137.8	69.7	1.058E-04
50	140.4	68.7	1.048E-04
75	143.0	68.2	1.026E-04
100	142.7	68.1	1.009E-04
150	145.6	67.5	9.288E-05
200	146.8	68.7	8.367E-05
250	144.7	69.8	7.542E-05
300	155.0	71.9	6.668E-05
350	162.6	74.6	6.097E-05
400	144.7	67.6	5.972E-05
450	169.9	76.3	5.824E-05

SPEC. NAME: 12995-4.2.2 Site 10

FIELD	DECL.	INCL.	MOMENT
0	119.7	73.1	6.358E-05
25	121.9	72.4	5.982E-05
50	124.3	71.5	5.795E-05
75	124.6	70.7	5.602E-05
100	126.9	70.3	5.477E-05
150	129.6	70.0	5.240E-05
200	132.9	69.8	4.795E-05
250	132.6	69.6	4.333E-05
300	134.7	66.8	3.755E-05
350	136.8	67.4	3.597E-05
400	137.8	69.1	3.364E-05
500	131.7	58.3	2.621E-05
600	137.1	68.1	3.464E-05

SPEC. NAME: 12995-5.2 Site 10

FIELD	DECL.	INCL.	MOMENT
0	125.0	83.3	1.527E-04
25	125.2	83.4	1.526E-04
50	128.9	82.5	1.513E-04
75	121.6	81.7	1.493E-04
100	134.5	80.2	1.471E-04
150	132.1	81.8	1.429E-04
200	130.9	78.2	1.344E-04
250	141.5	79.5	1.213E-04
300	124.0	78.3	1.030E-04
350	106.0	81.2	1.050E-04
400	224.9	82.6	8.932E-05
450	99.7	61.4	6.290E-05

SPEC. NAME: 12995-6.2 Site 10

FIELD	DECL.	INCL.	MOMENT
0	200.0	73.0	7.566E-05
25	199.2	72.8	7.542E-05
50	195.8	72.0	7.374E-05
50	196.0	72.1	7.348E-05
100	190.4	71.2	6.926E-05
150	189.2	69.7	6.335E-05
200	187.2	69.7	5.617E-05
250	188.4	68.0	4.777E-05
300	193.7	68.3	4.123E-05
350	183.6	69.6	3.918E-05
400	187.1	65.3	2.983E-05
500	204.7	65.3	3.185E-05
600	168.3	71.1	3.514E-05

SPEC. NAME: 13996-1.2 Site 14

FIELD	DECL.	INCL.	MOMENT
0	321.5	79.4	1.786E-05
25	317.6	78.7	1.429E-05
50	311.5	81.8	1.161E-05
75	265.2	83.5	9.284E-06
100	199.9	86.9	7.337E-06
125	133.4	89.3	6.103E-06
150	268.6	84.0	5.978E-06
200	302.0	89.2	4.058E-06
250	344.8	81.3	3.657E-06
400	34.1	67.6	3.037E-06

SPEC. NAME: 13996-2.2b Site 14

FIELD	DECL.	INCL.	MOMENT
0	328.5	85.9	1.220E-05
25	227.3	85.3	9.598E-06
50	229.5	87.9	8.881E-06
75	174.3	82.5	7.304E-06
100	132.6	80.9	6.249E-06
125	138.1	83.3	5.717E-06
150	108.3	84.0	5.134E-06
200	93.7	83.4	4.834E-06
250	92.1	83.7	4.345E-06
300	71.5	82.4	4.031E-06
400	135.6	86.9	3.448E-06
500	90.8	75.5	3.317E-06

SPEC. NAME: 13996-3.2 Site 14

FIELD	DECL.	INCL.	MOMENT
0	173.9	64.2	1.058E-03
25	158.9	65.6	1.045E-03
50	168.9	61.8	8.009E-04
75	177.2	64.2	5.778E-04
100	179.5	62.6	4.828E-04
125	175.8	63.2	3.733E-04
150	180.1	61.9	2.876E-04
175	180.4	60.4	2.362E-04
200	174.7	61.8	2.028E-04
250	190.6	62.5	1.395E-04
300	194.7	59.2	1.098E-04
350	184.6	65.2	9.648E-05

SPEC. NAME: 13996-4.1A Site 14

FIELD	DECL.	INCL.	MOMENT
0	20.6	76.2	5.733E-04
25	331.6	70.8	6.076E-04
50	326.6	82.6	4.433E-04
75	354.9	79.5	3.309E-04
100	304.6	80.2	2.530E-04
125	301.0	83.3	2.092E-04
150	296.0	79.3	1.529E-04
175	259.2	77.1	1.276E-04
200	265.1	74.3	1.144E-04
250	247.9	67.1	7.088E-05
300	223.9	66.9	5.454E-05

SPEC. NAME:13995-13.2bTH Site14

TEMP	DECL.	INCL.	MOMENT
0	117.3	70.2	9.302E-05
5	119.5	70.7	9.421E-05
10	121.7	70.7	9.096E-05
15	122.3	71.6	8.398E-05
200	126.6	70.8	8.202E-05
300	126.4	71.8	7.416E-05
350	125.7	72.8	6.733E-05
400	126.5	73.5	6.412E-05
450	118.5	75.6	5.473E-05
475	113.3	76.9	4.873E-05
500	90.0	78.2	3.679E-05
525	81.5	78.4	3.308E-05
550	50.6	80.2	2.530E-05
575	48.7	79.0	2.573E-05
600	57.1	79.2	2.442E-05
625	58.5	78.6	2.183E-05
650	64.0	79.7	1.509E-05
675	194.6	54.2	1.207E-06

SPEC. NAME:13995-14.2aTH Site14

TEMP	DECL.	INCL.	MOMENT
0	128.6	44.8	1.065E-04
5	129.7	46.1	1.041E-04
10	130.9	46.4	9.803E-05
200	134.2	46.6	8.721E-05
300	134.0	48.4	7.613E-05
350	135.1	51.2	6.647E-05
450	133.1	59.8	5.419E-05
475	134.5	63.7	4.967E-05
500	123.3	69.0	3.630E-05
525	122.2	69.6	3.547E-05
550	117.6	72.6	3.045E-05
575	115.0	73.1	2.810E-05
600	112.6	72.2	2.575E-05
625	115.4	69.6	2.125E-05
650	116.4	63.4	1.308E-05
675	349.7	32.1	3.915E-07

SPEC. NAME: 13995-15A Site 14

FIELD	DECL.	INCL.	MOMENT
0	229.2	84.2	1.356E-04
25	219.8	84.2	1.338E-04
50	208.5	82.8	1.311E-04
100	190.5	80.5	1.225E-04
150	190.8	79.4	1.140E-04
200	187.2	78.9	1.025E-04
300	183.9	81.0	7.012E-05
350	216.3	81.9	6.221E-05
400	151.7	84.9	6.973E-05

SPEC. NAME: 16995-17.2 Site 14

FIELD	DECL.	INCL.	MOMENT
0	6.6	67.5	1.451E-05
25	358.6	66.5	1.375E-05
50	1.5	69.4	1.332E-05
100	3.1	67.5	1.049E-05
125	9.2	68.8	9.119E-06
150	6.5	71.0	8.097E-06
200	11.9	72.5	6.616E-06
250	2.8	71.8	5.419E-06
300	18.9	67.1	4.325E-06
400	33.8	72.3	3.752E-06

SPEC. NAME: 16995-18.1 Site 14

FIELD	DECL.	INCL.	MOMENT
0	4.7	49.1	2.630E-05
25	2.4	49.6	1.843E-05
50	11.5	56.9	1.445E-05
75	24.1	57.6	1.014E-05
100	25.8	68.0	7.581E-06
125	34.9	72.1	6.584E-06
150	51.7	68.5	5.844E-06
200	38.9	68.1	4.715E-06
250	29.8	70.4	4.313E-06
300	54.4	68.7	3.345E-06
350	45.7	71.1	3.216E-06
400	77.8	57.9	2.825E-06
500	29.9	52.4	3.816E-06

SPEC. NAME: 16995-19 Site 14

FIELD	DECL.	INCL.	MOMENT
0	287.7	74.1	1.316E-03
25	289.5	74.2	1.292E-03
50	284.5	74.7	1.205E-03
75	289.4	73.3	1.126E-03
100	275.6	74.8	1.007E-03
125	277.6	75.5	8.794E-04
150	287.4	74.7	8.265E-04
175	280.6	74.6	7.098E-04
200	283.4	74.9	6.375E-04
250	282.8	73.9	5.183E-04
300	287.7	75.1	4.334E-04
400	295.7	73.8	3.091E-04
500	285.7	71.2	2.038E-04
600	276.7	78.0	1.581E-04
700	297.5	73.2	1.157E-04

SPEC. NAME: 21794-19.1a Site 7

FIELD	DECL.	INCL.	MOMENT
0	132.2	-4.7	1.391E-02
25	134.2	-12.6	1.359E-02
50	132.4	-15.4	1.282E-02
75	131.6	-19.5	1.218E-02
100	132.9	-22.8	1.058E-02
125	134.0	-25.5	9.180E-03
150	132.9	-26.5	7.798E-03
175	131.8	-27.9	6.186E-03
200	130.7	-27.9	5.108E-03
250	131.0	-28.0	3.586E-03
300	124.7	-23.5	2.751E-03
400	132.8	-23.8	1.083E-03

SPEC. NAME: 21794-20.1a Site 7

FIELD	DECL.	INCL.	MOMENT
0	125.6	-2.1	1.044E-02
25	129.5	-5.2	1.011E-02
50	132.1	-14.5	1.064E-02
75	136.8	-21.9	1.052E-02
100	136.4	-25.1	1.020E-02
125	136.1	-29.3	9.319E-03
175	136.9	-33.6	7.470E-03
200	136.8	-34.6	6.605E-03
250	137.9	-35.9	5.131E-03
300	135.4	-36.5	4.029E-03
350	137.5	-38.6	2.976E-03
400	135.0	-37.7	2.148E-03
500	126.8	-29.2	1.474E-03
600	166.0	-55.7	7.378E-04

SPEC. NAME: 21794-21.2 Site 7

FIELD	DECL.	INCL.	MOMENT
0	114.3	35.7	7.236E-03
25	117.3	24.4	6.479E-03
50	125.3	13.0	5.271E-03
75	131.3	-6.2	5.009E-03
100	136.7	-23.6	5.439E-03
125	138.0	-31.5	5.794E-03
150	141.9	-36.5	5.888E-03
175	142.6	-39.3	5.934E-03
200	145.0	-42.2	5.661E-03
225	145.4	-42.8	5.327E-03
250	144.5	-44.7	4.935E-03
300	146.2	-46.7	4.152E-03
350	145.6	-46.7	3.276E-03
400	142.5	-46.8	2.692E-03
450	151.4	-55.2	2.158E-03
500	143.3	-42.1	1.256E-03
600	126.2	-35.1	1.230E-03

SPEC. NAME: 21794-22.1a Site 7

FIELD	DECL.	INCL.	MOMENT
0	148.0	10.7	5.777E-03
25	148.8	4.8	7.423E-03
50	149.2	-9.7	7.932E-03
75	154.4	-17.8	9.077E-03
100	153.4	-24.1	9.671E-03
125	153.6	-28.9	1.011E-02
150	153.6	-31.4	1.005E-02
175	154.6	-33.1	9.666E-03
200	153.9	-34.6	9.055E-03
225	153.9	-35.6	8.331E-03
250	154.7	-36.3	7.583E-03
275	153.4	-37.0	6.691E-03
300	154.3	-37.9	6.003E-03
350	153.1	-37.3	4.888E-03
375	156.1	-39.1	4.211E-03
400	152.8	-39.8	3.583E-03
425	150.8	-36.9	3.385E-03
450	161.9	-42.3	2.815E-03
500	147.7	-41.9	2.187E-03
550	144.5	-43.1	1.521E-03
600	131.8	-26.5	1.747E-03

SPEC. NAME: 21794-23.1a Site 7

FIELD	DECL.	INCL.	MOMENT
0	350.3	84.1	1.679E-02
25	346.9	85.4	1.517E-02
50	358.7	84.2	1.294E-02
75	41.1	85.6	1.027E-02
100	59.0	86.5	8.003E-03
125	96.1	84.8	6.125E-03
150	99.7	84.0	4.710E-03
175	113.7	84.6	3.621E-03
200	112.3	81.6	2.925E-03
250	116.9	81.1	1.915E-03
300	116.3	83.3	1.319E-03

SPEC. NAME: 21794-24.1a Site 7

FIELD	DECL.	INCL.	MOMENT
0	317.1	89.7	9.389E-03
25	7.6	88.9	8.978E-03
50	180.5	87.8	7.985E-03
75	154.6	85.4	6.575E-03
100	137.5	81.4	5.115E-03
125	138.6	77.1	3.839E-03
150	138.0	73.2	2.990E-03
175	135.0	71.0	2.321E-03
200	133.8	69.4	1.876E-03
225	139.5	69.1	1.460E-03
250	125.2	69.2	1.168E-03
275	127.1	69.9	9.580E-04
300	127.0	66.6	8.057E-04
325	117.4	64.6	6.951E-04

SPEC. NAME: 17794-6.1b Site 2

TEMP	DECL.	INCL.	MOMENT
0	283.7	52.3	9.872E-03
5	286.0	29.7	9.178E-03
10	284.8	27.4	6.124E-03
200	280.1	14.6	3.852E-03
250	273.8	22.2	3.080E-03
300	266.9	27.6	2.511E-03
350	260.9	31.4	2.039E-03
450	247.7	40.7	1.622E-03
500	243.9	39.2	1.192E-03
520	232.0	43.2	1.079E-03
540	239.5	42.5	9.091E-04
560	240.0	45.0	7.730E-04
580	219.3	15.4	5.863E-04
600	207.3	32.6	3.712E-04
620	233.0	-25.2	5.996E-05
640	196.3	41.3	1.098E-04

SPEC. NAME: 17794-7.1a Site 2

FIELD	DECL.	INCL.	MOMENT
0	269.6	5.2	4.211E-03
25	268.8	3.7	3.719E-03
50	268.4	5.0	3.337E-03
75	267.4	6.0	2.868E-03
100	268.6	7.0	2.422E-03
125	268.0	9.3	1.994E-03
150	266.8	11.0	1.660E-03
200	267.8	15.9	1.202E-03
250	266.1	38.7	9.039E-04
300	235.1	-4.4	5.474E-04

SPEC. NAME: 17794-8.1 Site 2

FIELD	DECL.	INCL.	MOMENT
0	90.7	27.3	1.447E-02
25	91.9	26.3	1.313E-02
50	92.8	26.8	1.201E-02
75	94.1	27.2	1.067E-02
100	94.5	28.1	9.440E-03
125	96.1	29.4	8.455E-03
150	97.9	30.3	7.440E-03
175	98.3	31.5	6.568E-03
200	100.4	33.8	5.858E-03
225	104.6	32.4	4.912E-03
250	100.6	35.7	4.175E-03
275	94.6	42.6	4.165E-03
300	117.5	24.9	3.102E-03
325	87.6	45.2	2.249E-03

SPEC. NAME: 17794-9.2 TH Site 2

TEMP	DECL.	INCL.	MOMENT
0	243.4	0.3	5.362E-03
5	243.2	3.6	4.903E-03
10	244.2	10.2	4.062E-03
15	242.4	15.6	3.061E-03
20	243.3	20.0	2.269E-03
200	243.7	35.5	1.554E-03
300	243.3	36.9	1.230E-03
350	244.7	37.8	1.046E-03
400	244.8	39.2	9.400E-04
450	244.5	39.9	8.304E-04
475	251.9	40.9	7.263E-04
500	242.6	41.4	6.627E-04
525	242.4	42.5	6.198E-04
550	240.2	44.7	3.028E-04
575	240.1	46.2	2.262E-04
600	146.9	-24.5	1.791E-05

SPEC. NAME:17794-10.2b TH Site 2

TEMP	DECL.	INCL.	MOMENT
0	50.7	-2.0	5.348E-03
5	51.3	-0.4	5.247E-03
10	51.9	2.3	4.673E-03
15	54.0	5.5	3.989E-03
20	56.3	8.2	3.299E-03
200	65.3	17.4	2.129E-03
300	75.8	23.7	1.621E-03
350	82.2	25.0	1.323E-03
400	89.3	27.7	1.193E-03
450	87.9	27.7	1.024E-03
475	92.3	27.6	9.204E-04
500	92.4	26.7	7.985E-04
525	104.8	31.6	5.824E-04
550	181.6	38.6	6.992E-05

SPEC. NAME: 21794-26.1a Site 2

FIELD	DECL.	INCL.	MOMENT
0	30.4	27.9	2.641E-02
25	33.3	30.8	2.307E-02
50	33.1	36.0	2.038E-02
75	35.1	41.6	1.687E-02
100	37.2	46.1	1.331E-02
125	40.3	50.9	1.029E-02
150	49.2	57.3	7.707E-03
175	48.1	57.8	5.446E-03
200	55.2	62.8	4.517E-03
250	90.4	57.7	1.798E-03
275	17.9	59.5	1.848E-03

SPEC. NAME: 16995-1.2A Site 15

FIELD	DECL.	INCL.	MOMENT
0	239.9	69.3	1.334E-05
25	241.5	72.7	1.341E-05
50	223.3	78.7	1.149E-05
75	227.4	80.6	1.135E-05
100	211.3	78.9	9.854E-06
125	185.5	80.8	9.097E-06
150	194.2	81.1	8.736E-06
175	206.0	80.4	8.025E-06
200	172.7	85.5	7.381E-06
250	3.9	88.1	6.560E-06
300	283.7	81.3	6.462E-06

SPEC. NAME: 16995-2.2A Site 15

FIELD	DECL.	INCL.	MOMENT
0	315.0	79.0	1.648E-05
25	333.7	79.7	1.608E-05
50	339.4	80.1	1.184E-05
75	325.9	80.0	1.224E-05
100	354.7	79.6	1.260E-05
125	16.1	81.4	1.027E-05
150	12.0	79.5	9.947E-06
175	20.3	80.5	9.043E-06
200	16.2	80.6	8.345E-06
225	25.4	80.7	7.938E-06
250	19.2	82.9	7.298E-06
300	39.8	79.8	6.156E-06
350	21.6	75.4	6.708E-06
400	22.3	83.9	6.072E-06

SPEC. NAME: 16995-3.1 Site 15

TEMP	DECL.	INCL.	MOMENT
0	99.0	79.6	1.105E-03
5	69.8	85.1	9.867E-04
10	127.0	86.0	6.019E-04
15	233.2	85.3	3.595E-04
200	225.9	75.8	1.666E-04
300	284.0	78.5	1.325E-04
350	293.6	76.2	1.291E-04
450	248.9	78.5	1.140E-04
475	212.4	82.0	1.008E-04
500	303.0	81.8	8.314E-05
525	294.7	81.0	6.113E-05
550	208.0	49.6	4.267E-05

SPEC. NAME: 16995-4.2A Site 15

TEMP	DECL.	INCL.	MOMENT
0	21.6	69.5	1.405E-03
5	346.0	73.4	1.138E-03
10	336.6	75.1	6.765E-04
200	288.1	73.4	4.417E-04
250	256.0	74.9	2.542E-04
300	270.3	77.7	2.585E-04
350	251.5	75.3	2.467E-04
400	247.7	71.8	2.156E-04
450	240.3	63.4	1.951E-04
500	205.1	56.6	1.296E-04
520	227.3	45.0	1.313E-04
540	211.5	2.2	1.560E-04
560	194.0	17.2	5.124E-05
580	215.5	19.2	2.028E-05
600	210.6	1.1	3.035E-05

SPEC. NAME: 16995-5.1 Site 15

FIELD	DECL.	INCL.	MOMENT
0	38.4	25.2	7.123E-04
25	35.3	30.9	5.214E-04
50	31.2	48.3	3.720E-04
75	34.6	47.8	2.648E-04
100	32.6	52.9	1.734E-04
125	30.0	56.6	1.240E-04
150	33.6	56.8	9.298E-05
200	31.3	62.0	5.479E-05
225	37.6	70.6	4.916E-05
250	44.0	63.4	3.574E-05
275	14.6	66.7	3.037E-05

SPEC. NAME: 16995-6.1 Site 15

TEMP	DECL.	INCL.	MOMENT
0	239.9	82.0	2.152E-03
3	236.7	77.9	1.726E-03
5	227.9	81.4	1.376E-03
10	198.8	84.5	6.955E-04
200	160.8	81.8	2.963E-04
300	157.8	72.9	2.382E-04
350	168.1	77.7	2.244E-04
450	154.7	74.1	1.911E-04
475	175.5	71.7	1.694E-04
500	161.7	64.3	1.609E-04
525	157.6	66.0	1.459E-04
550	235.6	26.5	6.069E-05
575	196.4	34.3	2.217E-05

SPEC. NAME: 16995-20.2 Site 15

FIELD	DECL.	INCL.	MOMENT
0	41.7	45.3	1.023E-03
25	36.5	62.0	5.703E-04
50	51.3	63.5	4.915E-04
75	46.7	74.8	3.562E-04
100	60.0	70.5	2.475E-04
125	76.5	74.2	1.811E-04
150	71.6	74.8	1.362E-04
175	68.0	74.9	1.030E-04
200	74.1	80.3	9.003E-05
250	99.7	80.7	7.610E-05

SPEC. NAME: 13995-7.1A Site 13

FIELD	DECL.	INCL.	MOMENT
0	191.4	-43.0	4.000E-03
100	161.0	26.5	2.128E-03
150	155.5	36.8	2.313E-03
175	153.6	44.4	1.997E-03
175	152.7	44.2	2.005E-03
200	146.8	47.5	1.759E-03
225	150.2	49.1	1.592E-03
250	151.0	48.0	1.335E-03
275	142.4	50.4	1.145E-03
300	141.1	60.5	1.413E-03
325	152.0	45.6	8.231E-04
350	131.9	60.4	6.347E-04
375	153.7	58.5	5.640E-04
400	161.7	45.9	5.909E-04
425	74.7	49.6	5.298E-04
450	153.7	69.5	3.454E-04
475	166.5	23.7	4.019E-04
500	27.6	26.7	4.234E-04
525	122.7	80.8	3.097E-04
550	154.1	16.2	5.598E-04
575	19.7	11.2	5.125E-04
600	81.0	69.7	2.469E-04
625	167.7	28.8	5.479E-04

SPEC. NAME: 13995-8.3TH Site 13

TEMP	DECL.	INCL.	MOMENT
0	104.5	51.0	1.384E-02
5	104.2	52.2	1.203E-02
10	103.0	53.9	8.033E-03
15	104.6	55.6	4.916E-03
200	108.1	59.5	2.799E-03
300	106.0	60.1	2.157E-03
350	108.8	61.1	1.781E-03
400	111.4	61.9	1.485E-03
450	121.0	60.5	1.100E-03
475	125.8	61.6	1.000E-03
500	125.5	57.0	7.906E-04
525	150.5	49.9	4.785E-04
550	182.5	36.8	1.547E-04

SPEC. NAME: 13995-9A Site 13

FIELD	DECL.	INCL.	MOMENT
0	217.4	74.6	2.340E-02
100	223.0	80.3	1.020E-02
150	197.9	80.2	6.016E-03
175	210.5	81.9	4.446E-03
200	212.6	79.6	3.370E-03
225	208.4	79.7	2.754E-03
250	204.0	77.5	2.086E-03
275	201.2	77.7	1.642E-03
300	208.9	74.1	1.395E-03
325	208.8	75.3	8.760E-04
350	197.1	67.7	8.275E-04
375	191.3	69.7	8.070E-04
400	220.8	69.5	5.246E-04
425	211.6	63.7	4.089E-04

SPEC. NAME: 13995-10.1a Site 13

TEMP	DECL.	INCL.	MOMENT
0	32.3	65.8	1.976E-02
5	31.8	66.7	1.595E-02
10	33.4	69.7	1.111E-02
200	41.3	73.7	5.402E-03
250	50.5	74.7	4.362E-03
300	58.7	76.1	3.708E-03
350	72.0	78.0	3.148E-03
400	93.9	77.9	2.636E-03
450	122.5	78.1	2.052E-03
500	149.1	77.7	1.258E-03
520	169.0	72.3	1.157E-03
540	182.7	79.7	5.959E-04
560	206.3	78.1	4.223E-04
580	192.2	29.6	2.916E-04
600	206.6	-0.5	2.190E-04

SPEC. NAME:13995-11.1TH Site 13

TEMP	DECL.	INCL.	MOMENT
0	23.1	51.9	3.887E-03
5	22.6	55.6	3.042E-03
10	24.4	58.6	1.865E-03
15	24.0	59.2	1.117E-03
200	25.5	68.9	7.754E-04
300	33.9	67.4	6.280E-04
350	34.1	70.2	5.024E-04
400	42.0	70.0	3.951E-04
450	74.1	49.7	2.739E-04
475	47.2	75.6	2.231E-04
500	40.3	75.6	1.863E-04
525	191.8	53.4	7.280E-05

SPEC. NAME: 13995-12.2 Site 13

FIELD	DECL.	INCL.	MOMENT
0	57.2	71.0	1.161E-04
25	56.0	70.9	1.149E-04
50	56.8	71.2	1.144E-04
75	55.1	71.2	1.124E-04
100	55.9	71.2	1.097E-04
150	53.7	70.5	1.026E-04
200	51.3	69.5	9.395E-05
250	50.8	69.8	8.578E-05
300	48.0	68.9	7.541E-05
350	43.7	65.8	6.320E-05
400	47.9	70.3	5.316E-05
450	44.1	53.2	3.006E-05
500	32.9	56.8	3.472E-05

SPEC. NAME: 21794-1.1a Site 8

FIELD	DECL.	INCL.	MOMENT
0	187.6	24.7	5.437E-03
25	198.6	60.5	5.547E-03
50	168.3	52.6	4.724E-03
75	169.3	46.8	3.638E-03
100	161.9	46.8	2.561E-03
125	155.5	41.6	1.950E-03
150	157.5	38.1	1.504E-03
175	159.1	38.2	1.057E-03
200	154.5	37.2	8.857E-04
250	147.9	38.2	5.316E-04

SPEC. NAME: 21794-3.1b TH Site 8

TEMP	DECL.	INCL.	MOMENT
0	234.0	21.9	1.135E-02
5	214.4	24.2	6.847E-03
10	196.1	19.7	4.452E-03
15	185.8	17.8	3.102E-03
200	164.4	11.4	3.201E-03
300	158.1	8.4	3.073E-03
350	159.4	4.9	2.854E-03
450	156.4	2.3	2.150E-03
475	154.8	3.6	1.793E-03
500	154.5	4.1	1.381E-03
525	166.6	10.7	8.891E-04
550	162.5	25.6	4.597E-04
575	214.8	8.8	1.189E-04

SPEC. NAME: 21794-4.2 Site 8

FIELD	DECL.	INCL.	MOMENT
0	53.5	51.5	4.486E-03
25	66.7	56.3	5.135E-03
50	110.2	66.0	4.303E-03
75	114.8	59.9	3.580E-03
100	130.0	54.4	2.775E-03
125	131.2	49.1	2.169E-03
150	132.1	44.5	1.729E-03
175	134.5	42.3	1.428E-03
200	132.5	40.4	1.181E-03
250	135.1	40.4	8.136E-04
300	137.9	46.0	6.260E-04
350	143.7	48.5	3.871E-04

SPEC. NAME: 21794-5.1a Site 8

FIELD	DECL.	INCL.	MOMENT
0	138.3	17.5	7.263E-03
25	136.0	33.1	7.567E-03
50	141.6	34.8	6.692E-03
75	145.7	31.7	4.881E-03
100	149.7	23.6	3.652E-03
125	150.1	16.7	2.612E-03
150	152.1	14.2	2.064E-03
175	150.8	13.5	1.538E-03
200	153.2	12.4	1.126E-03
225	152.6	13.1	9.134E-04
250	152.3	14.7	6.859E-04
275	148.7	14.8	5.712E-04

SPEC. NAME: 21794-6.2 Site 8

FIELD	DECL.	INCL.	MOMENT
0	150.3	85.6	1.116E-02
25	153.6	83.1	1.061E-02
50	159.5	82.3	1.009E-02
75	148.0	77.9	8.234E-03
100	154.8	69.1	6.322E-03
125	154.4	58.3	4.867E-03
150	156.2	46.6	3.945E-03
175	155.7	33.4	3.290E-03
200	157.2	24.7	2.998E-03
225	156.0	16.6	2.637E-03
250	156.2	10.6	2.356E-03
300	155.1	0.4	1.896E-03
350	151.3	-2.9	1.361E-03
400	152.3	-4.5	1.274E-03
500	164.0	-28.7	6.683E-04

SPEC. NAME: 16995-22.1b Site 16

FIELD	DECL.	INCL.	MOMENT
0	337.3	58.6	9.620E-03
25	353.0	68.2	7.264E-03
50	347.5	68.1	5.173E-03
75	344.3	77.0	3.136E-03
100	351.6	84.2	2.020E-03
125	55.0	89.2	1.327E-03
150	194.4	84.9	9.104E-04
175	203.6	85.3	6.499E-04
200	175.4	83.0	4.928E-04
225	191.7	77.8	3.232E-04

SPEC. NAME: 16995-24.1a Site 16

FIELD	DECL.	INCL.	MOMENT
0	199.2	28.2	1.075E-02
25	194.4	26.8	8.086E-03
50	199.0	33.6	5.428E-03
75	201.8	39.0	3.477E-03
100	204.0	45.0	2.138E-03
125	204.2	52.3	1.400E-03
150	203.3	56.2	9.666E-04
175	203.9	61.2	6.590E-04
200	206.8	66.0	5.085E-04
225	191.6	67.0	3.915E-04
250	217.0	73.9	3.485E-04

SPEC. NAME: 16995-25.2 Site 16

FIELD	DECL.	INCL.	MOMENT
0	272.9	30.9	3.849E-03
25	263.3	25.0	3.895E-03
50	259.7	20.0	2.978E-03
75	256.9	15.8	2.467E-03
100	253.6	17.4	1.791E-03
125	249.1	17.6	1.335E-03
150	245.3	18.4	1.052E-03
200	225.1	20.9	6.582E-04
250	229.4	15.6	5.218E-04
300	308.1	45.4	2.268E-04

SPEC. NAME: 16995-26.1 TH Site 16

TEMP	DECL.	INCL.	MOMENT
0	57.4	29.8	1.132E-02
5	68.0	26.2	9.182E-03
10	76.9	26.6	6.160E-03
15	86.5	27.8	3.641E-03
200	119.6	19.4	2.499E-03
300	136.7	18.2	1.987E-03
350	142.5	16.5	1.700E-03
400	144.5	21.3	1.432E-03
450	150.4	28.6	1.072E-03
475	159.8	19.7	8.830E-04
500	153.7	23.0	6.817E-04
525	160.5	36.2	1.667E-04
550	166.0	33.8	1.664E-04

SPEC. NAME:17794-11.2 Amyg Test

FIELD	DECL.	INCL.	MOMENT
0	39.4	69.6	1.346E-02
50	48.3	63.4	7.824E-03
75	45.0	62.0	6.009E-03
100	50.5	53.0	4.776E-03
125	52.1	49.4	4.045E-03
150	55.0	44.8	3.475E-03
175	55.5	23.0	2.368E-03
200	55.8	40.5	2.447E-03
225	53.9	40.0	2.010E-03
250	56.8	40.3	1.647E-03
300	58.0	41.7	1.091E-03
350	57.3	47.1	7.167E-04

SPEC. NAME:17794-12.2B TH Amyg Test

TEMP	DECL.	INCL.	MOMENT
0	120.0	58.9	1.595E-02
3	102.8	65.1	1.016E-02
200	90.2	66.7	5.610E-03
250	91.0	67.0	4.559E-03
300	86.1	65.3	3.894E-03
350	90.2	64.8	2.981E-03
400	96.3	64.7	2.405E-03
500	78.3	67.1	1.083E-03
520	76.1	65.4	9.269E-04
540	117.5	73.1	4.783E-04
560	122.0	78.4	2.224E-04
580	175.2	24.4	2.238E-04
600	208.4	9.9	3.261E-04

SPEC. NAME:17794-13.1A Amyg Test

FIELD	DECL.	INCL.	MOMENT
0	72.0	82.2	1.872E-02
25	79.4	82.0	1.677E-02
50	71.5	80.0	1.499E-02
75	85.6	78.4	1.202E-02
100	90.1	76.3	9.748E-03
125	95.0	73.9	7.878E-03
150	103.3	70.1	6.638E-03
175	102.1	69.7	5.525E-03
200	104.2	65.5	4.644E-03
225	105.3	65.3	4.070E-03
250	104.3	65.0	3.592E-03
300	103.9	63.3	2.920E-03
350	105.3	62.3	2.202E-03
400	108.3	59.3	1.900E-03
450	103.3	61.3	1.258E-03

SPEC. NAME:17794-14.1A TH Amyg Test

TEMP	DECL.	INCL.	MOMENT
0	278.4	74.6	1.590E-02
3	294.3	69.1	1.429E-02
200	292.8	66.0	9.459E-03
250	287.7	63.4	7.984E-03
300	288.9	61.0	6.868E-03
350	288.5	57.3	5.641E-03
400	284.6	58.3	4.826E-03
500	269.5	65.8	2.032E-03
520	272.4	67.7	1.704E-03
540	256.3	69.0	1.375E-03
560	253.8	70.0	6.693E-04
580	218.1	37.4	6.184E-04
600	241.0	57.7	1.847E-04

SPEC. NAME:17794-15.2 Amyg Test

FIELD	DECL.	INCL.	MOMENT
0	115.7	83.1	1.383E-02
25	111.5	82.9	1.318E-02
50	136.7	79.6	1.187E-02
75	144.2	75.4	9.922E-03
100	149.7	71.6	8.550E-03
125	149.0	68.2	7.288E-03
150	150.7	65.5	6.378E-03
200	153.5	61.1	4.983E-03
250	156.3	58.7	3.837E-03
300	155.0	58.1	2.957E-03
350	155.2	57.3	2.315E-03
400	158.7	59.5	1.822E-03
500	152.7	65.1	1.070E-03

SPEC. NAME: 18794-1.3A TH Amyg Test

TEMP	DECL.	INCL.	MOMENT
0	110.2	70.6	1.355E-02
3	131.1	70.5	1.165E-02
200	165.3	58.7	7.322E-03
250	166.4	51.1	6.194E-03
300	167.5	43.9	5.260E-03
350	172.4	39.7	4.439E-03
400	171.6	37.6	3.858E-03
500	166.5	44.2	1.929E-03
520	169.4	43.9	1.635E-03
540	169.4	44.1	1.346E-03
560	171.1	48.0	9.734E-04
580	183.2	39.2	6.381E-04
600	175.4	29.1	2.378E-04
620	220.5	51.8	6.499E-05
640	199.0	4.8	1.582E-04

SPEC. NAME:18794-2.1A Amyg Test

FIELD	DECL.	INCL.	MOMENT
0	305.5	70.4	1.490E-02
25	298.9	70.9	1.340E-02
50	300.9	68.6	1.205E-02
75	292.5	67.4	1.003E-02
100	288.4	64.5	8.115E-03
125	284.0	60.9	6.656E-03
150	280.0	57.8	5.576E-03
200	275.5	50.4	4.142E-03
250	274.9	47.3	3.231E-03
300	273.6	44.2	2.526E-03
400	266.4	43.3	1.554E-03
500	273.4	36.5	9.946E-04

SPEC. NAME: 18794-3.3 Amyg Test

FIELD	DECL.	INCL.	MOMENT
0	135.4	76.6	1.322E-02
25	116.4	75.8	1.261E-02
50	137.5	73.2	1.049E-02
75	131.8	70.0	8.649E-03
100	125.2	70.2	6.826E-03
125	123.4	65.8	5.251E-03
150	125.4	60.5	4.059E-03
200	116.9	53.9	2.583E-03
250	115.7	50.2	1.691E-03
300	114.2	44.8	1.177E-03

SPEC. NAME: 18794-4.2 Amyg Test

FIELD	DECL.	INCL.	MOMENT
0	337.9	72.6	1.440E-02
25	331.0	72.4	1.366E-02
50	334.8	72.0	1.192E-02
75	333.0	71.9	9.540E-03
100	330.9	70.3	7.475E-03
150	327.3	66.9	4.651E-03
200	323.5	62.7	3.111E-03
300	316.4	58.8	1.755E-03
400	312.0	53.0	1.067E-03

SPEC. NAME: 18794-5.1 Amyg Test

FIELD	DECL.	INCL.	MOMENT
0	303.7	75.8	1.340E-02
25	301.4	78.1	1.232E-02
50	297.5	75.1	1.061E-02
75	288.5	76.1	8.643E-03
100	278.8	72.9	6.412E-03
125	276.4	70.2	4.893E-03
150	266.7	66.2	3.798E-03
200	265.4	62.2	2.576E-03
250	261.2	55.7	1.838E-03
300	264.4	51.4	1.317E-03

SPEC. NAME: 19794-11.2A Amyg Test

FIELD	DECL.	INCL.	MOMENT
0	178.8	82.6	1.395E-02
25	189.9	83.2	1.362E-02
50	181.5	78.8	1.184E-02
75	178.4	75.5	1.030E-02
100	176.4	72.3	8.705E-03
125	172.9	67.6	7.585E-03
150	172.6	63.7	6.458E-03
200	171.9	59.0	5.011E-03
250	171.0	56.1	3.864E-03
300	169.2	55.5	2.947E-03
400	167.1	52.4	1.801E-03
500	185.9	51.5	8.798E-04

SPEC. NAME: 19794-12.1A Amyg Test

FIELD	DECL.	INCL.	MOMENT
0	60.0	72.4	9.808E-03
25	42.7	74.0	9.738E-03
50	61.9	69.2	7.702E-03
75	69.3	69.1	5.590E-03
100	65.2	64.4	4.013E-03
125	65.8	63.2	3.083E-03
150	67.9	62.3	2.279E-03
200	55.2	62.8	1.384E-03
250	54.3	58.7	8.988E-04

SPEC. NAME:19794-13.2 Amyg Test

FIELD	DECL.	INCL.	MOMENT
0	290.0	83.8	1.028E-02
25	261.0	82.0	1.021E-02
50	280.1	83.4	8.611E-03
75	248.0	83.3	6.811E-03
100	214.2	83.3	5.251E-03
125	204.3	78.4	4.022E-03
150	193.4	73.5	3.132E-03
200	184.1	65.4	2.026E-03
250	186.5	57.6	1.377E-03
300	185.2	55.1	1.027E-03
350	169.9	48.0	8.419E-04

SPEC. NAME: 19794-14.2A Amyg Test

FIELD	DECL.	INCL.	MOMENT
0	44.3	84.5	1.359E-02
25	24.5	83.7	1.354E-03
50	43.0	83.1	1.242E-02
75	65.1	82.4	1.096E-02
100	70.3	79.6	9.371E-03
125	74.5	75.7	7.410E-03
150	78.2	70.9	5.917E-03
200	82.0	64.8	4.612E-03
250	83.2	57.9	3.629E-03
300	84.5	49.1	2.685E-03
400	87.3	40.0	1.732E-03
500	86.0	39.2	1.066E-03

SPEC. NAME: 19794-15 Amyg Test

FIELD	DECL.	INCL.	MOMENT
0	340.1	75.6	1.220E-02
25	341.4	74.7	1.159E-02
50	342.6	75.3	1.076E-02
75	344.3	75.7	9.349E-03
100	345.3	75.3	7.962E-03
150	355.2	73.8	5.069E-03
200	5.0	70.9	3.093E-03
250	11.1	66.6	2.059E-03
300	14.7	63.8	1.729E-03
400	22.8	54.2	1.019E-03

SPEC. NAME: 19794-1.4 Tryb Test

FIELD	DECL.	INCL.	MOMENT
0	275.4	57.7	2.503E-02
25	276.5	57.0	2.416E-02
50	276.6	56.6	2.385E-02
75	275.9	55.9	2.318E-02
100	275.2	54.8	2.202E-02
125	276.2	55.4	2.085E-02
150	275.6	55.2	2.011E-02
175	276.8	54.2	1.645E-02
200	278.2	54.6	1.421E-02
225	275.0	54.2	1.116E-02
250	275.3	54.3	9.120E-03
275	274.8	52.7	7.640E-03
300	277.2	54.5	6.352E-03
350	273.4	45.7	4.632E-03
400	274.9	59.5	2.905E-03
450	274.5	38.6	2.203E-03

SPEC. NAME: 19794-2.1 TH Tryb Test

TEMP	DECL.	INCL.	MOMENT
0	28.0	19.0	3.013E-02
3	29.5	16.0	2.978E-02
5	30.7	14.8	2.970E-02
8	31.1	12.8	2.953E-02
200	33.9	9.3	3.034E-02
250	34.1	8.8	3.024E-02
300	32.7	8.2	2.948E-02
350	33.8	7.5	2.705E-02
400	34.8	7.2	2.284E-02
450	33.0	6.8	1.914E-02
500	34.1	10.3	1.643E-03
520	34.7	13.8	1.126E-03
540	44.0	71.5	9.104E-04
560	22.9	19.6	2.018E-04
580	28.4	24.4	9.117E-05
600	65.3	31.5	3.546E-05

SPEC. NAME: 19794-3.1 Tryb Test

FIELD	DECL.	INCL.	MOMENT
0	115.5	19.2	1.285E-02
25	114.6	16.1	1.303E-02
50	114.8	11.6	1.259E-02
75	114.9	7.4	1.180E-02
100	114.0	5.3	1.028E-02
125	113.1	4.7	8.973E-03
150	114.4	4.2	7.336E-03
175	114.6	4.8	5.337E-03
200	114.5	3.9	4.381E-03
225	113.6	3.9	3.621E-03
250	114.2	3.4	2.980E-03
300	116.6	3.1	2.200E-03
350	111.5	5.4	1.768E-03
400	114.4	1.4	1.095E-03

SPEC. NAME: 19794-4.1 Tryb Test

FIELD	DECL.	INCL.	MOMENT
0	84.2	-44.0	9.429E-03
25	85.4	-46.3	9.925E-03
50	88.2	-48.2	1.062E-02
75	89.8	-49.9	1.053E-02
100	91.1	-51.9	9.719E-03
125	91.5	-51.7	9.659E-03
150	90.0	-52.7	6.669E-03
175	88.3	-51.8	5.100E-03
200	89.2	-52.3	4.182E-03
225	87.3	-52.1	3.433E-03
250	90.7	-50.3	2.785E-03
300	90.9	-52.9	1.944E-03
350	82.9	-48.2	1.578E-03
400	95.5	-39.4	1.145E-03
450	97.8	-33.5	9.302E-04

SPEC. NAME: 19794-5.2 Tryb Test

FIELD	DECL.	INCL.	MOMENT
0	52.2	57.2	2.764E-02
25	52.1	57.5	2.731E-02
50	52.2	56.3	2.682E-02
75	51.2	55.1	2.622E-02
100	51.9	55.2	2.558E-02
125	51.7	55.2	2.378E-02
150	52.1	54.6	2.191E-02
175	52.2	54.7	1.989E-02
200	51.6	54.8	1.722E-02
225	50.1	54.7	1.519E-02
250	52.1	54.5	1.280E-02
300	50.8	54.3	8.968E-03
350	42.6	50.9	7.061E-03
400	64.6	54.9	4.388E-03
450	42.4	42.8	2.416E-03

SPEC. NAME: 19794-6 Tryb Test

FIELD	DECL.	INCL.	MOMENT
0	167.2	76.9	2.001E-02
25	168.7	76.1	1.968E-02
50	170.8	74.6	1.866E-02
75	168.8	73.3	1.701E-02
100	170.6	72.5	1.501E-02
125	173.4	71.7	1.286E-02
150	173.6	71.0	1.053E-02
175	173.7	70.9	8.661E-03
200	173.6	71.2	7.511E-03
250	174.1	69.9	4.778E-03
300	171.8	66.5	3.694E-03
350	174.5	70.5	2.612E-03
400	173.2	75.1	1.700E-03
450	163.7	64.8	1.464E-03

SPEC. NAME: 19794-7 Tryb Test

FIELD	DECL.	INCL.	MOMENT
0	167.6	67.0	2.009E-02
25	166.6	65.3	1.961E-02
50	165.4	64.6	1.857E-02
75	164.7	63.4	1.741E-02
100	164.9	63.7	1.522E-02
125	164.7	63.0	1.281E-02
150	164.3	62.9	1.054E-02
175	163.6	63.0	8.613E-03
200	164.4	63.0	7.059E-03
225	163.0	64.5	5.868E-03
250	164.8	61.7	4.696E-03
300	170.3	62.2	3.342E-03
350	160.3	68.8	2.541E-03
400	160.5	71.3	1.973E-03

SPEC. NAME: 19794-8 Tryb Test

FIELD	DECL.	INCL.	MOMENT
0	94.5	84.0	1.441E-02
25	133.5	84.4	1.254E-02
50	98.6	75.2	9.339E-03
75	106.2	73.2	6.945E-03
100	112.1	71.4	4.949E-03
125	113.6	69.0	3.477E-03
150	117.3	68.4	2.536E-03
175	117.0	68.4	1.867E-03
200	119.0	68.4	1.514E-03
225	135.7	64.2	1.129E-03

SPEC NAME: 19794-9 Tryb Test

FIELD	DECL.	INCL.	MOMENT
0	281.3	-69.4	1.315E-02
25	281.9	-70.8	1.401E-02
50	277.7	-74.4	1.436E-02
75	277.3	-77.7	1.508E-02
100	274.3	-80.6	1.515E-02
125	275.6	-81.7	1.488E-02
150	273.5	-82.2	1.410E-02
175	277.8	-83.3	1.313E-02
200	280.0	-84.2	1.193E-02
225	283.0	-84.3	1.064E-02
250	285.2	-84.9	9.590E-03
275	283.2	-84.4	8.333E-03
300	296.9	-84.7	7.238E-03
350	281.6	-86.0	5.457E-03
400	288.3	-83.7	4.035E-03
450	203.1	-88.3	2.886E-03
500	280.1	-80.0	2.459E-03
550	355.7	-59.1	1.652E-03

SPEC. NAME: 19794-10 Tryb Test

FIELD	DECL.	INCL.	MOMENT
0	9.3	60.8	1.116E-02
25	4.4	56.8	1.038E-02
50	8.2	54.9	8.815E-03
75	7.0	53.5	6.951E-03
100	7.7	51.9	5.074E-03
125	8.7	51.5	3.951E-03
150	7.6	51.1	3.083E-03
175	7.1	50.2	2.516E-03
200	8.6	51.2	2.038E-03
250	8.6	49.9	1.457E-03
300	9.1	50.9	1.075E-03
350	8.9	50.1	8.407E-04

SPEC. NAME: 1993-1-1A Tryb Test

FIELD	DECL.	INCL.	MOMENT
0	151.6	65.8	7.708E-03
50	136.0	77.8	3.458E-03
75	134.5	77.6	3.122E-03
100	140.1	77.8	1.790E-03
125	140.9	78.5	1.391E-03
150	130.2	77.9	1.054E-03
175	136.7	75.8	8.463E-04
200	154.3	77.1	6.970E-04
225	135.5	75.1	5.648E-04
250	133.6	70.8	5.239E-04
275	134.6	71.0	4.365E-04
300	131.9	77.0	3.503E-04
325	149.4	74.0	3.048E-04
350	153.4	73.6	2.403E-04
375	202.4	88.3	2.295E-04

SPEC. NAME: 1993-2B.1A TH Tryb Test

TEMP	DECL.	INCL.	MOMENT
0	310.5	-6.9	8.923E-03
5	313.5	-17.9	9.605E-03
10	314.3	-22.2	9.050E-03
15	314.8	-24.1	7.016E-03
200	312.7	-26.7	7.225E-03
250	313.4	-27.1	7.348E-03
300	313.8	-27.7	7.313E-03
350	313.8	-28.5	6.932E-03
400	314.7	-28.6	6.287E-03
450	309.5	-23.8	5.792E-03
500	295.8	-21.0	7.498E-04
520	300.3	-13.9	3.800E-04
540	262.8	1.6	1.751E-04
560	233.9	-7.8	6.154E-05
580	197.1	9.6	1.565E-04
600	205.8	4.6	1.039E-04

SPEC. NAME: 1993-3 Tryb Test

FIELD	DECL.	INCL.	MOMENT
0	116.2	-11.5	1.619E-02
50	112.8	-12.9	1.624E-02
75	112.4	-14.5	1.626E-02
100	111.3	-16.0	1.585E-02
125	111.0	-16.6	1.522E-02
150	110.0	-17.3	1.397E-02
175	109.4	-17.8	1.251E-02
200	108.9	-18.1	1.093E-02
225	109.4	-18.5	9.235E-03
250	108.3	-18.3	7.771E-03
275	108.3	-18.0	6.625E-03
300	108.7	-20.7	5.204E-03
325	105.9	-19.1	4.247E-03
350	105.3	-20.1	3.474E-03
375	107.5	-18.0	3.300E-03
400	111.8	-32.1	2.247E-03
425	98.3	-18.1	1.854E-03
450	108.0	-15.0	2.248E-03
475	124.7	-56.3	1.240E-03

SPEC. NAME: 1993-4.1A Tryb Test

FIELD	DECL.	INCL.	MOMENT
0	195.9	-26.7	4.053E-03
50	205.7	21.6	1.844E-03
75	173.9	68.5	1.565E-03
100	72.9	80.1	1.877E-03
125	45.6	68.4	2.087E-03
150	36.8	63.2	2.136E-03
175	35.6	61.0	2.023E-03
200	33.4	59.4	1.850E-03
225	30.9	58.9	1.748E-03
250	28.8	55.5	1.597E-03
275	34.1	56.0	1.375E-03
300	30.6	57.9	1.285E-03
325	31.1	54.0	1.233E-03
350	21.9	54.8	9.672E-04
375	17.5	45.0	9.178E-04
400	54.2	54.4	6.787E-04
425	11.6	51.0	5.957E-04
450	13.4	30.7	7.893E-04
500	116.4	47.3	4.854E-04

SPEC. NAME: 1993-5.1 Tryb Test

FIELD	DECL.	INCL.	MOMENT
0	258.8	64.4	1.564E-02
50	252.9	58.5	1.535E-02
75	250.6	57.3	1.419E-02
100	250.9	55.6	1.169E-02
125	250.6	55.3	9.212E-03
150	252.3	56.5	7.326E-03
175	253.3	52.6	5.696E-03
200	251.4	53.9	3.925E-03
225	251.4	55.2	3.252E-03
250	255.7	55.4	2.188E-03
275	249.5	53.4	1.653E-03
300	252.9	52.7	1.446E-03
325	266.7	58.2	1.059E-03
350	247.8	52.6	8.325E-04
375	256.5	52.3	7.598E-04

SPEC. NAME: 1993-6.1A Tryb Test

FIELD	DECL.	INCL.	MOMENT
0	54.9	72.2	1.621E-02
50	112.7	76.3	1.356E-02
75	137.2	73.9	1.266E-02
100	143.0	73.3	1.111E-02
125	150.2	71.8	1.010E-02
150	156.9	71.0	9.139E-03
175	164.0	70.5	8.295E-03
200	169.7	72.1	6.948E-03
225	169.0	70.4	6.187E-03
250	174.5	72.5	4.894E-03
275	172.4	87.2	3.830E-03
300	164.4	67.2	3.432E-03
325	208.8	71.9	2.488E-03
350	355.3	63.5	2.282E-03
375	156.1	52.1	2.222E-03
400	245.0	57.5	1.285E-03

SPEC. NAME: 18794-13.1 TH Tryb Test

TEMP	DECL.	INCL.	MOMENT
0	218.8	-23.1	2.315E-02
5	216.1	-27.1	2.429E-02
10	214.1	-30.3	2.478E-02
15	213.8	-31.7	2.351E-02
200	210.9	-33.8	2.388E-02
250	211.8	-34.1	2.391E-02
300	211.9	-34.6	2.308E-02
350	211.6	-35.0	2.171E-02
400	211.1	-35.4	1.928E-02
450	214.8	-35.2	1.673E-02
500	209.4	-34.9	2.845E-03
520	209.7	-29.6	1.528E-03
540	211.8	-24.3	6.283E-04
560	201.4	-23.8	2.133E-04
580	196.3	-9.5	2.558E-04
600	204.7	-3.3	1.653E-04

SPEC. NAME:18794-14.1 Tryb Test

FIELD	DECL.	INCL.	MOMENT
0	188.1	39.4	1.195E-02
25	186.3	38.5	1.159E-02
50	187.8	33.3	1.143E-02
75	188.7	29.6	1.051E-02
100	190.0	26.7	9.079E-03
125	188.8	25.3	7.678E-03
150	190.4	24.1	6.388E-03
175	190.2	24.1	5.068E-03
200	189.8	23.5	4.226E-03
225	190.0	23.7	3.407E-03
250	189.0	23.1	2.838E-03
300	189.4	25.1	1.860E-03
350	183.8	24.2	1.384E-03
400	191.7	23.7	9.591E-04

SPEC. NAME:18794-15.1 Tryb Test

FIELD	DECL.	INCL.	MOMENT
0	297.9	59.3	1.564E-02
25	300.7	60.1	1.436E-02
50	297.7	57.4	1.273E-02
75	297.9	56.6	1.054E-02
100	298.9	54.9	8.350E-03
125	296.6	52.5	6.098E-03
150	298.2	52.7	4.943E-03
175	298.5	52.5	3.976E-03
200	297.7	52.5	3.288E-03
250	299.8	53.0	2.309E-03
300	298.4	50.7	1.624E-03
350	302.6	54.8	1.321E-03

SPEC. NAME:18794-16.2 Tryb Test

FIELD	DECL.	INCL.	MOMENT
0	182.9	3.7	1.307E-02
25	182.5	1.3	1.290E-02
50	180.7	-1.9	1.232E-02
75	180.7	-4.7	1.093E-02
100	180.2	-7.0	9.077E-03
125	180.1	-7.9	7.087E-03
150	180.0	-7.9	5.539E-03
175	179.7	-7.0	4.184E-03
200	180.4	-8.0	3.362E-03
225	179.8	-7.2	2.691E-03
250	178.7	-5.5	2.288E-03
300	180.7	-10.6	1.571E-03
350	178.6	-4.8	1.039E-03

SPEC. NAME:18794-17.2 Tryb Test

FIELD	DECL.	INCL.	MOMENT
0	97.7	-1.0	2.289E-02
25	97.8	-2.3	2.282E-02
50	98.8	-4.2	2.278E-02
75	98.9	-6.1	2.206E-02
100	99.1	-6.9	2.079E-02
125	99.2	-7.6	1.847E-02
150	98.3	-8.6	1.589E-02
175	97.8	-8.7	1.314E-02
200	97.9	-8.8	1.090E-02
225	97.7	-9.4	8.740E-03
250	95.9	-8.8	7.153E-03
275	97.3	-8.3	5.784E-03
300	97.3	-10.0	4.455E-03
350	89.3	-3.2	3.100E-03
400	100.6	-5.2	2.306E-03
450	97.4	-22.4	1.332E-03